Master's thesis

NTNU
Norwegian University of Science and Technology
Faculty of Natural Sciences
Department of Biotechnology and Food Science

Adshaha Arampu

Methanol-based production of putrescine and spermidine in *Bacillus methanolicus*

Master's thesis in Chemical Engineering and Biotechnology
Supervisor: Luciana Fernandes de Brito
Co-supervisor: Fernando Pérez-García
June 2023

NTNU
Norwegian University of
Science and Technology

Adshaha Arampu

Methanol-based production of putrescine and spermidine in *Bacillus methanolicus*

Master's thesis in Chemical Engineering and Biotechnology
Supervisor: Luciana Fernandes de Brito
Co-supervisor: Fernando Pérez-García
June 2023

Norwegian University of Science and Technology
Faculty of Natural Sciences
Department of Biotechnology and Food Science

NTNU
Norwegian University of
Science and Technology

Preface

This thesis is a part of the TBT4900 Biotechnology, Master's Thesis course for the biotechnology specialization of the five-year M.Sc. program in Chemical engineering and Biotechnology at the Norwegian University of Science and Technology (NTNU). The experimental work was conducted at the molecular genetics lab under the Department of Biotechnology and Food Science (IBT).

This report has been written under the supervision of researcher Luciana Fernandes de Brito, with post-doc Fernando Pérez-García as co-supervisor. I would like to express my sincere gratitude to Luciana Fernandes de Brito for her invaluable guidance, mentoring, support, and patience throughout this work. Her commitment to my academic growth has been truely remarkable. She has always been available to answer my questions, no matter how trivial or complex they may have seemed, providing me with the confidence and clarity needed to overcome obstacles.

I would also like to extend my appreciation to the rest of the Cell factories group for being including and for their collaboration in the lab. Finally, I would like to express my graditude to my family and friends for their support, understanding, and encouragement throughout these five-years and particular during this final year.

Abstract

Value-added compounds such as amino acids, are commonly produced through microbial fermentations with glucose as feedstock. Glucose is rising in price and creates undesirable competition in the food and feed industry. In contrast, methanol, a non-food, one-carbon (C1) feedstock, serves as a valuable carbon and energy source for C1-utilizing bacteria (*i.e.* methylotrophs), including *Bacillus methanolicus*. Moreover, biogenic diamines such as cadaverine, and putrescine, are readily used in the plastic industry for the production of synthetic polyamides. Another biogenic diamine that has received attention in pharmaceutical and food research is spermidine. Microbial production of these diamines has gained great interest, and the high titer production of putrescine and cadaverine has already been achieved in traditionally used cell factories like *Escherichia coli* and *Corynebacterium glutamicum* with glucose as feedstock. However, producing these diamines through the non-food feedstock methanol would contribute to the desired shift towards sustainable white biotechnology. Methanol-based cadaverine production has already been achieved in *B. methanolicus*, however, methanol-based putrescine and spermidine production have not been reported. Thus, this study aimed to achieve methanol-based putrescine and spermidine production by genetically engineering the methylotroph *B. methanolicus*.

To assess if *B. methanolicus* MGA3 is a suitable host for the production of putrescine and spermidine, tolerance towards the precursor arginine, alongside putrescine and spermidine, and the utilization of these as potential carbon or nitrogen sources was experimentally tested. The recombinant *B. methanolicus* strains, PUT^{Ec} and PUT^{Bm} are expressing the genes coding for arginine decarboxylase (SpeA) and agmatinase (SpeB) in the biosynthesis of putrescine heterologously or homologously, respectively. The constructed strains were cultivated and putrescine production was quantified through high-pressure liquid chromatography (HPLC).

The highest putrescine titer achieved was 47.5 $\pm$ 0.8 µM with PUT^{Ec}. Moreover, the optimization of growth conditions, including gene expression level, supplementation of putrescine biosynthesis precursors, and growth media composition was explored towards the increase in putrescine production by PUT^{Ec}. Out of the optimized growth conditions, 1 mM arginine supplementation resulted in 26.3 $\pm$ 1.5 µM, representing a 4.9-fold increase, and cultivation in a conventionally used CGXII medium resulted in 10.0 $\pm$ 0.0 µM, a 2-fold increase in putrescine titers, compared to the controls. PUT^{Ec} was subsequently used in the construction of a two-plasmid-based expression system. Here, homologous or heterologous expression of genes coding for spermidine synthase (SpeE) and/or S-adenosyl-methionine decarboxylase (SpeH) in spermidine biosynthesis was carried out both in that two-plasmid-based expression system ($PUT^{Ec}SPE^{Bm}$, $PUT^{Ec}SPE_{ii}{}^{Ec}$, and $PUT^{Ec}SPE_{ii}{}^{Bm}$) and solely in wild type *B. methanolicus* MGA3 (SPE^{Bm}, $SPE_{ii}{}^{Ec}$, and $SPE_{ii}{}^{Bm}$). A marginal improvement in spermidine titers was observed in the WT harboring homologous and heterologous expression of *speEH* genes. However, the two-plasmid-based expression system for genes involved in putrescine and spermidine biosynthesis did not lead to higher spermidine titers. In this study, it was evident that the growth of the strains played a crucial role in achieving high-production titers for both putrescine and spermidine.

This work provided valuable insight into the methanol-based production of the diamines putrescine and spermidine, and how compound toxicity and cell growth impact their production. Suggestions for achieving higher production titers are presented in this work, which contributes to the research on the sustainable production of diamines through methanol conversion.

Sammendrag

Verdiskapende forbindelser som aminosyrer produseres ofte gjennom mikrobiell produksjon ved bruk av glukose som råstoff. Dagens glukosepriser stiger, og i tillegg skaper bruk av glukose uønsket konkurranse i mat- og råstoff industries. I motsetning til dette kan metanol, et ikke-matbasert enkarbon (C1) råstoff, fungere som en verdifull karbon- og energikilde for C1-utnyttende bakterier (f.eks. metylotrofer), inkludert *Bacillus methanolicus*. Videre brukes biogene diaminer som kadaverin og putrescin allerede i plastindustrien til produksjon av syntetiske polyamider. En annen biogen diamine som har fått oppmerksomhet innen farmasøytisk og matforskning er spermidin. Mikrobiell produksjon av disse diaminkomponentene har vakt stor interesse, og høyproduksjon av putrescin og kadaverin er allerede oppnådd i tradisjonelle cellefabrikker som *Escherichia coli* og *Corynebacterium glutamicum* med glukose som råstoff. Produksjon av disse diaminkomponentene ved bruk av ikke-matbasert metanol bidra til en ønsket overgang til bærekraftig hvit bioteknologi. Metanolbasert produksjon av kadaverin er allerede oppnådd i *B. methanolicus*, men metanolbasert produksjon av putrescin og spermidin er ikke rapportert. Derfor hadde denne studien som mål å oppnå metanolbasert produksjon av putrescin og spermidin ved genredigering av metylotrofen *B. methanolicus*.

For å vurdere om *B. methanolicus* MGA3 er en egnet vert for produksjon av putrescin og spermidin, ble toleransen mot forløperen arginin, samt putrescin og spermidin, og utnyttelsen av disse som potensielle karbon- eller nitrogenkilder, testet eksperimentelt. De genredigerte *B. methanolicus*-stammene PUT^{Ec} og PUT^{Bm} uttrykker genene som koder for arginindekarboksylase (SpeA) og agmatinase (SpeB) i biosyntesen av putrescin henholdsvis på en heterolog eller homolog måte. De genredigerte stammene ble dyrket, og produksjonen av putrescin ble kvantifisert ved hjelp av høytrykksvæskekromatografi (HPLC).

Den høyeste putrescintiteren som ble oppnådd, var 47,5 $\pm$ 0,8 µM med PUT^{Ec}. Videre ble optimaliseringsforsøk for vekstforholdene, inkludert genuttrykksnivå, tilsetning av putrescinbiosyntese-forløpere og sammensetning av vekstmediet, utforsket for å øke produksjonen av putrescin med PUT^{Ec}. Av de optimaliserte vekstbetingelsene førte tilskudd av 1 mM arginin til en økning på 4,9 ganger med en titer på 26,3 $\pm$ 1,5 µM, og dyrking i et konvensjonelt brukt medium CGXII ga en økning på 2 ganger med en produksjon på 10,0 $\pm$ 0,0 µM sammenlignet med kontrollene. PUT^{Ec} ble deretter brukt i konstruksjonen av et to-plasmid-basert uttrykkssystem. Her ble homolog eller heterolog uttrykk av gener som koder for spermidinsyntase (SpeE) og/eller S-adenosylmetionindekarboksylase (SpeH) i spermidinbiosyntese utført både i dette to-plasmid-baserte uttrykkssystemet ($PUT^{Ec}SPE^{Bm}$, $PUT^{Ec}SPE_{ii}{}^{Ec}$ og $PUT^{Ec}SPE_{ii}{}^{Bm}$), og bare i villtype *B. methanolicus* MGA3 (SPE^{Bm}, $SPE_{ii}{}^{Ec}$ og $SPE_{ii}{}^{Bm}$). Det ble observert en marginal forbedring i spermidin produksjonen hos MGA3 som uttrykker homologe og heterologe *speEH*-gener. Det to-plasmid-baserte uttrykkssystemet for gener involvert i putrescin- og spermidinbiosyntese førte ikke til økt spermidin produksjon. Denne studien viste at at stammens vekst spilte en avgjørende rolle for å oppnå høy produksjon både for putrescin og spermidin.

Dette arbeidet ga verdifulle innsikt i metanolbasert produksjon av diaminkomponentene putrescin og spermidin, og hvordan toksisitet og cellevekst påvirker deres produksjon. Forslag til å oppnå høyere produksjon presenteres i dette arbeidet, og dette bidrar til forskningen på bærekraftig metanol basert produksjon av diaminkomponenter.

Table of Contents

List of Figures

List of Tables

List of abbreviations

ADC	arginine decarboxylase
AdoMet	S-adenosyl-l-methionine
AK	aspartokinase
BLAST	Basic Local Alignment Search Tool
Bp/kb	base pair/kilobases
BRENDA	Braunschwig enzyme database
C1	one-carbon
Cm^R	chloramphenicol resistant
C/N	carbon/nitrogen
CRISPR(i)	clustered regularly interspaced short palindromic repeats (interference)
dAdoMet	S-adenosyl-methioninamine
dCas9	endonuclease deficient Cas9
DHAP	dihydroxyacetone phosphate
dNTP	deooxynucleotide triphosphate
(g)DNA	(genomic) deoxyribonucleic acid
EPB	electroporation buffer
F6P	β-d-fructofuranose
FBP	fructose-1,6-biphosphate
GAP	glyceraldehyde 3-phosphate
G6P	glucose 6-phosphate
Hu6P	hexulose 6-phosphate
Hps	hexulose-6-phosphate synthase
Kan^R	kanamycin resistant
KEGG	Kyoto Encyclopedia of Genes and Genomes
Mdh	methanol dehydrogenase
mdh	methanol dehydrogenase (promotor)
NAD(H)	nicotinamide adenine dinucleotide (hydrogen)
ODC	ornithine decarboxylase
6PG	6-phosphogluconate

6PGL	6-phospho-glucono-1,5-lactone
PA	polyamide
PCR	polymerace chain reaction
P_{mtlR}	mannitol inducible promoter
Phi	6-photo-3-hexuloisomeras
RuMP	Ribulose monophosphate pathway
Ru5P	d-ribulose 5-phosphate
SBPase	sedoheptulose-1,7-bisphosphatase
SBS	spermidine biosynthesis
sgRNA	single guide RNA
SpeA/*speA*	arginine decarboxylase
SpeB/*speB*	agmatinase
SpeE/*speE*	spermidine synthase
SpeH/*speH*	S-adenosylmethionine decarboxylase
Ta	transaldose
TCA	tricarboxylic acid cycle
WT	wild type
xpx	xylose inducible promoter

1 Introduction

Amino acids and their derivatives are among the major products in biotechnology, and the global market is growing[1]. For example, the annual demand for diamines is at 7 000 000 tons, which is mainly produced by oil-based raw materials through chemical synthesis[2]. To reduce waste production, energy requirements, and environmental stress, production through biotechnological processes has shown ecological advantage without diminishing the product quality[3]. Microbial fermentation is already a dominant method used for the industrial production of amino acids, however, these are predominantly sugar-based, which presents environmental and economic challenges[4]. Methanol, a non-food, one-carbon (C1) compound, can therefore be utilized as the sole carbon source in microbial fermentation of C1-utilizing (*i.e* methylotrophic) *Bacillus methanolicus*, for sustainable methanol-based production of those products. Furthermore in this section, details regarding methanol as feedstock, *B. methanolicus* MGA3 as a model organism and production of diamines such as putrescine and spermidine will be presented.

1.1 Methanol as feedstock in microbial fermentations

The utilization of methanol as a feedstock in microbial fermentations is a subject of considerable interest in the field of white biotechnology. Historically, glucose and other sugars have served as the primary carbon substrate in such fermentations[5]. However, due to the increasing cost of these food-based substrates and the undesirable competition in the food and feed industries, alternative feedstocks are being explored for the sustainable production of value-added compounds[4]. One promising alternative is methanol, a pure C1 alcohol that can be used as a non-food carbon source for microbial fermentations with methylotrophic bacteria[5].

Methanol can be found naturally in the environment and is predominantly produced from syngas, a mixture of H_2, CO, and CO_2, which is a byproduct of incomplete combustion of natural gas[4,6]. Other methods for methanol production include direct conversion of natural gas and biogas, within mega-methanol production facilities which are currently under construction[6]. Pfeifenschneider et al. predicts that the availability of these facilities will result in lower methanol prices, which are presently at €488/ton[7], making it a more economically viable carbon substrate than sugar, which is presently at 25 U.S. cents/pound for raw sugar (€465/ton)[8,6]. Even with the current prices, Woolston et al. implies that methanol is comparable with the price of glucose, despite the higher energy density, and 50% higher degree of reduction per carbon mole of methanol[9]. In addition to the high availability and low pricing of methanol, its use as feedstock in microbial fermentations offers several advantages, such as its chemical purity, no significant fluctuations in the production of titers, minimal contamination in bioreactors compared to sugar feedstocks, and ease of transport and storage[10]. Aerobic methylotrophs as *B. methanolicus* generally exhibits high growth rates from 0.4 h^{-1}, on media containing methanol as the main carbon source, and nitrogen in the form of ammonium salts with key elements such as phosphorus, magnesium, and sulfur[10]. These supplements are low-cost, and combined with the cost-effective downstream and purification of simple biochemicals such as amino acids show that methanol has tremendous advantages in microbial fermentations. However, optimization of media compositions is essential to maintain an adequate carbon/nitrogen (C/N) ratio, and supplements of vitamins or amino acids are important against potential auxotrophies[10].

Although methanol holds potential as a sustainable feedstock for large-scale commercial and industrial

production, certain conditions need to be considered. Methanol can only be utilized by methylotrophic bacteria such as *B. methanolicus* natively. They possess the ability to utilize reduced C1 compounds as their sole carbon and energy source[5]. However, these microbes are not as well characterized with a less developed genetic toolbox compared to other conventionally used bacteria in microbial fermentations such as *Escherichia coli* and *Cornynebacterium glutamicum*. This may pose challenges in the metabolic engineering of methylotrophs for redirecting methanol-flux towards the production of specific value-added compounds[11]. Therefore, attempts on engineering synthetic methylotrophic *E. coli* and *C. glutamicum* have received increasing attention in recent years. In addition to a well-developed genetic toolbox, high growth rates of *E. coli* (0.65 h^{-1}) and *C. glutamicum* (0.52 h^{-1}) when utilizing glucose, and higher efficiency with regard to electron conservation and product yield makes synthetic methylotrophic engineering of the advantagous[12,13]. Presently, only *E. coli* have been engineered to utilize methanol as the sole carbon source, however, low biomass production was observed with maximum OD of 2[14]. Additionally, for higher biomass production of synthetic methylotrophs, methanol was not utilized as the sole carbon source, and low methanol-conversion to biomass production has been observed compared to methylotrophic bacteria[1,12,15]. Moreover, due to the higher reduction potential of methanol compared to sugar, more oxygen is required, resulting in higher energy demand for cooling systems in large-scale fermentations[5]. In addition to these aspects, the concentration of methanol should not be too excessive as methanol has an inhibitory effect on the cell, because methanol is oxidized to the cytotoxic compound formaldehyde (CHOH)[16]. The optimal concentration of methanol for fastest cell growth would therefore be between 0.5% and 2% for most methylotrophs with some variability[10]. Challenges with formaldehyde accumulation in bioreactors may resolve through continuous substrate (methanol) feeding, to hold the accumulation of formaldehyde under the toxicity threshold. Methanol concentration does therefore need to be monitored, with for example a methanol sensor. A combination of careful bioreactor design, which includes media composition, inoculum, feeding strategies, and online monitoring, is important for a sufficient dissolved oxygen concentration (usually at least 25% saturation), balanced biomass growth, and production of desired compounds. Overall, methanol is a promising candidate for large-scale production of value-added compounds[10,1].

1.2 *Bacillus methanolicus*: A model organism for conversion of methanol to value-added compounds

The first reports of isolated *B. methanolicus* strains from soil samples, wastewater treatment plants, and volcanic hot springs are dated from the 1980s[1]. *B. methanolicus* is a Gram-positive thermotolerant spore-forming bacteria that grow in the temperature range between 37 °C and 60 °C, with optimum growth at 50 °C[1]. However, sporulation occurs after the rapid change in temperature from 50 to 30°C[17,18]. The model strain *B. methanolicus* MGA3 is the most utilized for metabolic engineering of this bacterium for the purpose of overproducing value-added compounds such as amino acids and their derivatives through the conversion of methanol[1]. The bacteria is also a facultative methylotroph that can utilize multicarbon substrates as carbon sources, besides methanol, for energy and growth. It can utilize substrates such as glucose, arabitol, and mannitol for growth[19]. *B. methanolicus* is also advantageous in bioprocesses because of its high growth rate up to 0.4 h^{-1} at high temperatures of 50 °C[1]. Additionally, high temperatures in the reactors minimize the risk of contamination[1]. Generally, methanol fermentations are characterized by high oxygen demand compared to conventional sugar-based fermentations as methanol is more reduced than sugars, as mentioned above[1]. With higher oxygen

demands, heat in industrial bioreactors becomes a challenge, and cooling requirements represent additional production costs[1]. However, as *B. methanolicus* is thermotolerant, these cooling requirements decrease exceptionally compared to methylotrophic bacteria growing at 30 to 37 °C. Moreover, at about 200 m^3 reactor liquid volume, the cooling water requirements are reported to be similar for an organism growing on glucose at 35 °C and for *B. methanolicus* growing on methanol at 50 °C[1]. Overall, *B. methanolicus* has shown to be a promising candidate for cultivation in bioreactors.

The genome of *B. methanolicus* has been sequenced, which includes a chromosomal DNA of 3.4 Mb, native plasmid pBM19 of 19 kb, and native plasmid pBM69 of 69 kb[17]. The diversity of genetic tools for this strain includes compatible vectors that utilize theta- or rolling circle-replication mechanisms, as well as inducible and constitutive promoter systems[20]. Inducible promoters used for recombinant *B. methanolicus* are a mannitol inducible promoter P_{mtlR}, and a xylose inducible promoter, *e.g.* xpx[20]. However, P_{mtlR} was shown to be not as reliable as xpx for a controlled expression of cloned genes in *B. methanolicus*[21]. Moreover, xylose is not utilized in the bacteria for growth, hence, the xpx promoter has shown to be a promising promoter in *B. methanolicus*. As for constitutive promoters, the methanol dehydrogenase (*mdh*) promoter has been used for recombinant expression of genes in *B. methanolicus* MGA3[21]. Moreover, the expression of a reporter gene *gfpuv* was shown to be 15-fold higher in fully induced xpx promoted-derived plasmid, compared to the *mdh* promoter-derived plasmid[20]. The use of two separate plasmids in one cell facilitates the stable expression of multiple genes and pathways by enabling complex genetic engineering of *B. methanolicus* MGA3[21]. Additionally, the use of inducible promoter systems in expression vectors enables the controlled expression of genes, which potentially avoids toxic accumulation of intermediates in the applicable biosynthetic pathways during microbial fermentations[21]. Multiple transformation methods have been developed for introducing these plasmids, including electroporation and conjugation[21]. In addition to a well-developed, plasmid-based expression system, chromosomal gene editing has been developed in *B. methanolicus*. A CRISPR interference with deactivated Cas9 protein (CRISPRi-dCas9)-technique for gene repression has been reported in *B. methanolicus* through the construction of the vector PiCas[18]. One application was to target a sporulation protein to reduce the spore formation and increase the biofilm formation in *B. methanolicus* MGA3. CRISPRi can repress or activate the expression of specific genes, while the co-expression of dCas9 and a customizable single guide RNA (sgRNA), interferes with the RNA polymerase by disrupting the transcript elongation on DNA sequences complementary to the sgRNA[18]. Other omics tools available are a riboswitch-mediated regulatory system for metabolic flux control in *B. methanolicus*[22]. An l-lysine riboswitch was developed and showed promise for regulating genes encoding for the l-lysine pathway[22]. The genetic toolbox for *B. methanolicus* is restricted, however, the fast phase development of new genetic tools makes the utilization of *B. methanolicus* in bioprocessess promising.

As aforementioned, the interest in *B. methanolicus* in industrial biotechnology is mainly due to its potential as a sustainable cell factory, where methanol is utilized as an alternative to sugar feedstocks. In *B. methanolicus*, methanol is first oxidized to formaldehyde, catalyzed by NAD-linked methanol dehydrogenase in the cell. The expression of the *mdh* gene is activated by an activator protein denoted ACT, which works as a control mechanism for preventing the accumulation of toxic formaldehyde in the cells. After the oxidation of methanol, formaldehyde can either be assimilated for biomass production through the ribulose monophosphate (RuMP) cycle (Figure 1.1) or be dissimilated through a cyclic or linear dissimilatory pathway. The cyclic dissimilatory pathway has multiple common metabolites as the RuMP cycle and the pentose phosphate pathway (Figure 1.1)[1]. The native pBM19 plasmid in *B. methanolicus*

harbors the *mdh* gene and five of the RuMP pathway genes, *pfk*, *fba*, *tkt*, *glpX*, and *rpe*. Moreover, *B. methanolicus* MGA3 carries three *mdh* genes, two chromosomal and one in pBM19. For methanol-based growth, both chromosomal and plasmid genes encoding for the RuMP enzymes are required[17].

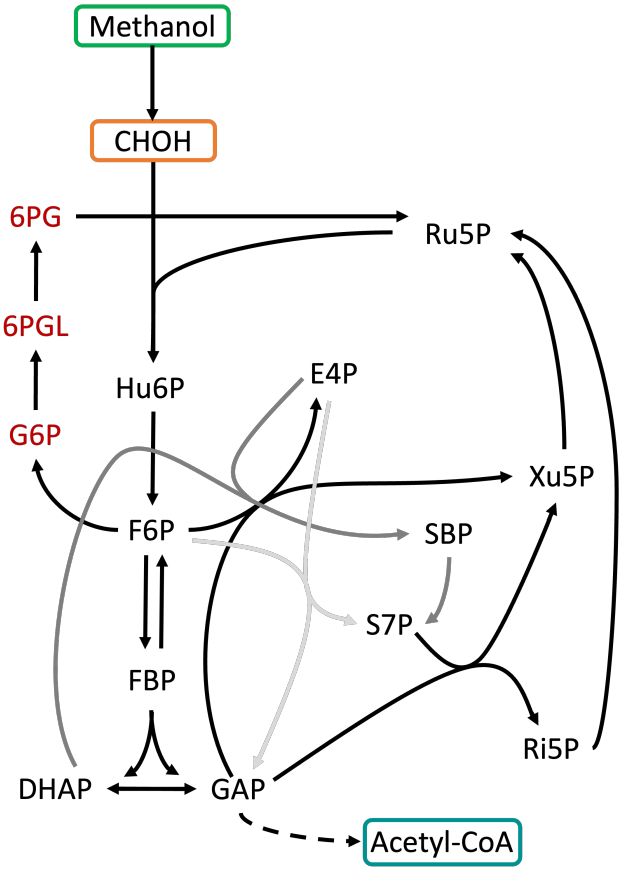

Figure 1.1: Schematic representation of the RuMP cycle (black) in *B. methanolicus*, with its SBPase variant (dark grey), and Ta variant (light grey).
Dashed arrows represent multiple reactions. The metabolites colored in red show the dissimilatory variant of the RuMP cycle. Metabolites: CHOH = formaldehyde, Ru5P = ribulose 5-phosphate, Hu6P = hexulose 6-phosphate, E4P = erythrose 4-phosphate, F6P = fructose 6-phosphate, FBP = fructose 1,6-bisphosphate, DHAP = dihydroxyacetone phosphate, GAP = glyceraldehyde 3-phosphate, S7P = sedoheptulose 7-phosphate, SBP = sedoheptulose 1,7- bisphosphate, Ri5P = ribose 5-phosphate, Xu5P = xylulose 5-phosphate, G6P = glucose 6-phosphate, 6PGL = 6-phospho-glucono-1,5-lactone, 6PG = 6-phosphogluconate. Adapted from Klein et al. [16]

The assimilatory RuMP cycle in methylotrophs can be described in three parts, fixation, cleavage, and re-arrangement (Figure1.1). In fixation, three formaldehyde molecules and d-ribulose 5-phosphate (Ru5P) are condensed to hexulose 6-phosphate (Hu6P) catalyzed by a hexulose-6-phosphate synthase (Hps). Hu6P is converted to β-d-fructofuranose (F6P), catalyzed by a 6-photo-3-hexuloisomerase (Phi). In the following step, F6P is phosphorylated to fructose-1,6-biphosphate (FBP). FBP is then cleaved to glyceraldehyde 3-phosphate (GAP) and dihydroxyacetone phosphate (DHAP) catalyzed by a FBP-aldolase, where GAP is rearranged to Ru5P by multiple steps, shown in Figure 1.1. The rearrangement step can follow two variants: the fructose FBP aldolase/transaldolase (FBPa/Ta) variant and the FBP aldolase/sedoheptulose-1,7-bisphosphatase (FBPa/SBPase) variant[16]. Both variants are present in *B. methanolicus*, however, the major rearrangement step follows the SBPase variant. GAP can further be converted to acetyl-CoA following multiple reactions with pyruvate as an intermediate, which leads to biomass production[16]. The cyclic dissimilatory pathway shares the activity of Hps and Phi as the assimilatory

pathway, followed by a series of enzymatic reactions from F6P to 6-phosphogluconate (6PG) followed by its decarboxylation leading to the regeneration of Ru5P, with the intermediates glucose 6-phosphate (G6P) and 6-phospho-glucono-1,5-lactone (6PGL). Notably, both the formaldehyde assimilatory and dissimilatory pathways play major roles in the generation of energy and reducing power in *B. methanolicus*, which compensates for the poor activity of the tricarboxylic acid (TCA) cycle[17, 23].

The backbones of amino acids are derived from intermediates in the TCA cycle, where the precursor of l-lysine is oxaloacetate, and the precursor of l-glutamate is α-ketoglutarate (Figure 1.2)[24]. Genetic engineering of the bacterial genomes, including overexpression of key genes and deletion of competing pathways may increase the desired amino acid titers by directing the carbon and nitrogen flux towards their biosynthesis[24]. This way, *B. methanolicus* have been engineered for the production of natural and non-native amino acids. l-Aspartate is an intermediate in the production of l-lysine from oxaloacetate, where the first enzymatic reaction from l-aspartate to l-lysine is catalyzed by aspartokinase (AK) enzymes. Overexpression of one of the AK enzymes encoded by the gene *yclM* resulted in titers of l-lysine up to 11 gL^{-1} in fed-batch methanol cultivation of *B. methanolicus* MGA3[24], which is 28-fold higher than the wild type (WT) strain. Moreover, as l-lysine is a precursor to multiple amino acids, the heterologous overexpression of essential genes in the appropriate biosynthetic pathways enables the biosynthesis of its derivatives[4]. For instance, cadaverine, a diamine derivative of l-lysine has been successfully produced from methanol in *B. methanolicus* MGA3 by heterologous expression of *cadA* and *ldcC* genes, both encoding l-lysine decarboxylase enzymes from *E. coli*, in combination with the overall increase in production levels of the precursor l-lysine[25]. *B. methanolicus* MGA3 can naturally produce l-glutamate with titers up to 59 gL^{-1}, in fed-batch methanol cultivation after 50 hours, which makes it an excellent host for producing amino acids derived from l-glutamate[17]. One example is the production of GABA in a methanol fed-batch fermentation to a final titer of 9 gL^{-1} after the shift of pH level to 4.6 from 6.0 after 27 hours and overexpression of the gene *gad* encoding glutamate decarboxylase from *Sulfobacillus thermosulfidooxidans*. Other derivatives of l-glutamate are the industry-relevant diamines putrescine and spermidine.

Similarly to cadaverine, the production of putrescine has been of high interest in the research field, where spermidine, a putrescine derivative, has gained attention in the pharmaceutical and food industry[26]. More about diamines and their production is presented in the following Section 1.3.

1.3 Applications and production of diamines

Diamines are low-weight molecules containing a carbon backbone with two amino groups and serve various functions both in nature and the industry due to their chemical properties[27]. They are used as stabilizers for anionic molecules such as phospholipids and DNA because of their cationic property in the cell[27]. Moreover, applications in which diamines and polyamines may be involved in are, pH homeostasis, cellular differentiation processes as signaling factors, and components in the membranes of Gram-negative bacteria[27].

In industry, the most essential applications for diamines are within pharmaceuticals, surfactants, agrochemicals, and polyamide plastics[27]. Conventional polyamide plastic is primarily synthesized chemically from petroleum, which often involves toxic precursors or intermediates[27]. Thus, bio-based plastics have gained interest in the past decade, where according to the latest market data, the production capacity will

increase from around 2.2 million tons in 2022 to approximately 6.3 million tons in 2027[28]. Biogenic diamines have gained momentum as monomers for polyamide plastics, such as putrescine (1,4-diaminobutane), and cadaverine (1,4-diaminopentane), which are alongside spermidine and spermine the most common diamines in bacteria and archaea[27]. Moreover, other diamines such as 1,3-diaminopropane, and 1,6-diaminohexane have also gained interest in microbial production. The synthesis of polyamides includes the condensation of different diamines with dicarboxylic acids[27]. They possess different properties, for instance, tensile strength, elasticity, and mechanical resistance. Accordingly, distinct polyamides serve different purposes in the industry based on their properties. For instance, polyamide plastic such as different nylons, is used in electrical and electronics applications, and in materials such as textiles[29]. Moreover, cadaverine can be used to synthesize PA-5.4, PA-5.6, and PA-5.10, while PA-6.6 and PA-6.10 can be synthesized from 1,6-diaminohexane[30]. Furthermore, putrescine yields the polyamides PA-4.10, and a nylon trademarked as Stanyl® (PA-4.6). PA-4,6 is synthesized through polycondensation of putrescine with adipic acid[31,27]. Spermidine is reported to display multiple health benefits, including protection against tumors, combatting skin aging, stimulation of human hair growth, treat type 2 diabetes, reducing inflammation, prevention of neurodegeneration, and cardiovascular protection[26]. Thus, spermidine and related amines have received attention within food research and the industry for production. Moreover, spermidine functional foods are commercially available by extracting spermidine from wheat germ. Presently, different products of spermidineLIFE® have been launched as dietary supplements, however, limiting resources of wheat germ presents a bottleneck in the application of spermidine in other related products[26]. Industrial production of spermidine is also based on chemical synthesis through addition, hydrogenation, and reduction of putrescine and acrylonitrile[32]. Furthermore, diamine biosynthesis through microbial production in bacteria is thus, a promising alternative to the production of diamines compared to chemical synthesis. In Section 1.4 the diamine biosynthesis pathways in bacteria with emphasis on putrescine and spermidine biosynthesis and the production of these through microbial fermentations are presented.

1.4 Diamine biosynthesis through microbial production in bacteria

The demand for diamines as raw materials for polyamides, pharmaceuticals, and other products has increased and the sustainable production of those is essential. Hence, there is an increasing interest in the production of diamines through bioprocessing in both research and industry[27]. Figure 1.2, shows the biosynthesis of diamines in bacteria through the C4 and C5 pathways, with oxaloacetate or α-ketoglutarate carbon backbone, respectively. The C4 pathway includes the biosynthesis of the diamines cadaverine and 1,3-diaminopropane which are derived from oxaloacetate, while the C5 pathway includes putrescine, spermidine, and also 1,3-diaminopropane biosynthesis which is derived from α-ketoglutarate. 1,3-diaminopropane biosynthesis pathways are only present natively in *Pseudomonas* and *Acinetobacter* species, through the C4 and C5 pathways, respectively[30].

The bio-based production of diamines has been developed in multiple cell factories, through the C4 and C5 pathways. The workhorse *C. glutamicum* and *E. coli* have both been utilized to produce cadaverine and putrescine through renewable feedstocks (Section 1.4.3). Production of putrescine and spermidine are described further in Section 1.4.1 and 1.4.2, respectively, and both degradation and transport pathways are mentioned as well.

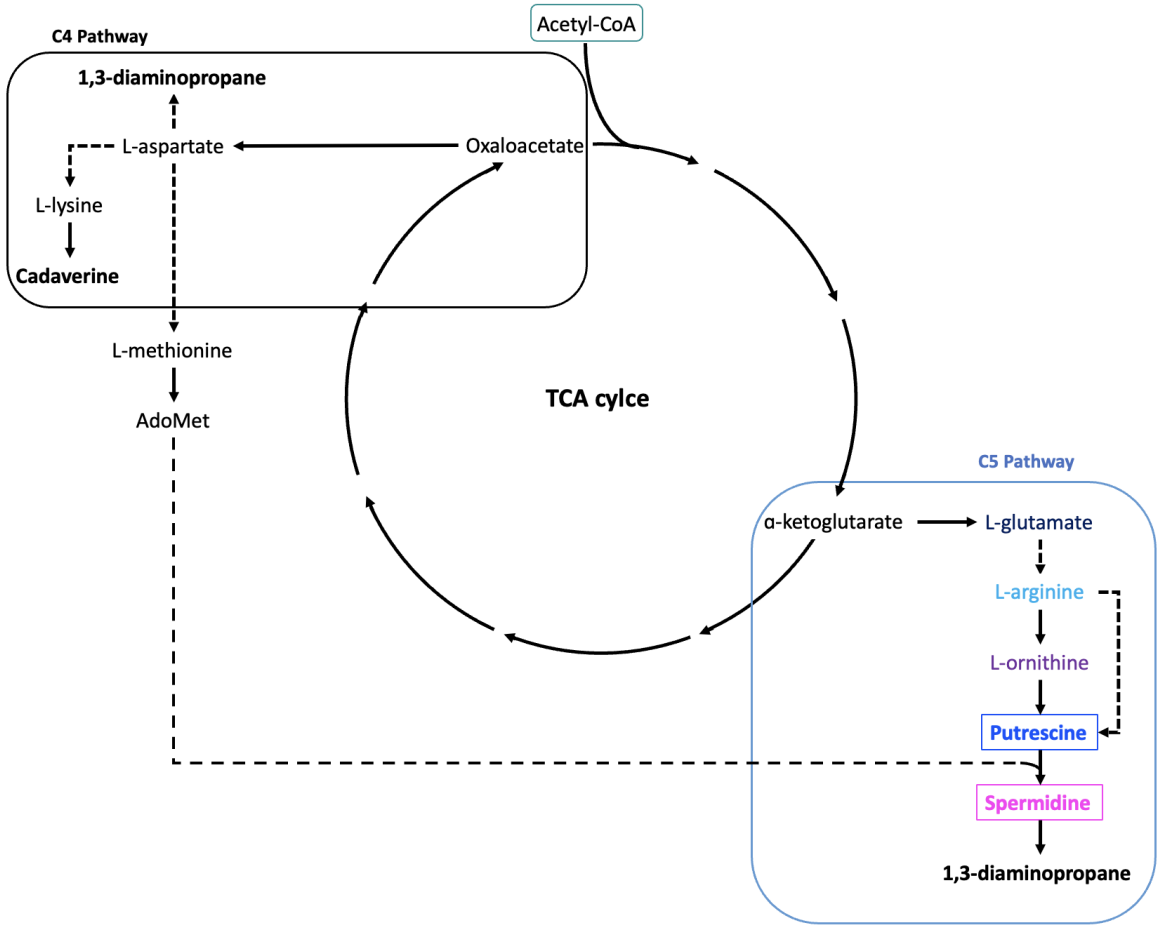

Figure 1.2: Schematic view of diamines biosynthesis through the C4 and C5 pathways in bacteria.
Dotted arrows implies multiple enzymatic reactions, while solid arrow implies one enzymatic reaction. Adapted from Pérez-García [30]

1.4.1 Putrescine

As aforementioned, putrescine has important applications in the industry, it is produced naturally in a wide range of organisms, and microbial production of putrescine has been achieved in well-known bacteria like *E. coli* and *C. glutamicum* [31, 33]. In *E. coli* among others, putrescine plays an important role in cell proliferation and normal cell growth. The regulation of putrescine in the cell involves the coordination of biosynthesis, degradation, uptake, and excretion pathways. Different bacteria possess variations of these pathways, which are regulated by multiple enzymatic reactions [31]. The putrescine biosynthesis, shown in Figure 1.3, includes the conversion of a carbon source to α-ketoglutarate through the TCA cycle, α-ketoglutarate conversion to l-glutamate, followed by the ornithine decarboxylase (ODC) in *e.g. E. coli* or arginine decarboxylase (ADC) pathways in *e.g. B. methanolicus* to putrescine production. *E. coli* can produce putrescine from both pathways, however, *B. methanolicus* can only produce putrescine from the ADC pathway. The ODC pathway yields putrescine directly from ornithine, while the ADC pathway yields putrescine from ornithine in a five-step reaction, with l-arginine being an intermediate. In the ADC pathway, l-arginine is decarboxylated and yields agmatine through an enzymatic reaction catalyzed by arginine decarboxylase (SpeA). Agmatine is thereafter converted to putrescine, through the cleavage of urea which is catalyzed by an agmatinase (SpeB) (Figure 1.3) [33].

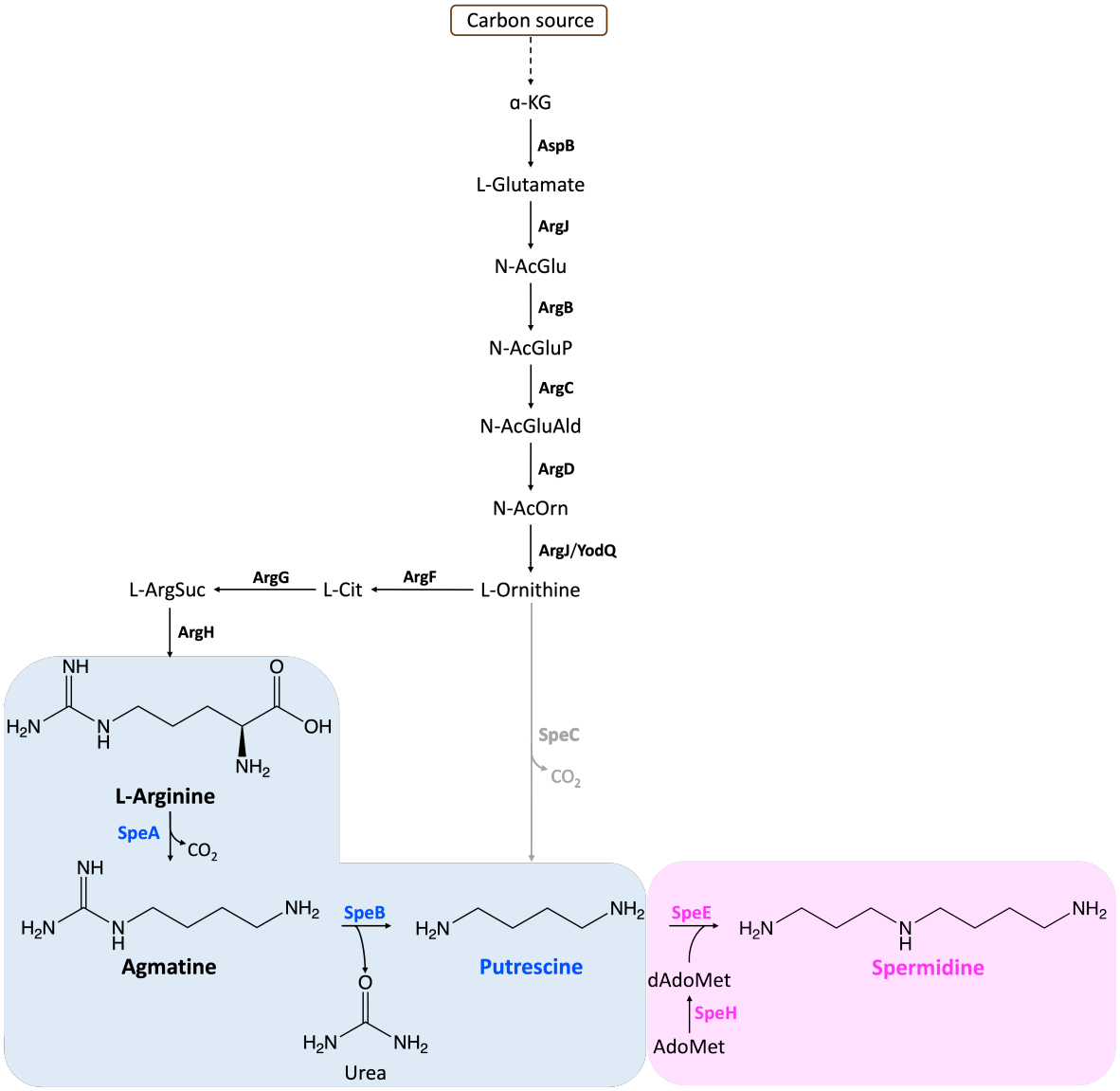

Figure 1.3: Schematic representation of putrescine and spermidine biosynthesis pathways through the ADC and the ODC pathways.
The dashed arrow represents multiple enzymatic reactions. Enzymes catalyzing the different reactions are in bold next to the arrows. The denotation of enzymes is based on enzymes found in *B. methanolicus*, except for SpeC. The ADC pathway is marked in blue, while the ODC pathway is highlighted in grey, and the spermidine biosynthesis (SBS) pathway is marked in pink. Enzymes directly connected to putrescine and spermidine biosynthesis are colored in blue, and pink, respectively. Adapted from KEGG[34]. Intermediates: α-KG = α-Ketoglutarate, N-AcGlu = N-Acetylglutamate, N-AcGluP = N-Acetylglutamylphoshate, N-AcGluAld = N-Acetylglutamate semialdehyde, N-AcOrn = N-Acetylornithine, l-Cit = l-Citrulin, l-ArgSuc = l-Argininosuccinate, AdoMet = S-Adenosyl-l-methionine, dAdoMet = S-Adenosyl-methioninamine. Enzymes: AspB = Aspartate aminotransferase [EC 2.6.1.1], ArgJ = amino-acid N-acetyltransferase [EC 2.3.1.1], ArgB = acetylglutamate kinase [EC 2.7.2.8], ArgC = N-acetyl-gamma-glutamyl-phosphate reductase [EC 1.2.1.38], ArgD = acetylornithine aminotransferase [EC 2.6.1.11], YodQ = acetylornithine deacetylase [EC 3.5.1.16], ArgJ = glutamate N-acetyltransferase [EC 2.3.1.35], ArgF = ornithine carbamoyltransferase [EC 2.1.3.3], ArgG = argininosuccinate synthase [EC 6.3.4.5], ArgH = argininosuccinate lyase [EC 4.3.2.1], SpeA = arginine decarboxylase [EC 4.1.1.19], SpeB = agmatinase [EC 3.5.3.11], SpeC = ornithine decarboxylase [EC 4.1.1.17], SpeE = spermidine synthase [EC 2.5.1.16], SpeH = S-adenosylmethionine decarboxylase [EC 4.1.1.50]

In *E.coli*, putrescine is degraded in the Puu pathway involving γ-glutamylation and the YdcW-YgjG pathway without γ-glutamylation, and it is also utilized in the production of spermidine. Putrescine can also be recycled as carbon and nitrogen source in *E. coli*, following multiple reactions to yield succinate, which is rechanneled into the TCA cycle[35]. Moreover, importers of putrescine in *E. coli*

are identified as PotFGHI, while a transporter which is both an importer and exporter is identified as PotE. Transportation of putrescine inside and outside of the cell is dependent on the membrane potential and putrescine-ornithine antiporter activity, respectively[36]. ArgR is a key pathway regulatory factor for the synthesis of l-arginine as it is a transcriptional repressor of the *arg* regulons, shown in Figure 1.3, encoding for l-arginine biosynthesis. Moreover, ArgA (equivalent catalytic property as ArgJ in *B. methanolicus*) is also feedback inhibited by the product l-arginine in *E. coli*, while ArgB is subjected to feedback inhibition in *C. glutamicum*[37, 30]. To achieve high-putrescine production in recombinant bacteria strategies concerning, knockout of degrading pathways, competing pathways, and importers of putrescine combined with overexpression of desired putrescine biosynthesis pathway genes, and overexpression of genes encoding putrescine exporters have been done. Multiple examples of high-putrescine producing recombinant *E. coli* and *C. glutamicum* will be presented further.

As the ODC pathway produces putrescine in one step from ornithine, the development of a putrescine overproducing pathway has been mainly focused around the ODC pathway. To create putrescine via the desirable ODC pathway, Qian et al. engineered *E. coli* by overexpression of the gene encoding the key enzyme for converting ornithine to putrescine (SpeC), deleting the degrading (Puu) and utilization (SpeE) pathways genes of putrescine, by attenuating the competing ADC pathway (Figure 1.3), and also deleting a stress response regulator RpoS as the overproduction of putrescine could cause stress in the cells[31]. This resulted in 24.2 gL^{-1} of putrescine in high cell density fed-batch cultures utilizing glucose as carbon source, with a productivity of 0.75 $gL^{-1}h^{-1}$ [31].

In *C. glutamicum*, Schneider and Wendisch introduced the ODC and ADC pathways from *E. coli* by heterologous expression of the genes encoding for the respective pathways[33]. A putrescine titer of 61 $\pm$ 6 mM was secreted in a recombinant *C. glutamicum* strain called PUT1, where the *speC* gene was overexpressed, and genes encoding an arginine repressor ArgR and the ornithine carbamoyltransferase ArgF were deleted to move the flux of ornithine towards the ODC pathway[33]. Moreover, production of putrescine through the ADC pathway yielded 1.3 $\pm$ 0.5 mM putrescine, which was achieved through plasmid-based overexpression of the genes *adiA* (encoding an arginine decarboxylase in *E. coli*) and *speB* in an arginine overproducing strain ARG1[33]. The strain ARG1 has a deletion of *argR*, and plasmid-based overexpression of the *argB* gene which was desensitized for feedback inhibition of arginine[38]. The ODC pathway engineering of PUT1 resulted in a 40-fold higher putrescine yield than the ADC pathway engineered ARG1 with overexpressed *adiA* and *speB*, where the highest putrescine titer of 6 gL^{-1} with a productivity of 0.1 $gL^{-1}h^{-1}$ were reached of PUT1 in shake-flask batch cultivation with glucose as carbon source. However, the supplementation of arginine was needed for growth. As the deletion of the *argF* gene lead to an arginine auxotrophy in PUT1, Schneider et al. developed a plasmid-based low-level *argF* expression and introduced the *speC* gene in this plasmid for stable production of putrescine without supplementation of arginine, which resulted in constructing of the strain PUT21. This strain produced putrescine titers up to 19 gL^{-1} with a productivity of 0.55 $gL^{-1}h^{-1}$ in fed-batch cultivation with glucose as carbon source[39]. Additionally, Nguyen et al. presented that deletion of a gene encoding a polyamine N-acetyltransferase (SnaA) increased the putrescine titers of PUT21 with 41%[40].

Moreover, Thongbhubate et al. have reported that the plasmid-based expression of the *speAB* genes from the ADC pathway produced more extracellular putrescine than plasmids containing *speC* or *speABC* in *E. coli* K-12[41]. Furthermore, they desensitized the feedback inhibition of ArgA by substituting a Tyr residue of the *argA* gene with Cys, creating the gene $argA^{ATG\ Y19C}$, to improve the putrescine titers through the plasmid-based expression of the constructed gene. In this gene, they changed the initiation

codon from GTG to the more active ATG, however, this did not impact the putrescine production. Moreover, they introduced the ADC pathway genes *speAB* into the *argA*$^{\text{ATG Y19C}}$ plasmid and used a strong T5 promoter for overexpression of the three genes. Disruption of putrescine catabolic pathways through deletion of *puuPA* (codes for Puu putrescine utilization pathway), and use of terrific broth which utilizes glycerol and higher yeast content for higher growth compared to LB media with glucose was also done. The deletion of *speH* (codes for putrescine utilization through spermidine synthesis), *speG* (codes for possible putrescine acetylation), and *potE* (codes for a transporter for putrescine uptake) was also done to prevent the possible loss of putrescine. The combination of genetic engineering described above resulted in an extracellular putrescine concentration of 19.8 mM in shake-flask batch cultivation[41].

Increased arginine biosynthesis through genetic engineering has shown to be beneficial for putrescine production. The aforementioned genetic engineering strategies for higher arginine availability concerned deletion of the *argR* gene and desensitizing the feedback inhibition of the *argA* and *argB* genes for *E. coli* and *C. glutamicum*, respectively. However, the *argGH* operon has been reported to be the rate-controlling step in arginine biosynthesis of *E. coli* and *C. glutamicum*[42]. Park et al. showed that the ArgGH activity increased by replacing the native promoter with a stronger one in *C. glutamicum*, and in combination with other metabolic engineering strategies concerning the removal of regulatory repressors as aforementioned, optimization of NADPH level, and disruption of an l-glutamate exporter to increase l-arginine precursors, resulted in high arginine titers of 92.5 gL^{-1} in 5 L fed-batch glucose fermentation[42].

1.4.2 Spermidine

Spermidine is widespread in living organisms, including microorganisms, plants, and animals at significantly different levels. It exhibits important biological activities, within DNA replication, transcription, translation, inducing autophagy, and regulation of cell growth and death[43]. As the cost of purification, and harsh reaction conditions of chemical synthesis are a disadvantage in spermidine production, the development of sustainable bioprocessing is gaining interest[26].

In bacteria, spermidine derives from putrescine and is produced through the donation of the aminopropyl group of S-adenosyl-methioninamine (dAdoMet) to putrescine, mediated by spermidine synthase (SpeE) (Figure 1.3). dAdoMet production is mediated by S-adenosylmethionine decarboxylase (SpeH) through decarboxylation of S-adenosyl-l-methionine (AdoMet). Both SpeE and SpeH are essential in the spermidine biosynthesis (SBS) pathway. AdoMet has a carbon skeleton derived from oxaloacetate, which is produced in the TCA cycle, in a series of enzymatic reactions, where l-aspartate and l-methionine are intermediates in the production of AdoMet (Figure 1.2)[26].

In recent years, the overproduction of spermidine has been attempted in microorganisms such as *Saccharomyces cerevisiae* and *Bacillus amyloliquefaciens*[43,44,45]. In *S. cerevisiae*, Kim et al. achieved production of 224 mgL^{-1} spermidine in fed-batch cultivation, through overexpression of a polyamine transporter, optimization of the cultivation media (pH, aeration, etc.), and the use of xylose as one of the carbon sources to overcome the glucose repression on spermidine production[43]. Moreover, Qin et al. achieved titers up to 2.3 gL^{-1} of spermidine in a glucose-limited fed-batch fermentation with a well-designed engineered *S. cerevisiae*, through overexpression of genes encoding the ODC and SBS pathways which increases access to putrescine and the co-factor dAdoMet, respectively, and through downregulation of spermidine utilizing pathways in *S. cerevisiae*[44]. Zou et al. genetically engineered *B. amyloliquefaciens*

to produce 227.4 mgL^{-1} spermidine titers, through heterologous expression of *speH* from *E. coli* and *speE* from *S. cerevisiae* in addition to an optimized fermentation medium consisting of xylose as a carbon source in batch cultivation. These current fermentation titers are relatively low and do not fulfill the commercial demand. Therefore, it is necessary to find microorganisms with high spermidine synthesis ability[26].

The spermidine concentration in the cell also depends on uptake, degradation, and secretion, in addition to biosynthesis. Uptake of spermidine is mediated by PotABCD in bacteria such as *E. coli*, which also facilitates the low-affinity uptake of putrescine[36]. Presently, information about the spermidine secretion system is limited. A secretion protein found in *E. coli* is denoted as MdtJI, and belongs to a small multidrug resistance family[46]. Spermidine is secreted when it is accumulated beyond the toxicity limits of the cell[46]. Moreover, Potter and Paton hypothesized that the PotD importer protein in *Synechocystis* also exhibits excretion abilities based on their data. Spermidine is also degraded through the biosynthesis of 1,3-diaminopropane, however, this pathway is only native in a few organisms including *Pseudomonas* and *Acinetobacter* species[29]. Furthermore, Wang et al. suggest that the lack of dAdoMet is a limitation for spermidine production and therefore also 1,3-diaminopropane production[29]. Additionally, according to a report from Zou et al., it has been found that the catalytic step performed by SpeE is the rate-limiting step in the biosynthesis of spermidine[45].

1.4.3 Renewable feedstocks for diamine production

Great efforts have been done to enable the bio-based production of diamines through the utilization of renewable feedstocks[30]. C1 substrates such as methanol, wood/plant-derived matter, side streams from industrial processes, and marine resources are attracting attention for this purpose[30]. The production of diamines, such as cadaverine and putrescine, has been developed through the utilization of green feedstocks especially in *C. glutamicum*[30].

Both native and non-native green carbon sources have been explored for multiple organisms. The non-native carbon source starch, a polysaccharide with glucose monomers has been utilized in cell factories like *C. glutamicum*, through the heterologous expression of amylases for the degradation of starch to glucose. Starch is considered more environmentally green than glucose as it is extracted from agricultural raw materials[30]. Moreover, xylose, arabinose, and glycerol derived from varied waste sources have also been utilized as feedstock for *C. glutamicum* for the production of cadaverine and putrescine[30]. However, the titers produced are not competitive with conventional glucose-based fermentations, which is a consequence of utilizing non-native carbon sources[30].

The bio-based production of cadaverine has been developed in *B. methanolicus* through the utilization of the native carbon source methanol[25]. The cadaverine titers of 17.5 gL^{-1} in strain MGA3 (pBV2mp-*cadA*) cultivated in fed-batch fermentation were severely lower than for glucose-based fed-batch production of cadaverine through conventionally used *C. glutamicum* (103.8 gL^{-1}), however higher than *E. coli* (12.6 gL^{-1})[20,48,49]. These findings show that utilization of methanol as a feedstock and implementing optimized genetic engineering of *B. methanolicus* MGA3 can result in potentially competitive titers of diamines such as putrescine and spermidine, compared to conventionally used glucose-fermentations with *E. coli* or *C. glutamicum*.

1.5 Objectives

Presently, the demand for sustainable production of value-added compounds is increasing. Production through microbial fermentation with renewable carbon sources has therefore drawn attention both in research and the industry. Methanol-based production of diamines through fermentations with the well-studied methylotrophic *B. methanolicus* is, therefore, a promising candidate for the sustainable production of diamines, such as cadaverine, putrescine, and spermidine. The overproduction of cadaverine is already established in *B. methanolicus* MGA3, however to this date, the overproduction of putrescine and spermidine in *B. methanolicus* MGA3 is not reported[25]. Therefore, the goal of this study is to achieve the methanol-based production of putrescine and spermidine through genetic engineering of *B. methanolicus* MGA3. For the overproduction of putrescine, the heterologous and homologous expression of the ADC pathway genes has been the focus of this study. Even though the ODC pathway has shown to be the most promising for overproduction of putrescine in both *E. coli* and *C. glutamicum*, *B. methanolicus* natively harbor the genes encoding the ADC pathway, but not the ODC pathway. Moreover, Thongbhubate et al. also implied that the ADC pathway produced more extracellular putrescine than the ODC pathway in *E. coli*, which is beneficial for high putrescine titers. Spermidine synthesis is also native in *B. methanolicus* MGA3, where the overexpression of the ADC pathway in addition to the overexpression of the SBS pathway genes is here hypothesized to result in the overproduction of spermidine. The main goal of this study will be reached by fulfilling the following objectives:

- Analysis of the expression host *B. methanolicus* MGA3 as a suitable putrescine and spermidine producer.
- Construction of *B. methanolicus* heterologously and homologously expressing the ADC pathway genes *speA* and *speB*, and the SBS pathway genes *speE*, and/or *speH*.
- Increased putrescine and spermidine production in genetically engineered *B. methanolicus* strains.
- Optimization of growth conditions for putrescine production in genetically engineered *B. methanolicus* strains.

2 Materials and methods

In this section, a comprehensive description of the experimental design, strain engineering, cultivation conditions, data collection, and analysis techniques employed in this study will be presented.

2.1 Media and solutions

The media and solutions used in this study are listed in Appendix A. All chemicals utilized in this study were purchased from Sigma-Aldrich® unless otherwise stated in the text.

2.2 Biological material

A list of bacterial strains obtained elsewhere and created for use in this study is presented in Table 2.1. *E. coli* DH5α was used as a cloning host for plasmid construction, and *B. methanolicus* MGA3 was used as the expression host. Genomic DNA (gDNA) (Section 2.4.1) from *B. methanolicus* MGA3 and *E. coli* K-12 MG1655 was used as a template for molecular cloning. A list of plasmids used and created in this study is shown in Table 2.2. Primers used for plasmid construction are highlighted in Table B.1.

Table 2.1: Characteristics of bacterial strains used for cloning and expression in this study, and recombinant bacterial strains used in this study.

Abbreviation	Strain	Characteristics	Reference
	Escherichia coli DH5α	Cloning host*	StrataGene
	Escherichia coli K-12 MG1655	Wild type strain	DSM 18039[50]
MGA3	*Bacillus methanolicus* MGA3	Wild type strain	ATCC 53907[17]
PBV	*B. methanolicus* MGA3(pBV2xp)	Kan^R	Donated by Luciana F. Brito
PUT^{Ec}	*B. methanolicus* MGA3(pBV2xp-$speAB^{Ec}$)	Kan^R	Donated by Luciana F. Brito
PUT^{Bm}	*B. mehtanolicus* MGA3(pBV2xp-$speAB^{Bm}$)	Kan^R	Donated by Luciana F. Brito
PTH	*B. methanolicus* MGA3(pTH1mp)	Cm^R	Donated by Luciana F. Brito
SPE^{Bm}	*B. methanolicus* MGA3(pTH1mp-$speE^{Bm}$)	Cm^R	This study
SPE_{ii}^{Ec}	*B. methanolicus* MGA3(pTH1mp-$speEH^{Ec}$)	Cm^R	This study
SPE_{ii}^{Bm}	*B. methanolicus* MGA3(pTH1mp-$speEH^{Bm}$)	Cm^R	This study
PBV PTH	*B. methanolicus* MGA3(pBV2xp)(pTH1mp)	Kan^R, Cm^R	Donated by Luciana F. Brito
$PUT^{Ec}PTH$	*B. methanolicus* MGA3(pBV2xp-$speAB^{Ec}$)(pTH1mp)	Kan^R, Cm^R	This study
$PUT^{Ec}SPE^{Bm}$	*B. methanolicus* MGA3(pBV2xp-$speAB^{Ec}$)(pTH1mp-$speE^{Bm}$)	Kan^R, Cm^R	This study
$PUT^{Ec}SPE_{ii}^{Ec}$	*B. methanolicus* MGA3(pBV2xp-$speAB^{Ec}$)(pTH1mp-$speEH^{Ec}$)	Kan^R, Cm^R	This study
$PUT^{Ec}SPE_{ii}^{Bm}$	*B. methanolicus* MGA3(pBV2xp-$speAB^{Ec}$)(pTH1mp-$speEH^{Bm}$)	Kan^R, Cm^R	This study
	E. coli DH5α(pTH1mp-$speE^{Ec}$)**	Cm^R	This study
	E. coli DH5α(pTH1mp-$speE^{Bm}$)	Cm^R	This study

Kan^R: kanamycin resistant. Cm^R: chloramphenicol resistant.
**fhuA2 lac(del)U169 phoA glnV44 ϕ80' lacZ(del)M15 gyrA96 recA1 relA1 endA1 thi-1 hsdR17.*
** Attempted to be created.

Table 2.2: Characteristics of plasmids used in this study.

Plasmid	Characteristics	Reference
pBV2xp	Kan^R, theta-replicating, induced gene expression controlled by xylose promoter (from *B. megaterium*). Derived from pHCMC04. Low copy number*: 3 ± 1	Drejer et al.[4]
pBV2xp-*speAB*^{Ec}	Kan^R, expression of *speAB* from *E. coli* under the control of a xylose promoter.	Donated by Luciana F. Brito
pBV2xp-*speAB*^{Bm}	Kan^R, expression of *speAB* from *B. methanolicus* under the control of a xylose promoter.	Donated by Luciana F. Brito
pTH1mp	Cm^R, rolling circle-replicating, constitutive gene expression controlled by *mdh* promoter (from *B. methanolicus*). Derived from pTH1mp-*lysC* where *lysC* was replaced with multiple cloning sites. Low copy number: 5 ± 1	Irla et al.[20]
pTH1mp-*speE*^{Ec**}	Cm^R, expression of *speE* from *E. coli* under the control of a *mdh* promoter.	This study
pTH1mp-*speE*^{Bm}	Cm^R, expression of *speE* from *B. methanolicus* under the control of a *mdh* promoter.	This study
pTH1mp-*speEH*^{Ec}	Cm^R, expression of *speE* and *speH* from *E. coli* under the control of a *mdh* promoter.	Donated by Luciana F. Brito
pTH1mp-*speEH*^{Bm}	Cm^R, expression of *speE* and *speH* from *B. methanolicus* under the control of a *mdh* promoter.	Donated by Luciana F. Brito

Kan^R: kanamycin resistant. Cm^R: chloramphenicol resistant. *mdh:* methanol dehydrogenase. *Copy number derived from parental plasmids. ** Attempted to be created

2.3 Cultivation

Media and solutions used for the cultivation of the different strains were prepared according to the recipes shown in Table A.1 and A.2, respectively. Cultivation for preparing chemically competent *E. coli* DH5α cells were done in Psi media at 37 °C and 225 rpm. All cultivations of *E. coli* recombinant strains were performed in LB media at 37 °C and 225 rpm in a Multitron shaker incubator (INFORS HT). All cultivation of *B. methanolicus* MGA3 was performed at 50 °C and 200 rpm in a New Brunswick™ Innovae 42R shaker incubator (Eppendrof). Selective antibiotics with concentrations shown in Table 2.3 were added to the liquid media before inoculating the respective bacterial strains. SOB and LB agar plates were prepared with appropriate antibiotics (Table 2.3) and their preparation details are further described in Appendix A. All SOB and LB agar plates were prewarmed at 50 °C and 37 °C, respectively, before plating out their respective strains.

On the preceding day, prior to conducting the growth experiments with *B. methanolicus* MGA3 strains, several pre-cultures were prepared to improve the likelihood of obtaining properly grown pre-cultures that were neither overgrown nor undergrown. These pre-cultures were subsequently used for reinoculation in the main culture. The pre-cultures were prepared in the morning and in the afternoon, by inoculating

from bacterial glycerol stocks to 25 or 40 mL of pre-warmed MVcMY media in 250 mL Erlenmeyer flasks (shake-flasks), and 100 mL of the same medium in 500 mL flasks. In addition, not pre-warmed pre-cultures were prepared. The pre-cultures with an optical density at 600 nm (OD_{600}) between 1 and 5 in the next morning were selected for inoculation of main cultures with an initial OD_{600} around 0.2. The main cultures were either prepared with 40 mL pre-warmed MVcM minimal media in 250 mL flasks, or in Deutz-plates with 2.5 mL pre-warmed minimal (MVcM, MVcM2, or CGXII) or rich (SOB) media depending on the executed experiment, which will be specified in the following sections. Before inoculation of main cultures, the pre-cultures were centrifugation at 7,830 rpm and 40 °C for five minutes, the supernatant was discarded, and cells were resuspended and washed once with the respective buffer of the main culture. All centrifugation was performed in the Eppendorf 5430R centrifuge (Eppendorf) if not stated otherwise.

Table 2.3: Concentration of antibiotics used for selection of recombinant bacterial clones.

Antibiotic	*E. coli*	*B. methanolicus*
Kanamycin	50 µg mL^{-1}	25 µg mL^{-1}
Chloramphenicol	15 µg mL^{-1}	5 µg mL^{-1}

For all growth experiments, growth was monitored by measuring OD_{600} every 2 hours until the cells reached the stationary phase. For strains harboring plasmid with a xylose inducible promoter, cultures were induced with xylose after doubling of initial OD_{600}, usually after 2 hours. Xylose concentrations and induction time differed in the executed experiments, which will be specified in the following sections. OD_{600} measurements were also performed after 24 hours and/or 48 hours. The growth rate was calculated based on an exponential fitted trend line, which was chosen from the data point at the exponential phase of growth. Final biomass was determined by subtracting the initial OD_{600} from the highest OD_{600} value recorded before the stationary phase of the cultures. Examples of both calculations are presented in Appendix D.

2.4 Molecular cloning

Molecular cloning is a combination of different techniques to isolate, amplify and purify a specific fragment of DNA into a cloning host organism for the purpose of producing multiple copies. It is an efficient technique that allows the construction of recombinant DNA, for desired applications in an expression host[51]. This section describes molecular cloning techniques performed in this study.

2.4.1 Isolation of genomic and plasmid DNA

To obtain a genetic template for polymerase chain reaction (PCR), gDNA isolation was performed. Bacteria were cultured overnight in LB (rich) media, followed by centrifugation at 3,000 rpm and 25 °C for one minute to harvest the cells. The Monarch® Genomic DNA Purification Kit (New England Biolabs, NEB) protocol for cells was employed for gDNA isolation, utilizing the solutions provided by the kit. To begin, proteinase K (Proteinase K, 10 µL) was added to the cell suspension to digest proteins and inactivate nucleases. Subsequently, a cell lysis buffer (Tissue Lysis Buffer, 100µL) was added. The mix was vortexed thoroughly and incubated at 56 ° C for 1-4 hours to complete cell lysis. All incubation

steps were carried out in a miniSpin® centrifuge (Eppendorf), at 13,400 rpm. Thereafter, ribonuclease (RNase A, 3 µL) was added as a catalyst to degrade the RNA, and incubated for 5 minutes at 56 °C. The addition of gDNA Binding Buffer (400µL), followed by pulse-vortexing of the mix, and transfer to a gDNA Purification Column pre-inserted into a collection tube facilitated the release and binding of gDNA after centrifugation. Thereafter, gDNA was washed twice and purified by a gDNA wash buffer in the same gDNA purification column inserted into a new Eppendorf tube and eluted in 35-100 µL of pre-heated (50 °C) gDNA elution buffer. Preheating the gDNA elution buffer was done to enhance the yield of gDNA.

Plasmid DNA was isolated for the purpose of further linearization, for performing transformations in the expression host, and as templates for sequencing analysis. The plasmids were isolated from the general cloning host, *E. coli* DH5α, by first cultivating DH5α strains as described in Section 2.3. The cells were then harvested by centrifuging 5 mL of the bacterial culture in a falcon tube at 7,830 rpm, at 22 °C for 5 minutes. The plasmids were isolated using the ZR® Plasmid Miniprep kit (Zymo Research, ZR), following the manufacturer's instructions. All centrifugation steps were performed using miniSpin® from Eppendorf, at 13,400 rpm. The cells were resuspended with a resuspension buffer (P1, 200 µL), lysed by the means of a cell lysis buffer (P2, 200 µL), and then neutralized by an alkaline protease buffer (P3, 400 µL) in Eppendorf tubes. After centrifugation, the supernatant from that mixture was then transferred to a Zymo-Spin™ IIN column in a collection tube, where the plasmid DNA was bound to the column. Plasmid DNA was washed with column wash buffer and eluted to an Eppendorf tube with 50 µL of MilliQ H_2O.

The concentration of both gDNA and plasmid DNA was measured on NanoDrop™ One (Thermo Scoentific™) using elution solution (MilliQ H_2O) as blank, and stored at either 4 °C or -20 °C, before further use in molecular cloning.

2.4.2 Plasmid restriction

For the purpose of assembling novel plasmids, linearization of parental plasmids occurred by digestion with restriction enzymes. The reaction mixture for PciI (New England Biolabs, NEB) restriction of the plasmid pTH1mp, shown in Table 2.4, was incubated for two hours at 37 °C. Linearization of plasmid was verified by agarose gel electrophoresis, described in Section 2.4.4.

Table 2.4: Reaction mixture for restriction of the plasmid pTH1mp.

Component	Volume (µL)	Amount (µg)
3.1 Buffer (NEB)	10	
Plasmid DNA		2
Restriction enzyme *Pci*I (NEB)	2	
MilliQ H_2O, to	100	

2.4.3 Polymerase chain reaction for amplification of DNA fragments

The purpose of PCR is to amplify specific DNA fragments *in vitro* from a gDNA template (Section 2.4.1). The PCR procedure involves three steps, which are repeated in multiple cycles. The first step is denaturation where gDNA is heated to allow untwirling of the DNA. In the second step, the single-stranded

DNAs are base-paired with an excess of synthetic primers by annealing. These primers are designed to include an overlapping region with the respective vector, and the annealing temperature is decided based on the characteristics of the primers. The final step is the extension, where DNA polymerase is used to replicate the DNA segment using the denatured DNA as a template and deoxynucleotide triphosphates (dNTPs, NEB)[52].

PCR was performed using Takara CloneAmp^{TM} Hifi PCR Premix protocol, following the conditions described in Table 2.5. All PCR programs were executed in a Mastercycler Nexus X2 (Eppendorf).

Table 2.5: Takara CloneAmp^{TM} reaction mixture and PCR conditions.

Reaction mixture			
Component		**Volume (µL)**	**Amount (ng)**
Takara CloneAmp^{TM} Hifi PCR Premix		12.5	
Forward primer		0.5	
Reverse primer		0.5	
DNA Template			90
MilliQ H_2O, to		25	
PCR program conditions			
Step	**Temperature (°C)**	**Time (s)**	**Number of cycles**
Denaturation	98	10	35
Annealing	55	15	35
Extension	72	5/kb	35
Storage	4	Infinite	1

In all PCR procedures, generated products were analyzed by agarose gel electrophoresis, described in Section 2.4.4.

2.4.4 Agarose gel electrophoresis

Agarose gel electrophoresis was used as a separation and visualization tool for DNA fragments derived from PCR products and linearized vectors. DNA samples were mixed with loading dye from Thermo Scientific^{TM} and loaded into a casted agarose gel with an appropriate number of wells, which was placed in a gel electrophoresis tank submerged with Tris-acetate-EDTA (TAE) buffer. The loading dye and DNA sample ratio were 1:6. For visualization and confirmation of DNA segments, a premade GelRed 0.8% (w/v) agarose gel in TAE buffer was used. Generuler 1 kb plus DNA ladder from Thermo Scientific^{TM} was used as a DNA marker. After loading all samples, a lid was placed which was connected to a power supply (PowerPac^{TM} Basic Power Supply, Bio-Rad). The electrophoresis tank harbors negative and positive electrodes on opposite sides which were connected to the lid. An electric current ran through the gel from the wells at the cathode to the anode. DNA fragments migrate towards the positive anode, as DNA has a net negative charge. The DNA fragments in one sample would therefore separate by size, with the smallest segments migrating furthest. The gel electrophoresis was executed at 100 V for 35 minutes, and visualized in UV-light by ChemiDoc XRS+ Gel Imaging System (BioRad). After confirmation of the correct band size, both PCR products and linearized vectors were purified following procedures described in Section 2.4.5.

2.4.5 Purification of DNA fragments

Purification of PCR products and linearized plasmid DNA was performed to remove impurities from the desired DNA products for further usage in molecular cloning. The DNA products were purified following QIAquick® PCR Purification Kit (QIAGEN). All solutions required were provided by the kit. All centrifugation steps were carried out in a miniSpin® centrifuge from Eppendorf, at 13,400 rpm.

The DNA products were mixed with a 5-times excess DNA binding buffer (Buffer PB) and transferred to the QIAquick column in a collection tube, which was further centrifuged to bind the DNA with the column. Subsequently, it was washed with a DNA washing buffer (Buffer PE) and eluted with 30 µL MilliQ H_2O. The concentration of all products was measured and stored as previously described (Section 2.4.1).

2.4.6 Gibson assembly for construction of expression vectors

Gibson assembly was used to join the overlapping ends belonging to PCR products and linearized plasmid[53]. The mix employs three enzymatic activities, a 5' exonuclease, the 3' extension activity of a DNA polymerase, and a DNA ligase activity. The 5' exonuclease activity creates single-stranded DNA with 3' overhangs of each fragment. These complementary sequences are then annealed. DNA polymerase extends the 3'ends to fill in the gap, and DNA ligase seals the remaining nicks. This results in an assembled DNA construct that can serve as a template for direct transformation[53].

The linearized vector and DNA insert (PCR product) were mixed with a premade Gibson assembly mix (NEB), routinely stored at -20 °C as 15 µL aliquots in PCR tubes(Table 2.6). The mixture (Table 2.7) was then incubated at 50 °C for one hour in a Mastercylcer Nexus X2 (Eppendorf). The equation used for the calculation of insert volume is shown in Equation 2.1, and it is based on the concentration and size of the DNA fragments. The size of the insert and vector refers to the length of the fragments in base pairs (bp).

Table 2.6: Composition of premade Gibson assembly mix.

Premade Gibson assembly mix Compound	Volume (µL)
Isothermal reaction buffer (IRB)	211.2
T5 Exonuclease (NEB; 10 U μL^{-1})	0.4
Phusion® High-Fidelity DNA Polymerase (NEB; 2 U μL^{-1})	13.2
Taq DNA Ligase (NEB; 40 U μL^{-1})	105.6
MilliQ H_2O	462.0
IRB **Compound**	**Volume (µL)**
2 M Tris-HCl	50
2 M $MgCl_2$	5
1 M Dithiothreitol (DTT)	10
100 mM NAD	10
10 mM dNTPs (NEB)	20
50% polyethylene glycol (PEG)-8000	100
MilliQ H_2O, to	1000

Table 2.7: Components in the Gibson assembly mix for plasmid construction.

Compound	Volume (µL)	Amount (ng)
Premade Gibson assembly mix	15	
Linearized vector		100
Insert		Insert quantity (Equation 2.1)
MilliQ H_2O, to	20	

$$\text{Insert quantity (ng)} = \text{Vector quantity (ng)} \cdot \frac{\text{Insert size (bp)}}{\text{Vector size (bp)}} \tag{2.1}$$

2.4.7 Preparation of chemically competent *E. coli* DH5α cells

The competence of a cell is referred to the cell's ability to bind, process, and take up foreign DNA introduced to the cell. To produce chemically competent *E. coli* DH5α cells, pre-cultures were first prepared in a 125 mL flask with 10 mL of Psi media and cultivated overnight according to Section 2.3. On the preceding day, 2 mL of the pre-culture was reinoculated in 200 mL Psi media, and cultivated at 37 ° C until OD_{600} reached 0.40-0.43. The cells were incubated on ice for 15 minutes and subsequently transferred to falcon tubes (2x 50 mL) for centrifugation at 4 ° C and 4,000 rpm for 5 minutes. The supernatant was discarded, and the cell pellet was resuspended carefully in 40 mL TFB1 for each container. The cells were then incubated for 5 minutes on ice, centrifuged at 4 °C, and 4,000 from for 5 minutes. Subsequently, the supernatant was discarded, the cell pellet was resuspended carefully in 6 mL of TFB2, and aliquoted in Eppendorf tubes of 100 µL. The tubes were then stored at -80 °C freezer (New Brunswick™ Innova C760 Ultra-Low temperature freezer, Eppendorf).

2.4.8 Transformation of chemically competent *E. coli* DH5α cells by heat-shock

After constructing a recombinant plasmid *in vitro* (Section 2.4.6), it was subsequently transferred to a chemically competent cloning host for replication *in vivo* (Section 2.4.7). The transformation was performed using heat shock, in which the cells undergo alternating cooling and heating cycles. This enhances the permeability of the cell membrane, facilitating the entry of plasmid DNA from the surrounding media into the cell[51].

An aliquot of 100 µL of competent cells in an Eppendorf tube was thawed on ice and mixed with 10 µL of Gibson assembly mix, followed by incubation of 30 minutes on ice, 45 seconds of heat-shock at 42 °C, and incubation of 90 seconds on ice. Next, 900 µL of LB-medium was added, the mixture was incubated for 45 minutes at 37 °C, and then centrifuged in a miniSpin® at 13,400 rpm for 3 minutes. The supernatant was discarded, the cell pellet was resuspended in the supernatant residue, and plated out on LB plates with appropriate antibiotics (Table 2.3). The plates were incubated at 37 ° until colonies were visible.

2.4.9 Colony PCR screening

Colony PCR was used as a screening tool to verify desired genetic constructs in *E. coli* DH5α clones, and was performed using GoTaq® PCR amplification protocol (Promega), following the procedure in Table 2.8. Primers used for the respective colony PCRs are indicated in Table B.1. The colony PCR master mix was prepared and aliquoted into PCR tubes with 10 µL. Single colonies that served as DNA templates were transferred to the aliquoted colony PCR master mix with a sterile pipette tip, after being stroked on a replica plate with selective antibiotics (Table 2.3). As a control, an empty vector also served as a DNA template. The PCR program was executed as described in Section 2.4.3. The replica plate was incubated overnight at 37 °C.

Table 2.8: GoTaq® PCR mix composition and PCR conditions.

Reaction mix			
Component	**Volume (µL)**		**Amount**
5X GoTaq® Buffer (Promega)	2.0		
10 mM dNTPs (NEB)	0.2		
10 mM forward primer	0.2		
10 mM reverse primer	0.2		
DNA Template	1	or	1 colony
GoTaq® DNA polymerase (5 U μL^{-1}) (Promega)	0.05		
MilliQ H_2O	7.35		

PCR program conditions			
Step	**Temperature (°C)**	**Time (min)**	**Number of cycles**
Initial Denaturation	95	10	1
Denaturation	95	1	35
Annealing	52	1	35
Extension	72	1/kb	35
Final extension	72	5	1
Storage	4	infinite	1

In all PCR procedures, generated products were analyzed by agarose gel electrophoresis, described in Section 2.4.4.

2.4.10 Sequencing

Sequencing was used to confirm the newly constructed plasmids. Isolated plasmid DNA (Section 2.4.1) from cloning hosts were sequenced, following requirements from Eurofins Genomics LightRun tubes sequencing services. Five µL of primer with a concentration of 5 µM was mixed with 5 µL of purified template DNA with a concentration of 50-100 ng μL^{-1} purified plasmid DNA. The sequencing results were compared with the template sequence *in silico* in Clone Manager V9 (Bioinformatics tool, Scientific & Educational Software) or in Benchling with the multi-alignment tool.

2.5 Construction of recombinant *B. methanolicus* strains

Constructed plasmid DNA was transformed into competent *B. methanolicus* cells. Foreign DNA can be introduced to *B. methanolicus* through electroporation, where an electric pulse is transmitted through the cells, which creates a temporary permeable cell membrane that makes the permeation of foreign DNA possible.

2.5.1 Preparation of electrocompetent *B. methanolicus* cells

Electrocompetent cells were prepared by first inoculating cells from *B. methanolicus* glycerol stock into 25 mL of pre-warmed SOB medium in a 250 mL shake-flask, and cultivated overnight at 50 °C and 200 rpm. Required antibiotics were used in all cultivations if needed (Table 2.3). The pre-culture was reinoculated to OD_{600} 0.1-0.2 in a second pre-culture of 50 mL pre-warmed SOB medium in a 500 mL shake-flask and continued to grow at 50 °C for approximately 4 hours. Main cultures consisting of 4 100 mL of pre-warmed SOB in 500 mL shake-flasks were prepared, inoculated to an initial OD_{600} of 0.05, and cultivated at 50 °C until reaching an OD_{600} of 0.25. The cell cultures were transferred to 50 mL falcon tubes (8 in total) and centrifuged for 5 minutes at 7,830 rpm and 25 °C. The supernatant was subsequently discarded, and cells were resuspended with 4.5 mL electroporation buffer (EPB) in each tube. Two cultures were combined into a total of 4 tubes and centrifuged for 5 minutes at 7,830 rpm and 25 °C. The supernatant was then discarded and 9 mL EPB was used to resuspend the cells by mixing gently. A final centrifugation of 10 minutes at 7,830 rpm and 25 °C was done, following the discarding of supernatant, and resuspension with left-over EPB. The cell suspension was aliquoted into sterile Eppendorf tubes with 100 µL. Electrocompetent cells were stored at -80 °C before use for transformation through electroporation (Section 2.5.2).

2.5.2 Transformation of competent *B. methanolicus* cells

Eppendorf tubes containing aliquots of 100 µL electrocompetent cells were thawed on ice for 10 minutes, and mixed with 0.5-1 µg plasmid DNA. An empty electroporation cuvette (0.2 cm) (VMR®) was pre-cooled in ice and the electrocompetent cells and DNA mixture was transferred into it, the cuvette was then incubated in ice for 30 min. Electroporation occurred by the following these conditions; 200 Ω, 25 µF, and 2.5 kV, in a GenePulser Xcell^{TM} (Bio-Rad) electroporator with time constant 4.5-5.5. After electroporation, 1 mL from a 25 mL shake-flask with 12.5 mL pre-warmed SOB was carefully transferred to the cuvette, mixed, transferred back to the flask, and incubated at 50°C and 200 rpm for 6 hours. Subsequently, cells were centrifuged at 25 °C and 7,830 rpm for 5 minutes, the supernatant was discarded, and the cell pellet was resuspended in the residue SOB. The resuspended cells were plated out on pre-warmed SOB plates supplemented with suitable antibiotics (Table 2.3), and incubated at 50 ° overnight or until colonies were visible. Fresh colonies from the plate were inoculated in 25 µL of MVcMY medium with appropriate antibiotics, and cultivated overnight. Glycerol stocks were prepared when the OD_{600} reached values between 2.0 and 2.5 (Section 2.6).

2.6 Storage of bacterial strains

To store and preserve the bacterial strains used in this study, glycerol stocks were prepared. For the preparation of *E. coli* glycerol stocks, colonies were cultivated in 5 mL of LB and grown to OD_{600} ~1.5. Subsequently, 650 µL of cell culture were mixed with 350 µL 87 % glycerol. For the preparation of *B. methanolicus* glycerol stocks, colonies were cultivated as mentioned in Section 2.5.2. Ninemilliliter cell culture was mixed with 3 mL of 87% glycerol in a 50 mL falcon tube. All the glycerol mixtures were aliquoted as 1 mL in Nunc® CryoTubes® (Merck), and stored at -80 °C in New Brunswick™ Innova C760 Ultra-Low temperature freezer (Eppendorf) in 1 mL aliquots.

2.7 Growth experiments with *B. methanolicus* strains

Bacterial strains presented in Table 2.1 were used for multiple growth experiments in this study. Firstly, growth experiments were done to assess the suitability of MGA3 as a host for putrescine and spermidine production. Optimization of putative putrescine production in *B. methanolicus*) overproducing strains (PUT^{Ec} and PUT^{Bm}) was first done by performing growth experiments with variating xylose induction. Furthermore, optimization of growth media towards enhanced putrescine production was done through cultivation of PUT^{Ec} with supplementation of putrescine pathway precursors. Growth in media containing different amounts of nitrogen was also analyzed. Lastly, growth experiments with putative spermidine overproducing strains derived from MGA3 and PUT^{Ec} parental strains were done with the optimized induction level proven from the previous induction level experiment. The optimized conditions were based on results from the quantification of putrescine and spermidine by HPLC (Section 2.8).

2.7.1 Suitability of *B. methanolicus* MGA3 as host for putrescine and spermidine production

To assess the feasibility of MGA3 as a host for putrescine and spermidine production, growth experiments were conducted using arginine, putrescine, and spermidine as carbon or nitrogen sources. Additionally, the tolerance of MGA3 towards these compounds was evaluated.

For the overproduction of diamines in microbial fermentations, it is desirable for the host to be unable to utilize the diamines as carbon or nitrogen sources, as the utilization of those products would decrease the final production titers. To evaluate if putrescine and spermidine could be utilized as carbon or nitrogen source, a growth experiment with the WT *B. methanolicus* strain MGA3 was performed in Deutz-plates with MVcM media according to Section 2.3. The medium carbon sources 200 mM methanol and nitrogen source 16 mM ammonium sulfate were replaced with putrescine, spermidine, or arginine at an equimolar concentration (Table 2.9).

Table 2.9: Concentration of carbon and nitrogen sources in MVcM media for cultivation of *B. methanolicus* MGA3.

Nitrogen source	Carbon source
Ammonium sulphate 16 mM	Arginine 50 mM Putrescine 50 mM Spermidine 28.6 mM
Arginine 8 mM Putresine 16 mM Spermidine 10.7 mM	Methanol 200 mM

Putrescine and spermidine have both been reported to be toxic to bacteria[31, 41]. *B. methanolicus* MGA3 has been reported to tolerate at least 100 mM putrescine[54], however, spermidine tolerance has not been assessed for this bacteria. Therefore, a tolerance experiment with cultivation of *B. methanolicus* MGA3 in SOB media supplemented with 0, 0.075, 0.75, 7.5, 15, and 30 mM putrescine, and spermidine separately and together were investigated to assess the potential synergistic effect. Arginine supplementation was also performed as low tolerance toward a precursor could result in low production titers. Main cultures were cultivated in Deutz-plates according to Section 2.3. Arginine and putrescine tolerance were tested in one experiment, while spermidine and the potential synergistic effect of putrescine and spermidine were tested in a second one.

2.7.2 Optimization of gene expression induction levels for putative putrescine overproducing *B. methanolicus* strains, PUT^{Ec} and PUT^{Bm}

In a previous study, it was observed that the expression of the reporter gene from the xylose-inducible promoter of the plasmid pTH1xpx-*gfpuv* exhibited a linear increase with xylose concentrations ranging from 0.01 to 0.1%, reaching a plateau at 0.5%[20]. The putative putrescine overproducing strains, PUT^{Ec} and PUT^{Bm}, harbor the xylose-inducible plasmid pBV2xp-*speAB* with *E. coli* and *B. methanolicus* as gene donors, respectively (see Table 2.1). In this growth experiment, various xylose concentrations (0, 0.01, 0.1, and 1%) were used to induce the plasmid and determine the optimal conditions for putrescine production. The PBV strain was cultivated under the same conditions and served as a empty vector control. The growth experiment was performed in shake flasks with MVcM media and cultivated for 48 hours, as described in Section 2.3. Samples for HPLC analysis (Section 2.8) were taken at 12, 24, and 48 hours of cultivation.

2.7.3 Supplementation of precursors and media selection for optimized putrescine production

For further optimization of putrescine production, a cultivation under media supplementation with putrescine biosynthesis pathway precursors, glutamate, arginine, and ornithine was performed. This way, 1 mM glutamate, arginine, and ornithine were supplemented in MVcM media, for the cultivation of strains PBV and PUT^{Ec} in Deutz-plates according to Section 2.3.

Insufficient nitrogen supply has shown to be a limiting factor for the production of amino acids and their

derivatives in microbial fermentation. Bacteria exhibit distinct degradation pathways for different nitrogen sources, indicating that the optimal nitrogen supply varies among bacterial species[55]. In Masuda et al. both urea and ammonium water were used as nitrogen sources for the production of l-threonine in *Serratia marcescens*, where the optimum nitrogen source was observed to be ammonium water[55]. Therefore, in this study, a growth experiment with PBV and PUT^{Ec} strains cultivated in different media (MVcM, MVcM2, and CGXII) regarding their nitrogen sources was performed for the purpose of enhancing the production of putrescine in those strains. They were cultivated in Deutz-plates according to Section 2.3. The media and their composition are presented in Table 2.10 with the total concentration of nitrogen calculated.

Table 2.10: Composition of media used for the optimization of putrescine production in *B. methanolicus* strains.

Compounds	MVcM	MVcM2	CGXII
K_2HPO_4	4.1 gL^{-1}	4.1 gL^{-1}	1.0 gL^{-1}
$NaH_2PO_4*H_2O$	1.5 gL^{-1}	1.5 gL^{-1}	/
KH_2PO_4	/	/	1.0 gL^{-1}
Urea	/	/	5.0 gL^{-1}
$(NH_4)_2SO_4$	2.1 gL^{-1}	4.2 gL^{-1}	10.0 gL^{-1}
Total Nitrogen (gL^{-1})	**0.2**	**0.4**	**4.4**

After cultivation of 24 hours, HPLC samples were prepared and analyzed, according to Section 2.8, for both experiments.

2.7.4 Production of spermidine in putative spermidine overproducing *B. methanolicus* strains derived from MGA3 and PUT^{Ec} as parental strains

A growth experiment with SPE^{Bm}, $SPE_{ii}{}^{Ec}$, $SPE_{ii}{}^{Bm}$, $PUT^{Ec}SPE^{Bm}$, $PUT^{Ec}SPE_{ii}{}^{Ec}$, and $PUT^{Ec}SPE_{ii}{}^{Bm}$ strains (Table 2.1) were performed in shake flasks, according to Section 2.3. The gene expression in PUT^{Ec}-derived strains was induced with a final concentration of 0.1 % xylose. HPLC samples were taken after 12 and 24 hours and analyzed according to Section 2.8.

2.8 Determination of putrescine and spermidine production in *B. methanolicus* MGA3 strains by high-pressure liquid chromatography

High-pressure liquid chromatography (HPLC) is used as an analytical tool that is able to quantify specific compounds in a solution. The secretion of putrescine, its precursor arginine, and further product spermidine in *B. methanolicus* strains were quantified based on cultivation supernatants. The supernatants were obtained as follows. The cell cultures (1 mL) were collected in an Eppendorf tube, and centrifuged for 15 min at room temperature and 14,000 rpm with Centrifuge 5424 (Eppendorf). Subsequently, the supernatant was transferred to a new Eppendorf tube to be further derivatized by the FMOC method[56]. All chemicals used were of the highest purity available (HPLC-graded) and solutions are presented in Table A.2. All HPLC sample vials were prepared by aliquoting 20 µL of samples (or standards), followed by aliquoting 60 µL sodium borate buffer (pH 9), and vortexing. Subsequently, 80 µL of FMOC solution was aliquoted to the vials, followed by vortexing and incubation of 45 seconds at room temperature. One

hundred microliters of EVA reagent was aliquoted, followed by vortexing and 45 seconds incubation as aforementioned. Finally, 540 µL of dilution buffer was added and the vials were vortexed one final time to complete the volume of the derivatized samples.

Quantification of arginine, putrescine, and spermidine, was carried out on Alliance e2695 XE HPLC System (Waters©) using Waters Symmetry C18 Column (100 Å, 3,5 µm, 4.6 mm x 75 mm) and a 2475 Fluorescence (FLR) detector (Waters©) at excitation 265 nm and emission 315 nm. The column was heated to 40 °C, and the pressure limit was set at 4,000 psi. The sample compounds were separated based on polarity. The mobile phase consists of a gradient of elution buffer (50 mM sodium acetate pH 4.2) and acetonitrile with composition gradient, shown in Table 2.11, at a 1.30 mL/min flow rate. Furthermore, the sample running time was 22 min. Under these chromatographic conditions, arginine, putrescine, and spermidine, in the samples could be separated. The quantification of the metabolites was done by making a linear regression using a standard curve with 0.1 mM, 0.05 mM, 0.025 mM, and 0.0125 mM of those compounds as described in Appendix E.

Table 2.11: Binary gradient in FMOC-based HPLC analysis consisting of eluent A (50 mM sodium acetate pH 4.2) and B (acetonitrile) from 0 to 22 minutes.

Time (min)	%A	%B
0	85	15
1	85	15
2	50	50
14	20	80
15	40	60
22	85.0	15.0

2.9 Software and computer analysis

Software and computer analysis used in this study are presented here. Clone Manager V9 (Bioinformatics tool, Scientific & Educational Software)[57] or Benchling[58] was used for plasmid visualization and interpreting sequencing results. Empower Chromatography Data Systems (Waters™) was used for running, visualizing, and interpreting HPLC analysis. Kyoto Encyclopedia of Genes and Genomes (KEGG) was used as a tool for pathway analysis[34]. Basic Local Alignment Search Tool (BLAST) was used for the alignment of specific genes used for gene expression in this study[59]. Braunschweig enzyme database (BRENDA) was used for screening enzymes of interest to find their kinetic characteristics[60]. Image Lab Software was used for the visualization of agarose gel electrophoresis[61].

3 Results

This section presents achieved results from an assessment of *B. methanolicus* MGA3 as a potential host for putrescine and spermidine overproduction (Section 3.1), including a comprehensive screening of heterologous enzymes for putrescine and spermidine biosynthesis (Section 3.1.1). Thereafter, results from growth experiments and HPLC analysis towards overproduction of putrescine with recombinant *B. methanolicus* strains (Section 3.2) is presented, followed by optimization of cell growth and putrescine production conditions (Section 3.3). Moreover, the construction of pTH1mp-derived plasmids done in this study (Section 3.4), and finally overproduction of spermidine by recombinant *B. methanolicus* strains (Section 3.5) are presented.

3.1 *B. methanolicus* MGA3 is a promising host for putrescine and spermidine overproduction

Genes encoding for putrescine and spermidine biosynthesis via the ADC and SBS pathway, respectively, have been identified through the genome annotation of *B. methanolicus* MGA3[17]. Thus, an assessment with two growth experiments was done to evaluate the suitability of *B. methanolicus* MGA3 as a host for putrescine and spermidine overproduction, in addition to a screening of the enzymes of interest (Section 3.1.1). The first experiment considered whether putrescine and spermidine could be utilized as carbon or nitrogen sources in the WT *B. methanolicus* MGA3 strain (Section 3.1.2), and the second assessed toxicity effects on cell growth of the diamines mentioned above (Section 3.1.3). In both assessments, the precursor arginine was also evaluated.

3.1.1 *B. methanolicus* MGA3 is putatively a suitable host for heterologous expression of the genes encoding arginine decarboxylase, agmatinase, spermidine synthase, and AdoMet decarboxylase

The enzymes of interest in this study, arginine decarboxylase, agmatinase, spermidine synthase, and AdoMet decarboxylase, encoded by *speA* (BMMGA3_05340), *speB* (BMMGA3_16210), *speE* (BMMGA3_16215), and *speH* (BMMGA3_13000), respectively, can be found natively in *B. methanolicus* MGA3[59]. However, little is known about their kinetic characteristic in that organism. A screening search through BRENDA was therefore performed, to investigate optimal pH, optimal temperatures, specific activities, and K_M values for all of the enzymes derived from *E. coli* and other microbial gene doners (Table 3.1).

Table 3.1: Properties of characterized enzymes in the putrescine and spermidine biosynthesis pathways used to establish overproduction of the aforementioned diamines by *B. methanolicus*

Enzyme	EC	Bacteria	Optimal pH	Optimal T (°C)	Sp. act. (U mg^{-1})	K_M (mM)	Reference
SpeA	4.1.1.19	*E. coli*	7.2-7.4	50	$2.8_{purified}$	0.03 (pH 7.5, 37°C)	Sun et al.[62]
		Bacillus subtilis	7.7	75	-	0.63-1.1 (pH 7.5, 37-70°C)	Burrell et al.[63]
		Pseudomonas	8.1	-	0.113	0.25	Rosenfeld and Roberts[64]
		Heliobacter pylori	8.5	50	-	$3.4_{purified}$ (pH 7.4, 37 °C)	Alam et al.[65]
SpeB	3.5.3.11	*E. coli*	7.3	42	-	1.2	Satishchandran and Boyle[66]
SpeE	2.5.1.16	*E. coli*	7.5[67]	50[67]	1.83[68]	0.0778* or 0.032**[67]	Bowman et al.[68], Lee et al.[67]
SpeH	4.1.1.50	*E. coli*	7.4[69]	-	0.06[70]	0.88[71]	Tabor et al.[69, 70, 71]

* putrescine. ** dAdoMet

As presented in Table 3.1, the low K_M value of 0.03 for the *E. coli* derived SpeA enzyme, indicates a high affinity of the substrate (arginine) to the enzyme[72]. The higher K_M values for the SpeA enzyme derived from *B. subtilis* (0.63-1.1 mM), *Pseudomonas* (0.25 mM), and *H. pylori* (3.4) indicates a lower affinity of the substrate arginine which correlates to a lower conversion rate of arginine to agmatine (Figure 1.3)[72]. Moreover, for the *E. coli* derived enzymes, the K_M value(s) of SpeE (0.0778 mM putrescine and 0.032 dAdoMet) showed the second-highest affinity to its substrate(s), followed by SpeH (0.88 AdoMet), and finally SpeB (1.2 mM agmatine). Furthermore, the specific activity is shown to be the highest for the SpeA enzyme (2.8 U mg^{-1}), followed by SpeE (1.83 U mg^{-1}), SpeH (0.06 U mg^{-1}), and no specific activity value was found for SpeE. Based on the observations from Table 3.1, it is evident that the enzymes derived from *E. coli* exhibit high optimal temperatures around 50 °C and generally neutral pH. These characteristics make *B. methanolicus* a hypothetical suitable host for the overexpression of these enzymes.

3.1.2 Evaluation of putrescine and spermidine as carbon or nitrogen sources in *B. methanolicus* MGA3

Here, Figure 3.1-A shows 200 mM methanol (control), 50 mM putrescine, 28.6 mM spermidine, or 50 mM arginine as carbon sources for the growth of MGA3. Furthermore, Figure 3.1-B shows 16 mM ammonium sulfate (control), 16 mM putrescine, 10.7 mM spermidine, or 8 mM arginine as nitrogen sources for the same strain.

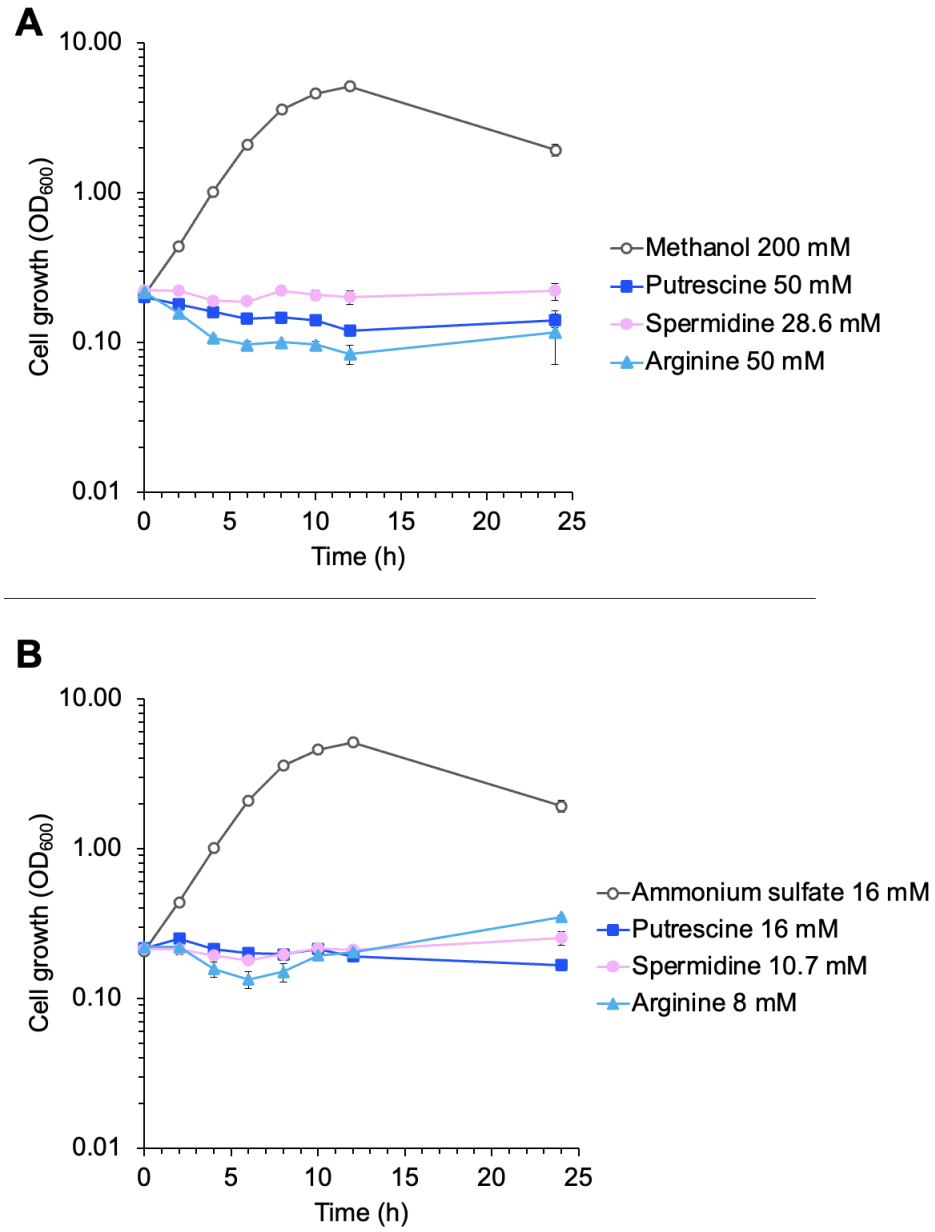

Figure 3.1: Growth of *B. methanolicus* MGA3 with putrescine, spermidine, or arginine as carbon or nitrogen sources. *B. methanolicus* MGA3 was cultivated in MVcM medium supplemented with putrescine, spermidine, or arginine as the sole carbon source (A) or nitrogen source (B), with methanol as the sole carbon source and ammonium sulfate as the sole nitrogen source as controls (red circles in A and B respectively). Values are presented as mean OD_{600} of triplicates. Standard deviations are presented as error bars.

Based on the growth curves presented in Figure 3.1, the results indicate that *B. methanolicus* MGA3 can not grow on putrescine, spermidine, or arginine neither as sole carbon nor nitrogen sources, as no growth is observed after 24 hours of cultivation in those conditions. In this assessment, MGA3 only grew on the combination of methanol and ammonium sulfate as carbon and nitrogen sources, respectively, with a growth rate of 0.39 $\pm$ 0.00 and a final biomass presented as OD_{600} of 4.92 $\pm$ 0.22 after 24 hours of cultivation.

3.1.3 Spermidine presents a toxic effect in *B. methanolicus* MGA3

An experiment assessing the toxic effects of putrescine, spermidine, and arginine on *B. methanolicus* MGA3 was conducted as described in Section 2.7.1. Growth curves of MGA3 supplemented with 0 to 30 mM arginine, putrescine, spermidine, or both putrescine and spermidine are presented in Figures C.1-A and C.1-B, C.1-C, and C.1-D, respectively. Furthermore, growth rates and final biomass production results for MGA3 supplemented with arginine and putrescine are presented in Table 3.2. Moreover, Figure 3.2-A and 3.2-B presents the growth rates and final biomass, respectively, of MGA3 at 0 to 30 mM of spermidine. Finally, Figure 3.3-A and 3.3-B presents the growth rates and final biomass, respectively, at 0 to 30 mM of both putrescine and spermidine.

Table 3.2: Growth rates and biomass production of *B. methanolicus* MGA3 in the presence of arginine and putrescine. *B. methanolicus* MGA3 was cultivated in SOB supplemented with 0, 0.075, 7.5, 15, or 30 mM arginine and putrescine. Values are presented as means of triplicates with standard deviations.

Compound	Concentration (mM)	Growth rate (h^{-1})	Final biomass (OD_{600})
Arginine	30	0.33 ± 0.01	3.41 ± 0.31
	15	0.47 ± 0.02	3.74 ± 0.29
	7.5	0.44 ± 0.02	4.10 ± 0.36
	0.75	0.49 ± 0.01	3.35 ± 0.15
	0.075	0.43 ± 0.02	3.21 ± 0.07
	0	0.50 ± 0.01	3.59 ± 0.07
Putrescine	30	0.47 ± 0.04	3.11 ± 0.16
	15	0.48 ± 0.01	3.37 ± 0.06
	7.5	0.50 ± 0.01	3.40 ± 0.22
	0.75	0.50 ± 0.01	3.49 ± 0.07
	0.075	0.49 ± 0.01	3.31 ± 0.12
	0	0.50 ± 0.01	3.38 ± 0.18

From Table 3.2, the growth rates and final biomass of MGA3 in the presence of arginine show no considerable changes caused by different supplemented arginine concentrations, except for 30 mM. In the presence of 30 mM arginine, a growth rate of 0.33 ± 0.01 h^{-1} was calculated, which is 1.5-fold lower than for MGA3 cultivated in 0 mM arginine (0.50 ± 0.01 h^{-1}). However, the final biomass for 30 mM arginine-cultivated MGA3 was not severely affected, compared to the control of 0 mM arginine. Moreover, the growth rates of MGA3 were not affected by the concentration of putrescine from 0 to 30 mM, however, the final biomass for MGA3 under 30 mM putrescine resulted in an OD_{600} value of 3.11 ± 0.16, which is 1.1-fold lower than that in the cultivation with 0 mM arginine (OD_{600} of 3.38 ± 0.18). Based on these observations, *B. methanolicus* MGA3 exhibits tolerance to arginine and putrescine concentrations of up to 30 mM.

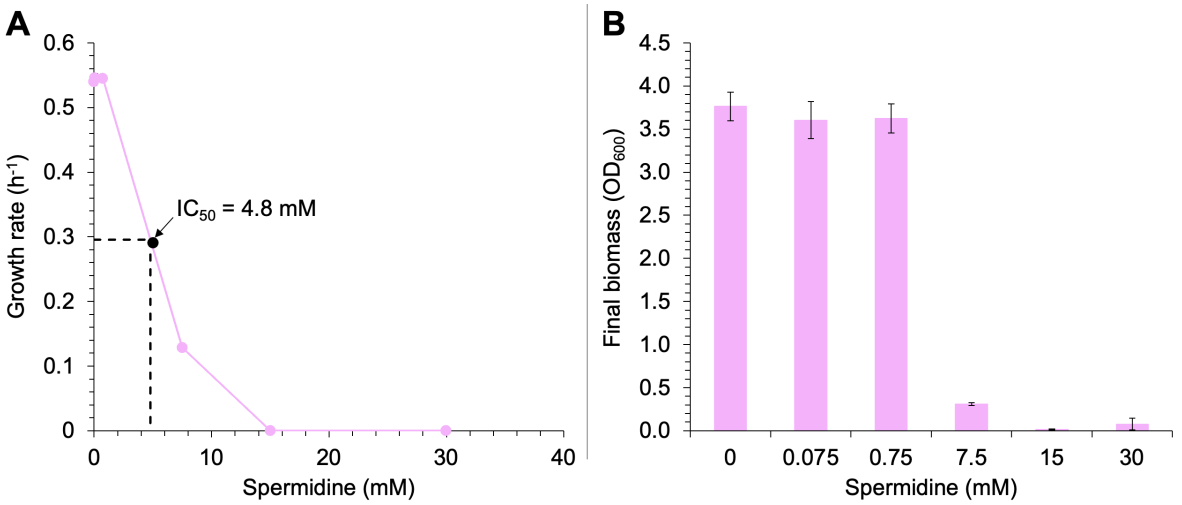

Figure 3.2: Spermidine IC_{50} in *B. methanolicus* MGA3 and its final biomass when cultivated with spermidine.
Growth rates (A) and final biomass (B) of *B. methanolicus* MGA3 cultivated in SOB medium and with increasing concentrations of spermidine. The IC_{50} value, which here describes the concentration of spermidine *B. methanolicus* MGA3 can tolerate before the growth rate is decreased by 50%, was determined to be 4.8 mM. The means of triplicates with standard deviations as error bars are shown.

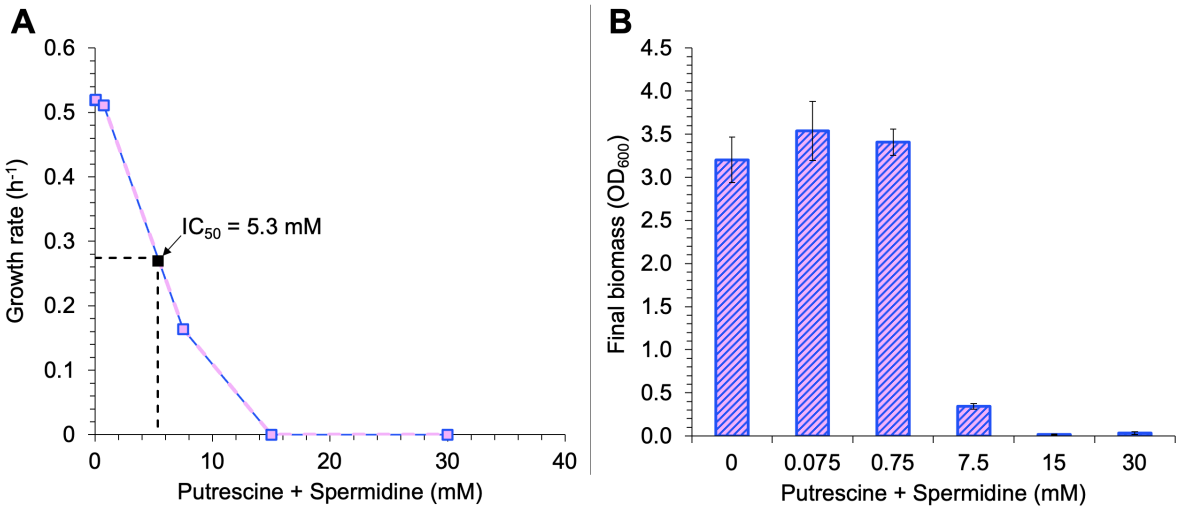

Figure 3.3: Putrescine and spermidine IC_{50} in *B. methanolicus* MGA3 and its final biomass when cultivated with putrescine and spermidine.
Growth rates (A) and final biomass (B) of *B. methanolicus* MGA3 cultivated in SOB medium and with increasing concentrations of putrescine and spermidine. The IC_{50} value, which here describes the concentration of putrescine and spermidine *B. methanolicus* MGA3 can tolerate before the growth rate is decreased by 50%, was determined to be 5.3 mM. The means of triplicates with standard deviations as error bars are shown.

Figure 3.2-A shows that spermidine severely hampers the growth of MGA3 at 7.5 mM, whereas the growth rate decreased 4-fold from 0.54 ± 0.01 h^{-1} at 0.75 mM to 0.13 ± 0.01 h^{-1} at 7.5 mM of that compound. This was also observed for the combined supplementation of spermidine and putrescine (Figure 3.3-A), where the growth rate decreased 3 times from 0.51 ± 0.02 h^{-1} at 0.75 mM to 0.16 ± 0.01 h^{-1} at 7.5 mM of the compounds. Moreover, the final biomass was also affected, by a 12 times decrease from OD_{600} of 3.62 ± 0.17 at 0.75 mM spermidine to 0.31 ± 0.02 at 7.5 mM spermidine (Figure 3.2-B). As for putrescine and spermidine synergistic effect, the final biomass decreased 10 times from OD_{600} of 3.41 ± 0.15 at 0.75 mM to 0.34 ± 0.03 at 7.5 mM of putrescine and spermidine (Figure

3.3-B). Furthermore, no or minimal growth was detected for concentrations over 15 mM of spermidine, and spermidine and putrescine together. Moreover, an IC_{50} value, which describes how much of a toxic compound a cell culture can tolerate before the growth rate is decreased by 50%, show a toxic effect of spermidine, presented by an IC_{50} value of 4.8 mM (Figure3.2-A). This value was also predicted for the inhibitory effect of putrescine and spermidine together in the cultivation of MGA3, which resulted in an IC_{50} of 5.3 mM putrescine and spermidine. However, as putrescine tolerance was observed for at least 30 mM (Table 3.2), the negative impact on the growth of *B. methanolicus* MGA3 cultivated with both putrescine and spermidine is assumed to be caused solely by spermidine supplementation.

3.2 Heterologous expression of arginine decarboxylase and agmatinase in *B. methanolicus* MGA3 strains leads to overproduction of putrescine from methanol

B. methanolicus MGA3 with heterologous and homologous expressions of *speA* and *speB* were used for putative putrescine overproduction, *i.e.* PUT^{Ec}, and PUT^{Bm} strains (Table 2.1). These strains harbor the pBV2xp-derived plasmid, which has a xylose-inducible promoter system[20]. To assess the most optimal xylose plasmid-borne induction levels, a growth experiment with 0, 0.01, 0.1, or 1% final xylose concentration was performed with the strains PBV (control), PUT^{Ec}, and PUT^{Bm} according to Section 2.7.2. The most optimal induction level would render the highest, most stable production of putrescine and a comparable growth rate to the empty vector control (PBV).

3.2.1 Heterologous *speA* and *speB* gene expression impacts the growth of *B. methanolicus* regardless of induction levels

The growth curve of *B. methanolicus* strains PBV, PUT^{Ec}, and PUT^{Bm} in different induction levels are shown in Figure C.2. The growth rates and final biomass for the respective strains with different induction levels are shown in Table 3.3.

Table 3.3: Growth rates and biomass production of the strains, PBV, PUT^{Ec}, and PUT^{Bm} cultivated with increasing induction levels of xylose.
Values are presented as means of triplicates with standard deviation.

Induction level (%)	Strain	Growth rate (h^{-1})	Final biomass (OD_{600})
0	PBV	0.42 ± 0.02	6.62 ± 0.41
	PUT^{Ec}	0.30 ± 0.00	6.20 ± 0.25
	PUT^{Bm}	0.39 ± 0.01	7.52 ± 0.50
0.01	PBV	0.41 ± 0.00	6.58 ± 0.19
	PUT^{Ec}	0.29 ± 0.01	6.12 ± 0.24
	PUT^{Bm}	0.40 ± 0.00	7.21 ± 0.46
0.1	PBV	0.41 ± 0.01	6.62 ± 0.23
	PUT^{Ec}	0.31 ± 0.01	7.26 ± 0.71
	PUT^{Bm}	0.40 ± 0.01	7.88 ± 0.54
1	PBV	0.41 ± 0.01	7.04 ± 0.09
	PUT^{Ec}	0.30 ± 0.02	6.66 ± 0.70
	PUT^{Bm}	0.38 ± 0.01	8.21 ± 0.12

Based on data from Table 3.3, the empty vector control strain PBV and the strain PUT^{Bm} had relatively

similar growth rates and around a 1.3-fold higher growth rate than PUT^{Ec} for all conditions, for instance, PBV had the highest growth rate (0.41 ± 0.01) compared to PUT^{Ec} (0.31 ± 0.01) at induction level of 0.1% xylose. Moreover, PUT^{Bm} produced the highest biomass in 0% xylose concentration, with a final biomass value of 7.52 ± 0.50, which is 1.1-fold higher than that value for PBV (OD_{600} of 6.62 ± 0.41), and 1.2-fold higher than that for PUT^{Ec} (OD_{600} of 6.20 ± 0.25). An equal effect was observed for biomass production of PBV and PUT^{Bm} strains in induction levels of 0.01, 0.1, and 1% xylose as well.

3.2.2 Quantification of putrescine production reveals higher production stability under partial xylose induction

An HPLC analysis was conducted, to determine which strain and at which induction level resulted in the most optimal putrescine production. Large error bars show little stability, which is not ideal for overproduction strategies. Here, quantification of extracellular putrescine, arginine (precursor), and spermidine (derivative) was done. Samples for HPLC were collected after cultivation of 12, 24, and 48 hours and analyzed according to Section 2.8. Figure 3.4, 3.5, and 3.6 show the production of arginine, putrescine, and spermidine, respectively, over time in the strains, PBV, PUT^{Ec}, and PUT^{Bm} under increasing xylose induction levels.

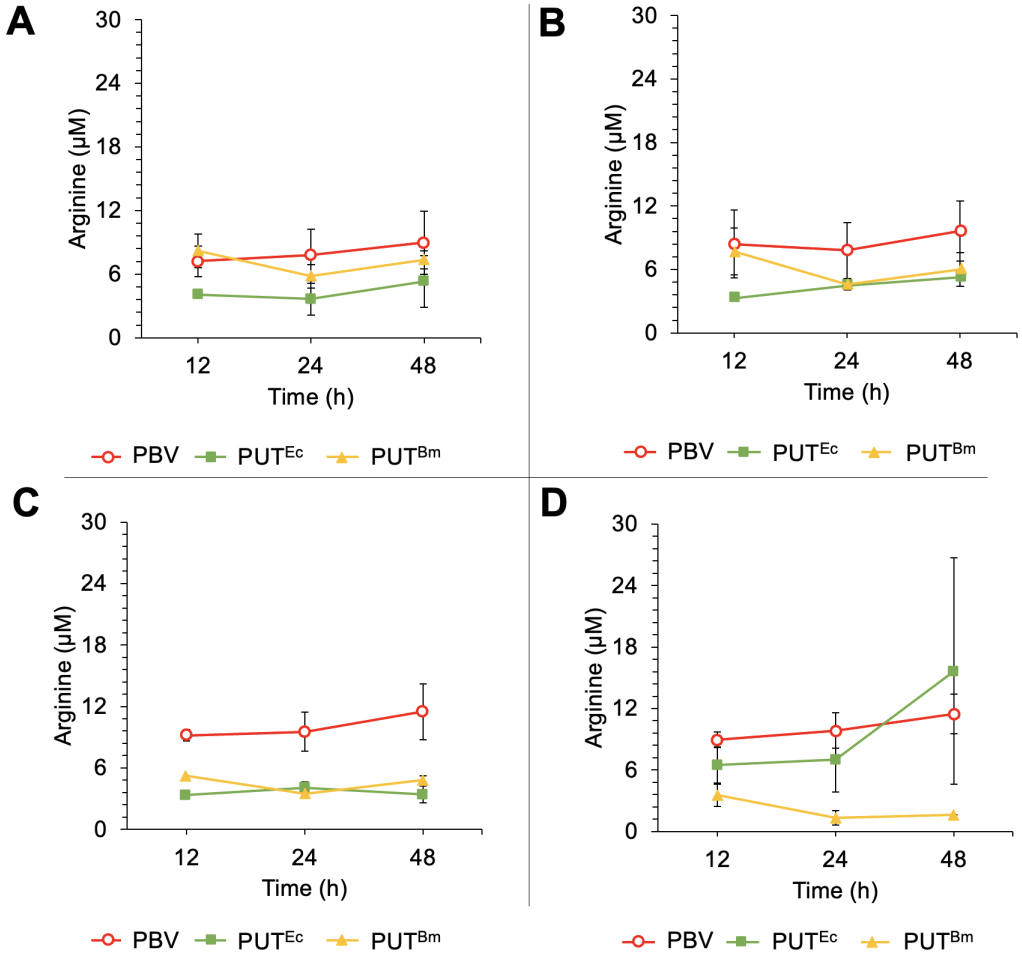

Figure 3.4: Production of arginine in the strains PBV, PUT^{Ec}, and PUT^{Bm} under plasmid-based gene expression induction with 0 (A), 0.01 (B), 0.1 (C), and 1% (D) xylose.
Measurements are taken at 12, 24, and 48 hours. Values are presented as means of triplicates with standard deviation presented as error bars.

In this experiment (Figure 3.4), arginine production was found to be relatively similar across different induction levels and times for each strain. Notably, under 0.1% xylose, and after cultivation of 24 hours, the arginine production of PUT^{Ec} (4.1 ± 0.5 µM) and PUT^{Bm} (3.5 ± 0.2 µM) was 2.3-fold and 2.7-fold less, respectively, compared to PBV (9.5 ± 1.9 µM) for the same conditions (Figure 3.4). The low levels of arginine production observed in the strains PUT^{Ec} and PUT^{Bm}, compared to the PBV strain, suggest that arginine is predominantly utilized within the cells rather than being secreted to the supernatant.

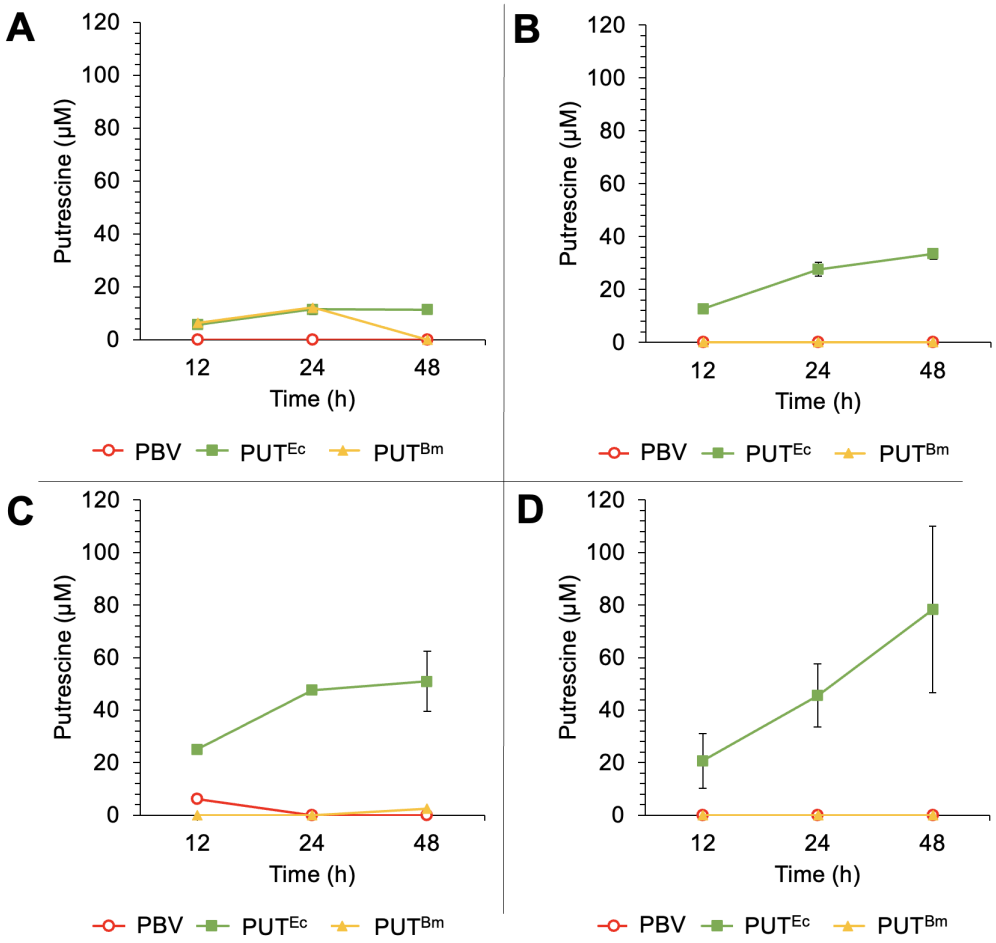

Figure 3.5: Production of putrescine in the strains, PBV, PUT^{Ec}, and PUT^{Bm} under plasmid-based gene expression induction with 0 (A), 0.01 (B), 0.1 (C), and 1% (D) xylose.
Measurements are taken at 12, 24, and 48 hours. Values are presented as means of triplicates with standard deviation presented as error bars.

Putrescine overproduction is mostly observed in PUT^{Ec} (Figure 3.5), with small putrescine production observed for strains PBV, and PUT^{Bm} (Figure 3.5-A, and 3.5-C, respectively). The concentration of putrescine increases from 12 to 48 hours for all conditions, however, from 24 to 48 hours, a plateau is observed under 0 (A), 0.01 (B), and 0.1% (D) xylose. For the 1% xylose condition, a large error is found at 48 hours of cultivation, with a 78.3 ± 32.7 µM putrescine production for the strain PUT^{Ec} (Figure 3.5-D). This shows low stability of putrescine production at 1% xylose concentration and cultivation after 48 hours. Moreover, the putrescine production for the PUT^{Ec} strain under 0.1 (Figure 3.5-C), and 1% (Figure 3.5-D) xylose after 24 hours of cultivation is relatively equal, with high titers of 47.5 ± 0.8 and 45.6 ± 12.0 µM, respectively, however, the lower error for PUT^{Ec} strain under 0.1% xylose after 24 hours of cultivation renders that this strain with these conditions is the most optimal for putrescine

overproduction. Unexpectedly, the putrescine production of PUT^{Bm} was comparable to that of PBV, despite the lower arginine production in PUT^{Bm} compared to PBV. Based on these observations, cultivation of PUT^{Ec} under 0.1% xylose induction level, with cells harvested after 24 hours was chosen for further putrescine-production optimization experiments.

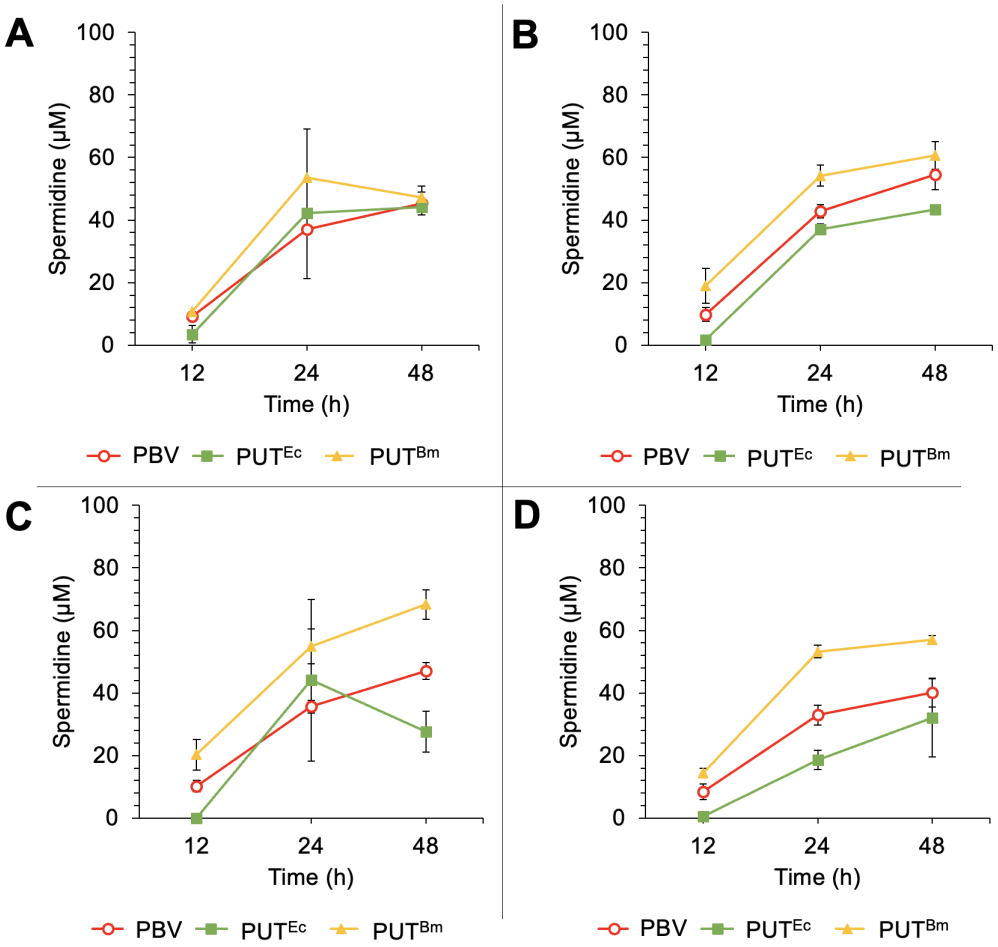

Figure 3.6: Production of spermidine in the strains, PBV, PUT^{Ec}, and PUT^{Bm} under plasmid-based gene expression induction with 0 (A), 0.01 (B), 0.1 (C), and 1% (D) xylose.
Measurements are taken at 12, 24, and 48 hours. Values are presented as means of triplicates with standard deviation presented as error bars.

The results from Figure 3.6 show that spermidine production is observed in all strains and increases with time, where the PUT^{Ec} strain renders the lowest titers of by-product (spermidine) formation, followed by the PBV strain and then the PUT^{Bm} strain with the highest overall values. Moreover, spermidine production stays relatively similar for each strain in the different induction levels. Unexpectedly, in Figure 3.6-A (0% xylose) and 3.6-C (0.1% xylose), the PUT^{Ec} strain cultivated after 24 hours show higher spermidine production than the PBV strain, however large error bars indicate that this data is not reliable. Furthermore, spermidine production was the least for the PUT^{Ec} strain when induced with 1 % xylose (Figure 3.6-D), which is beneficial for less putrescine utilization, and would indicate higher final putrescine production titers. Moreover, based on these results (Figure 3.6-C) PUT^{Bm} shows the highest spermidine production with a value of 68.3 $\pm$ 4.7 µM after 48 hours of cultivation and an induction level of 0.1%, which would indicate that this strain in these conditions is not advantageous for putrescine overproduction. The overall lower spermidine production in PUT^{Ec}, is advantageous for higher putrescine titers.

3.3 Amino acids and nitrogen supply impact putrescine production in *B. methanolicus* PUT^{Ec}

Based on the results from the previous Section 3.2, the optimal induction level was 0.1% xylose, by which putrescine production was the highest after 24 hours of cultivation for the PUT^{Ec} strain. As PUT^{Bm} did not show a putrescine production different from the empty vector control strain, this strain was not included in further experiments. Further optimization of cultivation conditions for higher putrescine production was therefore performed by supplementation of putrescine precursors, and growth in different media containing variating supplies of nitrogen. Therefore, 1 mM of glutamate, arginine, or ornithine was supplemented in the cultivation of PBV and PUT^{Ec}, additionally, growth of those strains in MVcM, MVcM2, or CGXII was recorded, according to Section 2.7.3, followed by an HPLC analysis (Section 2.8) for quantifying the extracellular putrescine and spermidine.

3.3.1 Growth of *B. methanolicus* strains, PBV and PUT^{Ec} is slightly impacted by supplementation of putrescine precursors

Growth rates and final biomass production (Table 3.4) were derived from Figure C.3-A and C.3-B which presents the growth curves of PBV, and PUT^{Ec} respectively, in cultivation with MVcM supplemented with 1 mM glutamate, arginine, or ornithine.

Table 3.4: Growth rates and biomass production of *B. methanolicus* strains PBV and PUT^{Ec} cultivated with 1 mM of putrescine precursors, glutamate, arginine, and ornithine.
Values are presented as means of triplicates with standard deviation.

Strain	1 mM amino acid	Growth rate (h^{-1})	Final biomass (OD_{600})
PBV	-	0.35 ± 0.00	5.03 ± 0.52
	Glutamate	0.36 ± 0.01	4.87 ± 0.32
	Arginine	0.36 ± 0.01	5.09 ± 0.47
	Ornithine	0.36 ± 0.00	4.99 ± 0.54
PUT^{Ec}	-	0.30 ± 0.00	5.00 ± 0.41
	Glutamate	0.32 ± 0.00	5.20 ± 0.48
	Arginine	0.28 ± 0.00	4.91 ± 0.33
	Ornithine	0.30 ± 0.01	4.98 ± 0.28

The results presented in Table 3.4 show that the growth rate of the PUT^{Ec} strain cultivated with the supplementation of arginine (0.28 ± 0.00 h^{-1}), is slightly less than the control PUT^{Ec} strain with no supplementation (0.30 ± 0.00 h^{-1}). Notably, the growth rate of the PUT^{Ec} strain supplemented with glutamate (0.32 ± 0.00 h^{-1}), is slightly higher than the control PUT^{Ec} strain with no supplementation (0.30 ± 0.00 h^{-1}). The growth rate of the strain PBV supplemented with ornithine (0.36 ± 0.00 h^{-1}) is slightly higher than the control strain PBV with no supplementation (0.35 ± 0.00 h^{-1}). Final biomass is not considerably affected by the supplementation of amino acids for the respective strains, PBV and PUT^{Ec}.

3.3.2 Putrescine production is enhanced when the PUT^{Ec} strain is cultivated with putrescine precursors

Here, the HPLC results of PBV, and PUT^{Ec} cultivated in supplementation of 1 mM glutamate, arginine, and ornithine after 24 hours are presented (Figure 3.7). Figure 3.7-A show results for the PBV strain, while Figure 3.7-B show results for the PUT^{Ec} strain.

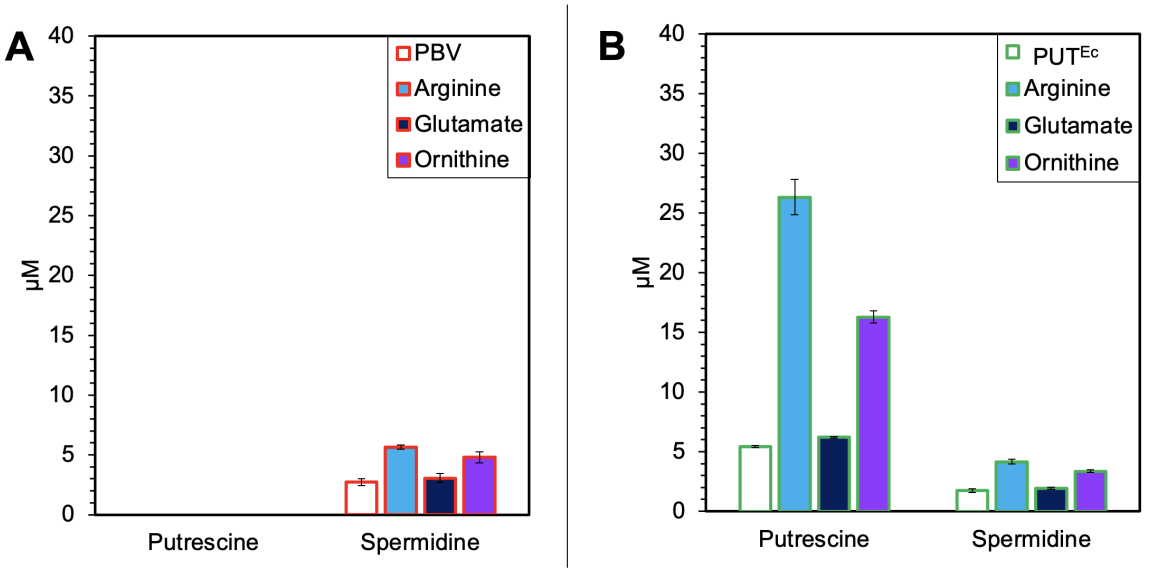

Figure 3.7: Production of diamines in *B. methanolicus* strains PBV (A) and PUT^{Ec} (B) cultivated in MVcM supplemented with 1 mM putrescine-precursors, glutamate, arginine, and ornithine.
Values are presented as means of triplicates with standard deviation presented as error bars.

As expected from previous results, putrescine was not detected in PBV strains, despite the supplementation of precursor (Figure 3.7-A). On the other hand, the spermidine production for PBV with supplementation of arginine (5.6 ± 0.2 µM), and ornithine (4.8 ± 0.5 µM), increased 2-fold and 1.8-fold, respectively, compared to PBV with no supplementation (2.7 ± 0.3 µM). For PUT^{Ec}, putrescine production was highest for cultivation with arginine (26.3 ± 1.5 µM), which was expected as arginine is a more direct precursor for putrescine biosynthesis in *B. methanolicus* (Figure 3.7-B). Moreover, compared to PUT^{Ec} cultivated without any supplementation (5.4 ± 0.1 µM), arginine supplementation results in 4.9-fold, ornithine supplementation results in 3-fold putrescine production increase (16.3 ± 0.5 µM), and glutamate supplementation resulted in 1.1-fold (6.2 ± 0.1 µM) higher putrescine production (Figure 3.7-B). Spermidine production in PUT^{Ec} supplemented with the different amino acids showed a similar, but slightly lower outcome as that for PBV, described above. Based on the presented results, it can be concluded that arginine supplementation in the cultivation of the PUT^{Ec} strain resulted in the highest production of putrescine. However, it also led to an increase in the production of the derivative spermidine, compared to no supplementation.

3.3.3 Growth of the PUT^{Ec} strain is negatively affected by cultivation in CGXII

Figure C.4 presents the growth curve of PBV and PUT^{Ec}, cultivated in MVcM, MVcM2, or CGXII. The growth rate and final biomass results of these strains and media conditions are presented in Table 3.5.

Table 3.5: Growth rates and biomass production of *B. methanolicus* strains PBV and PUT^{Ec} cultivated in MVcM, MVcM2, and CGXII.
Values are presented as means of triplicates with standard deviation.

Strain	Cultivation media	Growth rate (h^{-1})	Final biomass (OD_{600})
PBV	MVcM	0.35 ± 0.02	4.96 ± 0.44
	MVcM2	0.38 ± 0.00	4.93 ± 0.20
	CGXII	0.30 ± 0.00	3.36 ± 0.38
PUT^{Ec}	MVcM	0.36 ± 0.00	5.10 ± 0.34
	MVcM2	0.36 ± 0.01	4.56 ± 0.29
	CGXII	0.27 ± 0.01	3.12 ± 0.07

In MVcM2, PBV demonstrated the highest growth rate (0.38 ± 0.00 h^{-1}), while in CGXII, the growth rate is 1.2-fold lower (0.30 ± 0.00 h^{-1}) compared to the growth rate of PBV in MVcM (0.35 ± 0.02 h^{-1}). Moreover, the growth rates of PUT^{Ec} in MVcM and MVcM2 are similar, with values of 0.36 ± 0.00 h^{-1} and 0.36 ± 0.01 h^{-1}, respectively. However, in CGXII, the growth rate was 1.3-fold lower (0.27 ± 0.01 h^{-1}) compared to cultivation in MVcM. The final biomass production was relatively similar for both strains cultivated in MVcM and MVcM2. However, for PBV cultivation in CGXII (3.36 ± 0.38), the biomass production was 1.5 times less than that for PBV in MVcM (4.96 ± 0.44). Similarly, the biomass production was 1.6 times less for PUT^{Ec} grown CGXII (3.12 ± 0.07), compared to PUT^{Ec} in MVcM (5.10 ± 0.44).

3.3.4 Putrescine production in *B. methanolicus* strains PBV and PUT^{Ec} are directly related to growth parameters

In this section, results from the HPLC analysis (Section 2.8) of the strains PBV, and PUT^{Ec} cultivated in MVcM, MVcM2, and CGXII after 24 hours are presented (Figur 3.8). Figure 3.8-A shows production results for the PBV strain, while Figure 3.8-B shows production results for the PUT^{Ec} strain.

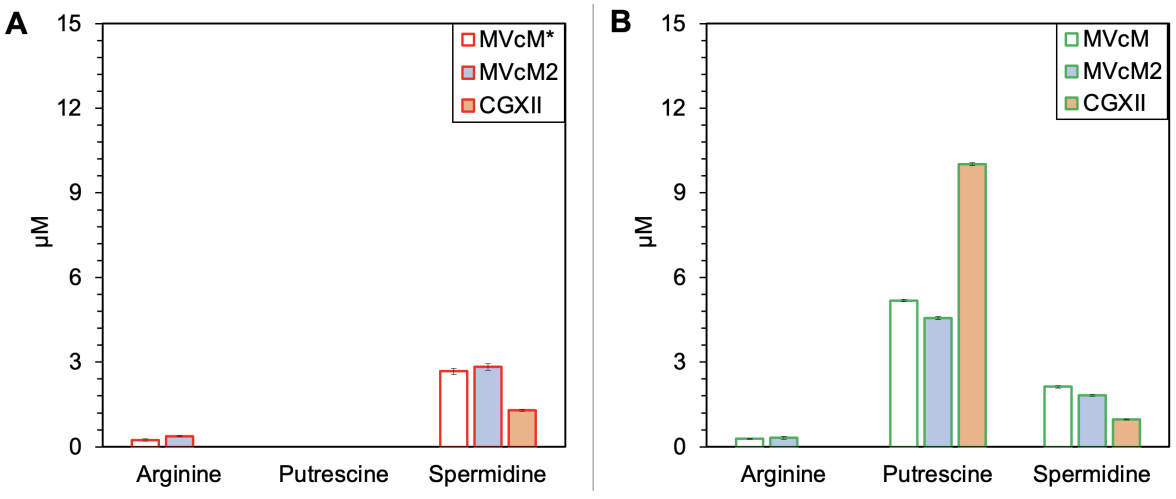

Figure 3.8: Production of diamines in *B. methanolicus* strains PBV (A) and PUT^{Ec} (B) cultivated in MVcM, MVcM2, and CGXII.
Values are presented as means of triplicates with standard deviation as error bars. "*" symbolizes duplicates instead of triplicates.

Arginine production was detectable in minimal quantities for MVcM and MVcM2 cultivation of PBV (Figure 3.8-A) and PUT^{Ec} (Figure 3.8-B). Moreover, putrescine production was only detectable for the PUT^{Ec} strain, where the highest putrescine concentration was 10.0 ± 0.0 µM for PUT^{Ec} cultivated in CGXII, which is 2-fold higher than for PUT^{Ec} cultivated in MVcM (5.2 ± 0.0 µM). Production of the derivative spermidine was lowest for PBV and PUT^{Ec} cultivated in CGXII, with values of 1.3 ± 0.0 µM, and 1.0 ± 0.0 µM, respectively. Based on the presented results, it can be concluded that PUT^{Ec} cultivated in CGXII results in the highest putrescine production. Interestingly, a correlation between low growth (Table 3.5) and high putrescine production in CGXII cultivation of PUT^{Ec} can be observed.

3.4 Construction of pTH1mp-derived plasmids towards production of spermidine

The spermidine synthase encoded by *speE* catalyzes the production of spermidine through the transfer of the aminopropyl group of dAdoMet to putrescine. While the AdoMet decarboxylase encoded by *speH* produces the co-factor dAdoMet, through the decarboxylation of AdoMet (Figure 1.3)[45]. Moreover, SpeE has been shown to be the rate-limiting step for the production of spermidine, while SpeH derived from *E. coli* has shown to produce high titers of spermidine in *B. amuloliquefaciens*[45]. As spermidine inhibits the growth rate of *B. methanolicus* (Figure 3.2), it was hypothesized that overexpression of the *speE* gene, encoding the rate-limiting step of spermidine synthesis, could improve spermidine production without significantly hampering the growth rate compared to the overexpression of both *speE* and *speH*.

Thus, pTH1mp-*speE*^{Ec} and pTH1mp-*speE*^{Bm} were constructed according to Section 2.4. The insert *speE* from *E. coli* K-12 MG1655 (984 bp) and *B. methanolicus* MGA3 (891 bp) was PCR amplified and their band size was confirmed by agarose gel electrophoresis shown in, lanes 2 and 3, respectively (Figure 3.9-A). The linearization of the backbone pTH1mp (5,873 bp) was also confirmed, which is displayed in lane 1, in comparison to the undigested pTH1mp as control C1 (Figure 3.9-A). For confirming a successful Gibson assembly, colony PCR was performed according to section 2.4.9 and resulted in the correct band size of the insert in pTH1mp-*speE*^{Ec} in lanes 1, 2, and 7 (Figure 3.9-B), and pTH1mp-*speE*^{Bm} in lanes 6, 7, and 11 (Figure 3.9-C).

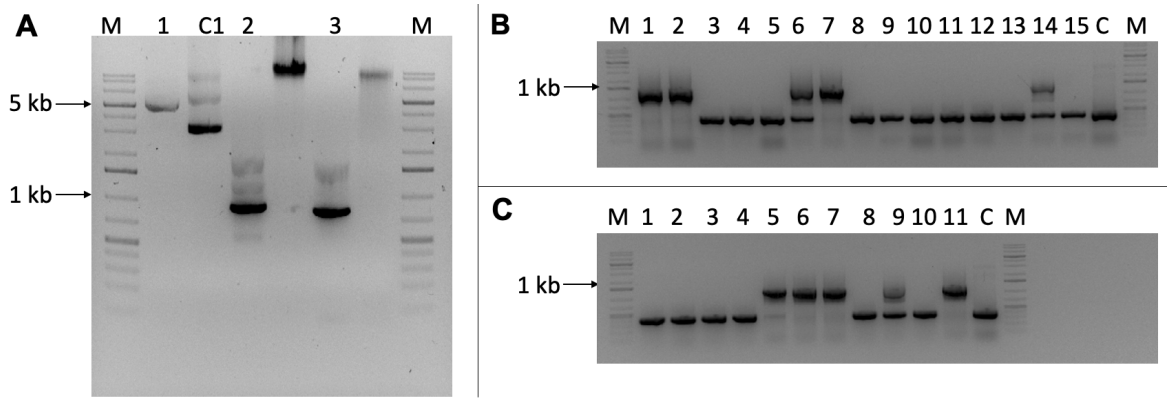

Figure 3.9: Agarose gel electrophoresis images showing the construction of pTH1mp-*speE*^{Ec} and pTH1mp-*speE*^{Bm}. Agarose gel electrophoresis showing A: *Pci*I digested pTH1mp (1) and undigested pTH1mp (C1) as control, PCR amplified *speE* (2) from *E. coli* K-12 MG1655, and PCR amplified *speE* (2) from *B. methanolicus* MGA3. B: Colony PCR results showing correct band size of insert in pTH1mp-*speE*^{Ec} (1, 2, and 7), and empty vector pTH1mp as control C. C: Colony PCR results showing correct band size of insert in pTH1mp-*speE*^{Bm} (6, 7, and 11), and empty vector pTH1mp as control C. Samples are applied next to 1 kb plus DNA ladder (M).

Agarose gel electrophoresis only confirms the assembly of the insert and backbone. However, mutation may occur during Gibson assembly or transformation to the cloning host. Therefore, plasmid DNA from positive colonies shown in Figure 3.9, were sent to sequencing twice (Section 2.4.10), and successful cloning of pTH1mp-*speE*^{Bm} was confirmed. However, sequencing results of plasmids from two colonies with pTH1mp-*speE*^{Ec} showed a mutation (deletion) at the beginning of the insert gene sequence, causing a frameshift in the sequence. This is shown in Figure 3.10 for colony numbers 2 (Figure 3.10-A) and 7 (Figure 3.10-B), by a deletion at the position 1,105 bp and 1,096 bp, respectively. The frameshift mutation in both colonies 2 and 7 were confirmed through two rounds of sequencing, representing *e.g.* "speeEEc_fw1" and "speeEEc_fw2", for the first and second sequencing results of *speE*^{Ec}, respectively. Therefore, only the plasmid pTH1mp-*speE*^{Bm} was transformed into both *B. methanolicus* MGA3 and PUT^{Ec} strains, and further used in achieving spermidine overproduction.

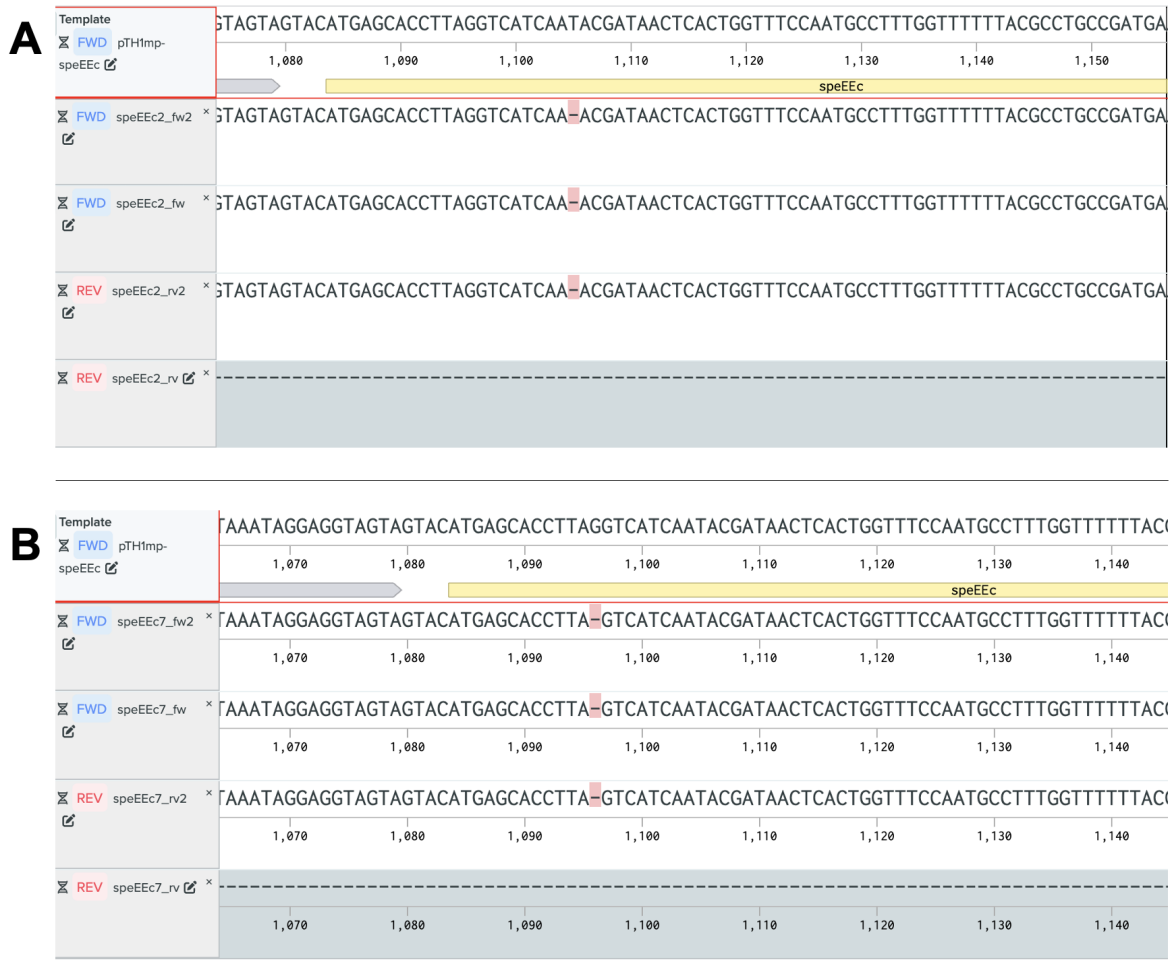

Figure 3.10: Multiple-alignment of sequencing results of pTH1mp-*speE*^{Ec} from colonies 2 (A) and 7 (B).
The template DNA for sequencing was the isolated plasmid pTH1mp-*speE*^{Ec}. "speEEc_fw" and "speEEc_rv" are forward strand and reverse strand sequencing results, respectively, from the first sequencing. "speEEc_fw2" and "speEEc_rv2" is from the second sequencing. In both instances, the corresponding plasmids exhibited the same point mutation (deletion). The deletion is marked in red and is located at the beginning of the gene sequence at position 1,105 bp and 1,096 bp, respectively.

3.5 Heterologous and homologous expression of spermidine synthase and AdoMet decarboxylase for overproduction of spermidine in *B. methanolicus* strains

Putrescine production in *B. methanolicus* MGA3 has been proved through HPLC analysis (Section 3.2), and in these results, the putrescine derivative spermidine production is also detected. The overproduction of spermidine was therefore attempted. Moreover, spermidine is toxic to the cell as proved earlier (Section 3.1.3), therefore overproduction of spermidine under the toxicity level is desirable. Multiple strains were constructed to assess which is the most optimal metabolic engineering strategy for spermidine overproduction. After construction of pTH1mp-*speE*^{Bm}, homologous expression of spermidine synthase in *B. methanolicus* strains was successfully created, however as pTH1mp-*speE*^{Ec} was not successfully constructed. The growth and quantification of spermidine in the donated and created strains PTH, SPE^{Bm}, SPE$_{ii}^{Ec}$, and SPE$_{ii}^{Bm}$ are presented in Section 3.5.1. Moreover, as the PUT^{Ec} strain have an increased putrescine production compared to the PBV strain, the construction of strains, PUT^{Ec}SPE^{Bm}, PUT^{Ec}SPE$_{ii}^{Ec}$, and PUT^{Ec}SPE$_{ii}^{Bm}$, was hypothesized to render higher spermidine titers. The growth and spermidine production of the mentioned strains, in comparison to the controls PBV PTH, and PUT^{Ec}PTH were analyzed in Section 3.5.2.

3.5.1 Spermidine production is benefited by overexpression of *speH* in combination with *speE*

The strains PTH, SPE^{Bm}, SPE$_{ii}^{Ec}$, and SPE$_{ii}^{Bm}$ were further used in growth experiments (Section 2.7.4), and in spermidine production quantification (Section 2.8). Growth curves for the respective strains cultivated in MVcM are shown in Figure C.5. The growth rates, final biomass, and quantification of arginine, putrescine, and spermidine for the respective strains are presented in Table 3.6. The quantification of the produced diamines is based on 24 hours of cultivation, and HPLC data after 12 hours showed lower titers (data not shown).

Table 3.6: Growth rates, final biomass, and quantification of arginine, putrescine, and spermidine in PTH, SPE^{Bm}, SPE$_{ii}^{Ec}$, and SPE$_{ii}^{Bm}$ cultivation after 24 hours.
Values are presented as means of triplicates with standard deviation.

Strain	Growth rate (h^{-1})	Final biomass (OD_{600})	Arginine (μM)	Putrescine (μM)	Spermidine (μM)
PTH	0.44 ± 0.01	5.19 ± 0.19	0.5 ± 0.3	0.0 ± 0.0	5.2 ± 0.1
SPE^{Bm}	0.40 ± 0.01	5.86 ± 0.24	0.5 ± 0.1	0.1 ± 0.0	5.1 ± 0.4
SPE$_{ii}^{Ec}$	0.44 ± 0.01	5.54 ± 0.22	0.6 ± 0.2	0.1 ± 0.0	6.2 ± 0.4
SPE$_{ii}^{Bm}$	0.41 ± 0.01	5.70 ± 0.18	0.4 ± 0.2	0.1 ± 0.0	6.3 ± 0.4

Based on results from Table 3.6, the strains, PTH and SPE$_{ii}^{Ec}$ presented the highest growth rates of 0.44 ± 0.01 h^{-1}, followed by SPE$_{ii}^{Bm}$ (0.41 ± 0.01 h^{-1}) and finally SPE^{Bm} (0.40 ± 0.01 h^{-1}) with the lowest growth rate. The final biomass production is relatively similar for these strains. As for diamine production, the arginine titers were relatively similar for all strains. Putrescine production was detected in minimal quantities of 0.1 ± 0.0 μM in SPE^{Bm} and SPE$_{ii}^{Ec}$. Moreover, SPE$_{ii}^{Ec}$ and SPE$_{ii}^{Bm}$ produced the highest spermidine titers of 6.2 ± 0.3 μM, and 6.3 ± 0.4 μM, respectively. This is 1.2-fold higher than spermidine production for PTH (5.2 ± 0.1 μM) and SPE^{Bm} (5.1 ± 0.4 μM).

3.5.2 Growth and spermidine quantification of PUT^{Ec}SPE^{Bm}, PUT^{Ec}SPE$_{ii}^{Ec}$, and PUT^{Ec}SPE$_{ii}^{Bm}$ reveal no improvement in spermidine production by employment of PUT^{Ec} as background strain

The results from Section 3.5 show that the combined expression of *speE* with *speH* results in slightly higher spermidine titers. However, to increase the current titers, the heterologous and homologous expression of the aforementioned genes in the putrescine-producing strain PUT^{Ec} have been hypothesized to enhance the availability of the precursor putrescine and subsequently increase in spermidine production. PUT^{Ec}SPE^{Bm}, PUT^{Ec}SPE$_{ii}^{Ec}$ and PUT^{Ec}SPE$_{ii}^{Bm}$ were therefore cultivated in MVcM for 24 hours, with PBV PTH and PUT^{Ec}PTH as controls. Figure C.6 presents the growth curves of the aforementioned strains. The PBV PTH strain grew without any lag phase, along with PUT^{Ec}SPE^{Bm}, and PUT^{Ec}SPE$_{ii}^{Bm}$. PUT^{Ec}PTH had a lag phase for 6 hours before it grew exponentially, and PUT^{Ec}SPE$_{ii}^{Bm}$ did not grow at all. The growth rates, final biomass, and quantification of arginine, putrescine, and spermidine for the respective strains are presented in Table 3.7. The quantification of the compounds is based on 24 hours of cultivation. HPLC data after 12 hours showed lower titers (data not shown).

Table 3.7: Growth rates, final biomass, and quantification of arginine, putrescine, and spermidine in PTH, SPE^{Bm}, SPE$_{ii}^{Ec}$, and SPE$_{ii}^{Bm}$ cultivation after 24 hours.
Values are presented as means of triplicates with standard deviation.

Strain	Growth rate (h^{-1})	Final biomass (OD_{600})	Arginine (μM)	Putrescine (μM)	Spermidine (μM)
PBV PTH	0.36 ± 0.01	5.65 ± 0.50	0.4 ± 0.1	0.1 ± 0.0	4.3 ± 0.2
PUT^{Ec}PTH	0.22 ± 0.00	3.51 ± 0.90	0.4 ± 0.0	4.8 ± 0.2	1.3 ± 0.3
PUT^{Ec}SPE^{Bm}	0.31 ± 0.01	4.95 ± 0.16	0.7 ± 0.1	1.7 ± 0.0	3.9 ± 0.4
PUT^{Ec}SPE$_{ii}^{Ec}$	0.24 ± 0.02	4.33 ± 0.08	0.2 ± 0.1	3.3 ± 0.2	2.7 ± 0.1
PUT^{Ec}SPE$_{ii}^{Bm}$	n.a.	0.09 ± 0.01	n.a.	n.a.	n.a.

Based on the results presented in Table 3.7, the strain PBV PTH presented the highest growth rate (0.36 ± 0.01 h^{-1}) and final biomass (5.65 ± 0.50) in comparison to the other tested strains. Moreover, PUT^{Ec}SPE^{Bm} had a growth rate of 0.31 ± 0.01 h^{-1} which is 1.2 times lower than the PBV PTH control, and the final biomass (4.95 ± 0.16) was 1.1-fold lower than the PBV PTH control. The PUT^{Ec}PTH control had the lowest growth rate of 0.22 ± 0.00 h^{-1}, which is 1.6 times lower than the PBV PTH control. Its final biomass was measured to 3.51 ± 0.90, however, based on the growth curve shown in Figure C.6, this measurement was taken when the OD_{600} decreased due to cell lysis. The PUT^{Ec}SPE$_{ii}^{Ec}$ strain had a 1.5 times lower growth rate (0.24 ± 0.01 h^{-1}), and a 1.3-fold lower final biomass (4.33 ± 0.08), than the PBV PTH control. The PUT^{Ec}SPE$_{ii}^{Bm}$ growth strain presented no growth in this cultivation.

The arginine production was more expressive in the strains PUT^{Ec}SPE^{Bm} with a titer of 0.7 ± 0.1 μM. Here, the best producer of spermidine among the strains tested was the control PBV PTH, with a final titer of 4.3 ± 0.2 μM. The second-best producer was PUT^{Ec}SPE^{Bm} with a titer of 3.9 ± 0.4 μM spermidine, which is 1.1-fold lower in comparison with the PBV PTH strain. Furthermore, PUT^{Ec}SPE$_{ii}^{Ec}$ had spermidine titers of 2.7 ± 0.1 μM, which is 1.6-fold lower in comparison with PBV PTH. The control PUT^{Ec}PTH had the lowest spermidine titers of 1.3 ± 0.3 μM which is 3.3-fold lower than the PBV PTH strain. These results indicate that when spermidine biosynthetic genes are overexpressed in the PUT^{Ec} strain, the spermidine titers are not improved, however, some conversion of putrescine to spermidine may be indicated as PUT^{Ec}SPE^{Bm}, and PUT^{Ec}SPE$_{ii}^{Ec}$ had lower putrescine titers and higher spermidine titers than PUT^{Ec}PTH.

4 Discussion

Sustainable production of value-added compounds, such as amino acids and their derivatives, is rapidly gaining attention in research and the industry. The large-scale production of amino acids has already been established through cell factories such as *C. glutamicum* and *E. coli*[39,73]. Moreover, amino acid derivatives like diamines are important for the plastic industry, as they are building blocks for diverse polyamides. As plastic consumption is encouraged to decrease, the market for bioplastic is growing[30]. The sustainable production of biogenic diamines through microbial fermentation with renewable feedstocks will therefore be the cornerstone in the green production of polyamides. Furthermore, the use of the diamine spermidine in the pharmaceutical and food industry is gaining interest. Methanol is an alternative non-food feedstock, which does not compete with the feed industry[5]. However, the conventional cell factories *E. coli* and *C. glutamicum*, does not utilize methanol[6]. *B. methanolics* MGA3 can utilize methanol, and developments within its genetic toolbox have increased over the years. In recent years, this methylotrophic bacteria has been explored for methanol-based production of multiple amino acids, such as l-glutamate, and l-lysine[17]. In this section, the suitability of *B. methanolicus* for the overproduction of putrescine and spermidine will be discussed in relation to the findings of this study as well as previous research.

B. methanolicus MGA3 was shown to be a suitable host for putrescine overproduction in this study. Firstly, diamines such as putrescine have been reported to have toxic effects when accumulated in multiple organisms, which could affect the growth of the cell[27]. Low tolerance of the product in a production host is undesirable, as it could result in cellular stress and hinder cell growth rates, ultimately leading to reduced production capacity[74]. Putrescine tolerance was observed in up to 30 mM putrescine dihydrochloride (2.6 gL^{-1} putrescine) in this study (Table 3.2), which is in agreement with previously reported putrescine tolerance of at least 100 mM (8.8 gL^{-1} putrescine) in *B. methanolicus*[54]. However, the response of *B. methanolicus* to higher than 100 mM putrescine has not been tested. In comparison, *E. coli* cells grew well in 250 mM putrescine dihydrochloride (equivalent to 22 gL^{-1} putrescine, however, the growth rate was 40% less than the control (cultivation with no putrescine)[31]. Moreover, in *C. glutamicum* a high putrescine tolerance, with growth in 750 mM putrescine dichloride (66 gL^{-1} putrescine), with a reduction in the growth rate of 34%. In regard to the observed putrescine intolerance in *E. coli* and *C. glutamicum*, putrescine intolerance could potentially be observed for higher concentrations than 100 mM for *B. methanolicus*. However, this needs to be experimentally tested. In comparison to cadaverine tolerance, *B. methanolicus* tolerates up to 200 mM cadaverine dihydrochloride (35 gL^{-1} cadaverine), which was found to be similar to the *E. coli* tolerance, with a reduced growth rate of 20% and 35 %, respectively[25]. Secondly, no utilization of putrescine neither as a carbon nor as a nitrogen source was observed in this study (Figure 3.1). The utilization of putrescine for biomass production would result in lower putrescine titers. For instance, the Puu pathway in *E. coli* utilized extracellular putrescine for the production of succinate, through the intermediate GABA[31]. Succinate is thereafter utilized for growth through the TCA cycle[31]. Moreover, putrescine is utilized for spermidine production. Qian et al. reported that the deletion of the Puu pathway genes, and *speE* encoding for spermidine synthase, combined with overexpression of *speC*, which increases the flux towards the ODC pathway resulted in high-level putrescine production in the recombinant *E. coli* strain, compared to the equal strain with the Puu pathway genes. However, as this pathway was reported to not exist in *B. methanolicus* MGA3, no deletion of degradation pathways is necessary[75]. Finally, *B. methanolicus* MGA3 has shown to be a competitive producer of the putrescine equivalent C4 diamine cadaverine, with production levels of 0.5 gL^{-1} and 11.3

gL^{-1} in shake-flask, and fed-batch methanol fermentation, respectively[25]. Furthermore, an increase in the overall l-lysine production gave higher cadaverine titers[25]. Moreover, *B. methanolicus* MGA3 has the ability to produce up to 59 gL^{-1} of glutamate in fed-batch cultivations[1], which is advantageous for the overproduction of downstream metabolites like putrescine. As glutamate is a precursor for other amino acids, overproduction of those in *B. methanolicus* is therefore possible through genetic engineering. *B. methanolicus* has already been engineered for the overproduction of glutamate-derived metabolites, such as GABA (9.0 gL^{-1} in fed-batch methanol fermentation) through heterologous expression of glutamate decarboxylase[75]. To summarize, *B. methanolicus* is a potentially efficient putrescine-producing bacteria, as it is an efficient l-glutamate producer, has a high tolerance to the product and its precursor arginine (Table 3.2), as well as lacking a degradation pathway.

Low spermidine tolerance in *B. methanolicus* MGA3 might have been a bottleneck for spermidine production. Spermidine accumulation has been reported to decrease the number of viable cells and inhibits growth in a *E. coli* strain deficient in spermidine acetyltransferase (SpeG)[76]. SpeG catalyzes the acetylation of polyamines such as putrescine and spermidine, which regulates the intracellular content of those diamines[76]. Most polyamines are found as RNA-polyamine complexes intracellularly and stimulate protein synthesis through structural changes in the Shine-Dalgarno (SD) sequence in mRNA to facilitate the formation of the initiation complex[76]. However high concentrations of these have been observed to be cytotoxic mainly due to increased alterations in the bulged-out region of the mRNA structure, which causes an inhibitory effect on protein synthesis[76]. The *E. coli* strain deficient in SpeG was shown to be less tolerant towards spermidine supplementation (4 mM) compared to the parental *E. coli* strain harboring the gene encoding SpeG[76]. In this present study, a 4-fold and 12-fold reduction of growth rate and final biomass, respectively, of *B. methanolicus* MGA3 was observed in 7.5 mM spermidine (1 gL^{-1}) compared to the control (Figure 3.2). Moreover, an IC_{50} of 4.8 mM spermidine (0.7 gL^{-1}), and 5.3 mM spermidine (0.8 gL^{-1}) of combined putrescine and spermidine were observed (Figure 3.2 and 3.3). The synergistic inhibitory effect is most likely caused by spermidine inhibition, based on the higher putrescine tolerance of *B. methanolicus* (Table 3.2). Indeed, the findings of this study indicate that *B. methanolicus* MGA3 exhibits a similar level of spermidine intolerance as the *E. coli* strain deficient in SpeG. This similarity can be attributed to the fact that *B. methanolicus* MGA3 also lacks the gene responsible for SpeG expression[59], similar to *E. coli*. Moreover, *B. methanolicus* MGA3 was incapable to utilize spermidine as the sole carbon or nitrogen source for growth (Figure 3.1), which makes it a possible host for spermidine overproduction, however, the low tolerance towards spermidine is a disadvantage, as growth will be impaired, and consequently potential spermidine titers would be low[54].

In this study, the heterologous expression of *speAB* in *B. methanolicus* (PUT^{Ec}) resulted in the putrescine titers of 47.5 $\pm$ 0.8 µM (4.1 mgL^{-1}) by means of 0.1% xylose induction. Moreover, the homologous expression (PUT^{Bm}) did not result in higher putrescine titers in comparison to the empty vector control strain (Figure 3.5). A reason for this could be that the different enzymes have different optimal conditions and activities. From a screening of four distinct heterologous SpeA enzymes (Table 3.1) the most optimal enzyme was rendered to be SpeA derived from *E. coli*. Based on the K_M value (0.03 mM) and specific activity (2.8 U mg^{-1}) of purified enzyme), SpeA had the highest affinity to the substrate arginine, and the highest specific activity compared to the other three heterologous SpeA enzymes. Additionally, the *E. coli* SpeA enzyme displayed optimal performance at neutral pH and a temperature of 50 °C, which are advantageous traits for cultivation in *B. methanolicus*. Therefore, the use of *E. coli* as the gene donor for *speA* offered advantages over other donors. The properties of SpeB from *E. coli* were found to be

suitable for expression in *B. methanolicus* in terms of pH and temperature as well. This compatibility between the expression conditions and the host strain's growth conditions likely contributed to the high putrescine titers achieved through heterologous expression of $speAB^{Ec}$ in *B. methanolicus*. Moreover, the enzymatic properties of *B. methanolicus* SpeAB are not characterized. However, SpeA in *B. methanolicus* presumably have similar properties, of optimal pH and temperature, as the closely related *B. subtilis*, the soil bacteriaspecies *Pseudomonas*, or other Gram-positive bacteria such as *H. pylori*, which in addition had lower enzyme activities compared to SpeA derived from *E. coli*. This could be the reason why the heterologous expression of SpeAB from *E. coli*, resulted in higher putrescine concentrations than that with homologous expression. However, the enzymatic activity of homologous SpeAB in *B. methanolicus* remains to be experimentally tested.

The PUT^{Ec} strain is a pBV2xp-based strain with a xylose promoter, which has shown to be stable in industrial production of compunds[20]. Xylose is not utilzed in *B. methanolicus* MGA3 as a carbon source, making it suitable as a gratuitous plasmid inducer[20]. Irla et al. presented multiple advantages of a xylose promoter, herein, the low background expression of genes in an uninduced state, and higher production titers compared to constitutive *mdh* promoter when fully induced with 1% xylose[20]. Moreover, expression levels of the reporter gene *gfpuv* in different xylose induction levels were presented, where a plateau in gene expression was reported from 0.5% to 1% induction[20]. Here in this study, a similar plateau effect was observed where the optimal putrescine production with 0.1% xylose induced and full plasmid induction in the PUT^{Ec} strain resulted in similar putrescine-titers, however, a larger error was observed at fully induced state which indicates lower production stability. The induction with 0.5 % xylose was not performed in this study, however, the similar production titers observed for PUT^{Ec} from 0.1 to 1% xylose induction (Figure 3.5-C and 3.5-D), indicates that 0.5% xylose induction would result in similar production titers.

The highest and most stable putrescine titer and productivity measured in PUT^{Ec} (4.1 mgL^{-1} and 0.17 $gL^{-1}h^{-1}$, respectively) are substantially lower than the putrescine titer and productivity produced from *E. coli* (43.0 gL^{-1} and 1.26 $gL^{-1}h^{-1}$, respectively) and *C. glutamicum* (19 gL^{-1} and 0.55 $gL^{-1}h^{-1}$, respectively)[77,39]. Firstly, in this study, shake-flask cultivations were performed for 24 hours, while Noh et al. and Schneider et al. performed cultivations in fed-batch cultivations for *E. coli* XQ52(p15SpeC) and *C. glutamicum* PUT21, respectively, with glucose as feedstock. Fed-batch cultivations often give higher production titers, as media composition is regulated through feeding strategies[1]. Moreover, strategies that involved overexpressing the ODC pathway were performed in those studies, whereas in the present study, the ADC pathway was utilized because of its nativity in *B. methanolicus* MGA3. Furthermore, the overexpression of the ADC pathway in *E. coli* have been reported to increase extracellular putrescine production compared to the expression of *speC* or *speABC*[41]. Thongbhubate et al. produced titers of 19 mM (1.7 gL^{-1}) putrescine in shake-flask cultivation with glycerol as carbon source, which gave high putrescine titers because of higher precursor arginine availability[41]. The increased arginine availability was achieved by knock-out of the *argR* repressor gene, and desensitizing the feedback inhibition of arginine on ArgA in *E. coli* (Section 1.4.1)[41]. Consistent with these findings, the supplementation of 1 mM arginine in the cultivation of PUT^{Ec} in this present study resulted in a 4.9-fold increase in putrescine production compared to no supplementation (Figure 3.7).

Moreover, amino acid production requires an efficient supply of nitrogen. It has been observed that the improvement in nitrogen supply can enhance the production of l-threonine in *C. glutmaicum*[55]. This bacterium is a workhorse for large-scale production of amino acids which utilizes the nitrogen-rich CGXII as media for growth and production[78]. Here, cultivation of PUT^{Ec} in the nitrogen-rich CGXII media

(4.4 gL^{-1} nitrogen) increased the putrescine production 2-fold, in comparison to cultivation in MVcM (0.2 gL^{-1} nitrogen) (Figure 3.8). In the media, urea and ammonium sulfate are the nitrogen sources[78]. Urea has shown to be an efficient and cheap nitrogen source for *C. glutamicum*, and was shown to have a strong positive influence on cell growth[79]. However, in the cultivation of the *B. methanolicus* strain PUT^{Ec} in CGXII a decrease in growth rate and biomass production of 1.2-fold and 1.5-fold, respectively, was observed in comparison to the control (MVcM) (Table 3.5). The decrease in growth rate may be a consequence of the metabolic burden imposed by putrescine production in the cell[76]. Even though putrescine tolerance is high in *B. methanolicus* (Table 3.2), overexpression of target genes requires energy that comes from the cellular resources of the host, which could cause stress upon the host[80]. Furthermore, the effect of pH could also explain the higher putrescine production in the PUT^{Ec} strain cultivated in CGXII. Here, the initial pH of the cultivation media was neutral (pH around 7) in MVcM, MVcM2, and CGXII. This is known to be optimal for the activity of SpeAB enzymes from *E. coli* (Table 3.1). However, Nærdal et al. observed that the acidification of cultivation media (MVcM) occurred when the diamine cadaverine was produced in *B. methanolicus*[75]. This suggests that the production of putrescine with the PUT^{Ec} strain could also contribute to the acidification of MVcM media which may inhibit further putrescine production in this medium[75]. Additionally, CGXII media contains a MOPS buffer which is known to provide a constant pH in cultivation over time[78,81]. The cultivation in constant pH 7 is beneficial for the SpeAB enzymes based on the optimal pH values observed from the screening of the heterologous enzymes (Table 3.1), which would explain the higher putrescine titers in CGXII media. However, it should be noted that the pH of the media under cultivation was not measured in this study, and further investigations are needed to determine the impact of pH changes during putrescine production. To summarize, an increase in arginine supply and media optimization, emphasized on nitrogen supply, was shown to be important for high putrescine-titers through the ADC pathway in *B. methanolicus*, where neutral pH was indicated to be beneficial for putrescine production through cultivation in CGXII. By combining the optimized conditions identified in this study, it is possible to achieve higher putrescine production from PUT^{Ec}. This could potentially make the strain competitive compared to other putrescine-producing strains that utilize the ADC pathway[41].

As spermidine toxicity is observed in multiple bacteria[76], it could also explain the difficulty in the cloning of plasmid pTH1mp-*speE*^{Ec} (Section 3.4). pTH1mp is a rolling circle replicating plasmid with a constitutive *mdh* promoter[20]. This *mdh* promoter is classified as a constitutive promoter due to high background expression without the addition of methanol and is known to be active in *E. coli*[21,82]. This would indicate that the *speE* gene could be expressed when transformed to *E. coli* DH5α. This could trigger a defense mechanism in *E. coli*, *e.g.* Insertion Sequence (IS)-mediate mutations, resulting in a frameshift mutation[83].

Unexpectedly, the PUT^{Bm} strain induced with 0.1% xylose produced the highest spermidine titers of 68.3 $\pm$ 4.7 µM (9.9 mgL^{-1}) after 48 hours of cultivation (Figure 3.6). Putrescine concentration was not detected for this strain (Figure 3.5), however a 2.3-fold decrease in arginine concentration, compared to the control PBV was observed for this condition, similar to the decrease in arginine concentration found in the putrescine producing PUT^{Ec} strain (Figure 3.4). The high spermidine production in PUT^{Bm} compared to spermidine production in empty vector control strain (PBV) suggests that the activity of homologous SpeAB results in a metabolic pull that deregulates flux through the ADC and SBS pathways. While in PUT^{Ec} the heterologous expression of *speAB* exerts a metabolic pull deregulating flux through the ADC pathway for putrescine production. Similarly Nærdal et al. reported high cadaverine titers in

the production strain compared to the l-lysine titer in the empty vector control strain, attributing this difference to a similar metabolic pull that deregulated flux through the l-lysine biosynthesis pathway[25].

Multiple plasmids expressing heterologous and homologous SpeE or SpeEH were produced in both *B. methanolicus* MGA3 and the putrescine producing strain PUT^{Ec}. Based on data from this study (Table 3.6), $SPE_{ii}{}^{Ec}$, and $SPE_{ii}{}^{Bm}$ produced the highest spermidine titers, with 6.2 ± 0.4 µM (0.9 mgL^{-1}) and 6.3 ± 0.4 (0.9 mgL^{-1}) µM respectively, which was 1.2-fold higher than the control, PTH, and SPE^{Bm}. This indicates that a presumably increase in dAdoMet through overexpression of the *speH* gene, increases the spermidine production through co-expression with the *speE* gene. In *B. amyloliquefaciens*, Zou et al. showed that expression of the *speH* gene from *E. coli* and *speE* gene from *S. cerevisae* gave spermidine titers of 227.4 mg L^{-1} after 84 hours of batch cultivation with maximum OD_{600} at around 20. The significantly lower spermidine titers observed in $SPE_{ii}{}^{Ec}$, and $SPE_{ii}{}^{Bm}$ could therefore be because of low growth (5.54 ± 0.22 and 5.70 ± 0.18, respectively) compared to the recombinant *B. amyloliquefaciens* strain.

The insufficient supply of putrescine was initially hypothesized to be the reason for only a 1.2-fold increase in spermidine titers in this study (Table 3.6). However, the increased putrescine supply through the expression of the *speE* or *speEH* genes in PUT^{Ec}, did not result in higher spermidine titers compared to the control PBV PTH (4.3 ± 0.2) (Table 3.7). This indicated that SpeE and SpeH are insufficient to convert putrescine and dAdoMet to spermidine, compared to the control. Moreover, SpeH is highly dependent on a pyruvoyl cofactor during the decarboxylation of AdoMet[45]. Even with overexpression of *speH*, it cannot be assumed that the availability of the pyruvoyl cofactor necessarily increases which might be why the expression of *speEH* did not convert putrescine efficiently in the strain $PUT^{Ec}SPE_{ii}{}^{Ec}$.

Notably, the final biomass of $PUT^{Ec}SPE^{Bm}$, and $PUT^{Ec}SPE_{ii}{}^{Ec}$ was 1.1-fold and 1.3-fold lower than PBV PTH (Table 3.7). The growth could therefore have an effect on the insufficient conversion of putrescine to spermidine. Moreover, Zou et al. did indeed suggest that spermidine production was partly growth-coupled, where cell growth entered a stationary phase at 48 hours, and the maximum spermidine titer was reached after 84 hours. They also measured the concentration of precursor AdoMet, in comparison to spermidine production in their best producer of spermidine, HSAM2(PDspeD-SspeE), which showed a sharp drop in the AdoMeth concentration, accompanied by an increase in spermidine titers after 24 hours. This indicated that AdoMet was utilized for spermidine biosynthesis[45]. Similarly in this study, putrescine titers for $PUT^{Ec}SPE^{Bm}$, and $PUT^{Ec}SPE_{ii}{}^{Ec}$ was 2.8-fold and 1.5-fold lower, respectively, while their spermidine titers where 3-fold and 2-fold higher, respectively, compared to the control PUT^{Ec}PTH. This indicates that putrescine was converted to spermidine, however as the quantification of the precursor was still high, more conversion to spermidine could be possible through further genetic engineering. Moreover, $PUT^{Ec}SPE^{Bm}$ grew better than $PUT^{Ec}SPE_{ii}{}^{Ec}$, which could be the reason why 1.4-fold higher spermidine titers were observed for $PUT^{Ec}SPE^{Bm}$.

Growth of *B. methanolicus* MGA3 was observed to be inhibited by spermidine (Figure 3.2), the overexpression of spermidine could therefore be the major reason for inhibited growth in strains $PUT^{Ec}SPE^{Bm}$, $PUT^{Ec}SPE_{ii}{}^{Ec}$ and no growth of $PUT^{Ec}SPE_{ii}{}^{Bm}$. The constitutive expression of the gene encoding for the SBS pathway could have a negative effect on the production, as high cell densities were not able to be achieved as genes for the SBS pathway are getting expressed. The toxic effect of this could be a major reason for low growth and therefore also inhibition in the production of more spermidine[76]. In contrast, the use of an inducible expression system (such as pBV2xp) in acetoin production with *B. methanolicus*

MGA3 allowed for the decoupling of growth from the production of acetoin. This decoupling was beneficial because acetoin had been shown to inhibit the growth of MGA3. By achieving high cell densities before induction, the inhibitory effects of acetoin were minimized, enabling more efficient production[4].

A similar two-plasmid-based expression system as this study was shown in Klein et al. for the overproduction of riboflavin in *B. methanolicus* MGA3. They observed that the introduction of both pBV2xp and pTH1mp plasmids in *B. methanolicus* MGA3 did not impact production stability, compared to only the introduction of pBV2xp[3]. The riboflavin titers of strain BV_RIB^{BI}(TH-Ctr) harboring the pBV2xp plasmid with *rib* operon and empty vector pTH1mp produced 34-fold higher titers than the BV_RIB^{BI} strain. Klein et al. observed that the concentration of riboflavin increased when supplementation with sublethal chloramphenicol concentrations, which was hypothesized to be because of increased copy number of pBV2xp, which finally increased the riboflavin production. However, this is not in compliance with this present study (Table 3.7), as the PUT^{Ec}PTH (4.8 $\pm$ 0.2 mM) produced 10-fold lower putrescine titers compared to PUT^{Ec}. However, this discrepancy could be because of the lower growth of the PUT^{Ec}PTH (OD_{600} of 3.51 $\pm$ 0.90) compared to PUT^{Ec} (OD_{600} of 7.26 $\pm$ 0.90), in similar conditions of 0.1% xylose induction and cultivation in shake-flasks. The lower growth observed remains unknown and requires further investigation. Additionally, the two-plasmid-based expression system should be further experimentally tested.

4.1 Outlook

PUT^{Ec} is a promising strain for methanol-based putrescine production. The supply of precursor arginine and increased nitrogen source enhanced putrescine titers, a combination of those strategies could lead to higher putrescine titers, which would be more competitive. The rate-controlling step in arginine biosynthesis of *E. coli* and *C. glutamicum* is reported to be the operon *argGH*[42]. As this operon is also found in *B. methanolicus*, it could be a rate-controlling step in arginine biosynthesis in this organism as well[84]. The overexpression of the *argGH* genes, and the *speAB* genes through a two-plasmid-based expression system could increase the availability of precursor arginine towards an elevated conversion to putrescine, which is advantageous, as expensive supplementation is unwanted. To increase arginine concentration further, possible negative feedback inhibition of the compound on enzymes in the arginine biosynthesis pathway of *B. methanolicus* should be desensitized. In *E. coli*, the desensitizing of arginine inhibition on ArgA was done[41], while in *C. glutamicum* the desensitizing of arginine inhibition of ArgB was done[38], in combination with deletion of the ArgR repressor in both organisms to increase arginine supply. As *B. methanolicus* is not found to have ArgA and is observed to have a similar arginine biosynthesis pathway as *C. glutamicum* the regulatory approaches done for higher arginine supply in *C. glutamicum* could be done for *B. methanolicus*[38, 34]. A search through the *B. methanolicus* MGA3 genome showed an equivalent arginine repressor AhrC (BMMGA3_11380), which could similarly be deleted for higher production of arginine[84]. Arginine catabolism through competitive pathways of the ADC pathway should also be depleted, where the *rocF* (BMMGA3_00985) gene encoding for an arginase that catabolizes arginine to ornithine should be downregulated. Available tools for gene repression in *B. methanolicus* MGA3 could be through the use of CRISPRi/dCas9-tool developed by Schultenkämper et al., which could be used to contribute to increased flux towards putrescine biosynthesis in *B. methanoliocus* through the depletion of the mentioned genes. Moreover, the export of arginine would decrease available intracellular arginine for putrescine conversion, therefore these transporters should be further analyzed. Two putative

arginine/ornithine antiporters (BMMGA3_09205 and BMMGA3_01150) have been identified which allow high-efficiency energy conversion in the arginine deiminase pathway, which is an anaerobic route for arginine degradation[84, 85]. As *B. methanolicus* MGA3 grow aerobically[6], the expression of these genes is unlikely, however, they should still be functionally characterized to ensure minimal arginine degradation through competitive pathways.

A comprehensive review of diamine transport in *B. methanolicus* should be considered before genetic engineering to uncover potential transporters. Moreover, a quantification of the intracellular content of putrescine and spermidine would help with the unraveling of the interplay between biosynthesis, export, and potential catabolism of putrescine and spermidine. Intracellular content and enzymatic activity could be measured by quantifying the compounds in the crude extract as previously described for measuring lysine decarboxylase activity in *B. methanolicus*[25]. Increased putrescine export would be beneficial for higher putrescine titers. Three putative spermidine/putrescine transporters have been identified in *B. methanolicus*[20]. The gene BMMGA3_08890 is denoted as a spermidine/putrescine importer ABC transporter permease PotC in the *B. methanolicus* genome and PotA is denoted as a spermidine/putrescine import ATP-binding protein, which in *E. coli* is a part of the spermidine-preferential uptake system in *E. coli* PotABCD[36]. The uptake of spermidine would decrease the extracellular concentration, therefore knock-down strategies should be done to prevent the decrease in *B. methanolicus*.The gene BMMGA3_08895 is denoted as a spermidine/putrescine ABC transporter which could encode for other putrescine/spermidine transporters such as the PotFGHI putrescine importer or PotE putrescine exporter/importer in *E.coli*. However, further characterization is needed to confirm their activity in *B. methanolicus*.

In *E. coli*, the overexpression of the *potE* gene and knock-out of the *puuP* gene increased extracellular putrescine[31]. The PotE functioned as an exporter at acidic pH, while in neutral pH it was functioning as an importer[46]. The identified exported in *E. coli* should be explored more for diamine export in *B. methanolicus* through heterologous expression. A spermidine exporter MdtJI in *E. coli* has been identified for the export of spermidine at neutral pH[46]. Moreover, the heterologous expression of putrescine and spermidine exported could result in decreased cell growth because of possible low tolerance to the products. Putrescine tolerance has been shown to be at least 100 mM, however, the tolerance should be tested in higher concentrations. The low spermidine tolerance was indicated to be the reason for the low spermidine production of the putative spermidine overproducing strains from this study. This tolerance could be increased through adaptive laboratory evolution approaches, which was successfully done for increased *B. methanolicus* tolerance to 5AVA[54]. ALE involves subjecting cells to a gradual increase in product concentration through a series of passages, where cells are harvested and their product tolerance is assessed to select the most tolerant strain[54]. After selection of a higher spermidine tolerant *B. methanolicus* strain, methanol-based spermidine overproduction could be achieved.

As optimal pH levels for increased putrescine and spermidine production would depend on both the optimal pH of the enzymes for biosynthesis and the export enzymes, an optimized pH regulation should therefore be experimentally tested, which would be possible through cultivation in a bioreactor with the possibility to regulate pH after different growth phases. This was done in the optimal production of GABA in *B. methanolicus*, through decreasing the pH of the medium at stationary phase[75]. The higher putrescine titers in PUT^{Ec} cultivated in CGXII indicate optimal pH around 7 for putrescine overproduction, however, optimal pH levels for both putrescine and spermidine excretion should be experimentally tested in *B. methanolicus*, to confirm the observations in this study. Moreover, the utilization of CGXII medium for *B. methanolicus* cultivation should be further explored. The higher putrescine production was most likely

because of higher nitrogen concentration in the medium and more stable pH, however, the metabolism of urea and ammonium sulfate in *B. methanolicus* should be explored further.

Indications of SpeAB activity were observed in PUT^{Ec} through increased putrescine production. The increased spermidine titers for $SPE_{ii}{}^{Ec}$ and $SPE_{ii}{}^{Bm}$ also indicated SpeEH activity. However, in order to confirm the increased titers in recombinant *B. methanolicus* strain are indeed due to the increased activity of the expressed enzymes, it is necessary to test the enzymatic activity of SpeAB and SpeEH. This can be achieved through enzyme assays, as explained in Nærdal et al., where the specific activity of lysine decarboxylase was calculated by measuring the conversion of lysine to cadaverine over time using HPLC and measuring protein concentration through Bradford assay[25].

For spermidine production, cultivation of 48 hours could result in higher spermidine titers as observed in Zou et al., which should be experimentally tested[45]. Finally, up-scaling in fed-batch fermentation could give competitive putrescine and spermidine titers as already established putrescine producers *E. coli* and *C. glutamicum* and spermidine producers *B. amyloliquefaciens* and *S. cerevisae*[73, 33, 45, 43], through the regulation of nitrogen uptake, pH, and temperature.

5 Conclusion

In this study, methanol-based overproduction of putrescine through metabolic engineering of the ADC pathway was achieved, and insights into methanol-based spermidine overproduction are presented. PUT^{Ec}, an recombinant *B. methanolicus* strain with xylose inducible plasmid-based expression of *speA* and *speB* genes was the best-performing strain for putrescine production of 47.5 $\pm$ 0.8 µM. Optimal conditions for the highest and most stable putrescine production were shown to be at an induction level of 0.1% xylose. Further optimization showed that supplementation of arginine and higher nitrogen supplementation in the media resulted in 4.9-fold and 2-fold, respectively, higher putrescine production titers than the control.

Spermidine production was analyzed to be natively higher than putrescine production in *B. methanolicus* MGA3, as a consequence of spermidine being downstream to putrescine production. An increase in spermidine titers through the heterologous and homologous expression of SpeE and/or SpeH in *B. methanolicus* was attempted which resulted in highest titers of 6.2 $\pm$ 0.4 µM and 6.3 $\pm$ 0.4 µM spermidine in SPE_{ii}^{Ec} and SPE_{ii}^{Bm}, respectively. An increase in these titers was expected when the spermidine precursor putrescine was made available by means of *speAB* overexpression, however $PUT^{Ec}SPE_{ii}^{Ec}$ produced lower spermidine titers than the control, while $PUT^{Ec}SPE_{ii}^{Bm}$ did not grow. With respect to spermidine production, the experimental results revealed clear challenges regarding the growth of recombinant strains engineered for increased spermidine production, the effectiveness of the SpeEH enzymes in a two-plasmid-based expression, and also regarding the construction of plasmid pTH1mp-spe^{Ec}. Efforts should be made to increase spermidine tolerance in *B. methanolicus*, and an analysis of the enzymatic activity of the enzymes regarding both putrescine and spermidine biosynthesis should be done.

In summary, this study has provided valuable insights regarding the methanol-based overproduction of putrescine and spermidine through the use of *B. methanolicus* MGA3 as a cell factory. Additionally, this study will contribute to the green shift in industrial biotechnology, by decreasing the use of nonrenewable feedstock and introducing alternative green feedstocks for the production of value-added compounds.

References

[1] Trygve Brautaset, Øyvind M Jakobsen, Kjell D Josefsen, Michael C Flickinger, and Trond E Ellingsen. *Bacillus methanolicus*: a candidate for industrial production of amino acids from methanol at 50 c. *Applied microbiology and biotechnology*, 74:22–34, 2007. URL https://doi.org/10.1007/s00253-006-0757-z.

[2] Judith Becker and Christoph Wittmann. Diamines for bio-based materials. *Industrial Biotechnology: Products and Processes*, pages 391–409, 2017.

[3] Vivien Jessica Klein, Luciana Fernandes Brito, Fernando Perez-Garcia, Trygve Brautaset, and Marta Irla. Metabolic engineering of thermophilic *Bacillus methanolicus* for riboflavin overproduction from methanol. *Microbial Biotechnology*, 2023. URL https://doi.org/10.1111/1751-7915.14239.

[4] Eivind B Drejer, Dennis Tin Chat Chan, Carsten Haupka, Volker F Wendisch, Trygve Brautaset, and Marta Irla. Methanol-based acetoin production by genetically engineered *Bacillus methanolicus*. *Green Chemistry*, 22(3):788–802, 2020. URL https://doi.org/10.1039/C9GC03950C.

[5] Jonas EN Müller, Tonje Heggeset, Volker F Wendisch, Julia A Vorholt, and Trygve Brautaset. Methylotrophy in the thermophilic *Bacillus methanolicus*, basic insights and application for commodity production from methanol. *Applied microbiology and biotechnology*, 99(2):535–551, 2015. URL https://link.springer.com/article/10.1007/s00253-014-6224-3.

[6] Johannes Pfeifenschneider, Trygve Brautaset, and Volker F Wendisch. Methanol as carbon substrate in the bio-economy: Metabolic engineering of aerobic methylotrophic bacteria for production of value-added chemicals. *Biofuels, Bioproducts and Biorefining*, 11(4):719–731, 2017. URL https://doi.org/10.1002/bbb.1773.

[7] Methanex. https://www.methanex.com/about-methanol/pricing/, 2023.

[8] United states department of agriculture. chrome-extension://efaidnbmnnnibpcajpcglclefindmkaj/https://www.ers.usda.gov/webdocs/outlooks/106577/sss-m-417.pdf?v=5346.4, 2023.

[9] Benjamin M Woolston, Jason R King, Michael Reiter, Bob Van Hove, and Gregory Stephanopoulos. Improving formaldehyde consumption drives methanol assimilation in engineered *E. coli*. *Nature communications*, 9(1):2387, 2018. URL https://doi.org/10.1038/s41467-018-04795-4.

[10] Volker F Wendisch, Gregor Kosec, Stéphanie Heux, and Trygve Brautaset. Aerobic utilization of methanol for microbial growth and production. In *One-Carbon Feedstocks for Sustainable Bioproduction*, pages 169–212. Springer, 2021. URL https://doi.org/10.1007/10_2021_177.

[11] Bo Gao, Ning Zhao, Jieying Deng, Yang Gu, Shiru Jia, Ying Hou, Xueqin Lv, and Long Liu. Constructing a methanol-dependent *Bacillus subtilis* by engineering the methanol metabolism. *Journal of Biotechnology*, 343:128–137, 2022. URL https://doi.org/10.1016/j.jbiotec.2021.12.005.

[12] J. E. Müller, F. Meyer, and B. Litsanov. Engineering *Escherichia coli* for methanol conversion. *Metabolic Engineering*, 28:190–201, 3 2015. doi: 10.1016/j.ymben.2014.12.008. URL http://dx.doi.org/10.1016/j.ymben.2014.12.008.

[13] Eugen Pfeifer, Cornelia Gätgens, Tino Polen, and Julia Frunzke. Adaptive laboratory evolution of *Corynebacterium glutamicum* towards higher growth rates on glucose minimal medium. *Scientific reports*, 7(1):1–14, 2017. URL https://doi.org/10.1038/s41598-017-17014-9.

[14] Frederic Y-H Chen, Hsin-Wei Jung, Chao-Yin Tsuei, and James C Liao. Converting *Escherichia coli* to a synthetic methylotroph growing solely on methanol. *Cell*, 182(4):933–946, 2020. URL https://doi.org/10.1016/j.cell.2020.07.010.

[15] Anh Duc Nguyen, In Yeub Hwang, Jeon Young Chan, and Eun Yeol Lee. Reconstruction of methanol and formate metabolic pathway in non-native host for biosynthesis of chemicals and biofuels. *Biotechnology and Bioprocess Engineering*, 21(4):477–482, 2016. URL https://doi.org/10.1007/s12257-016-0301-7.

[16] Vivien Jessica Klein, Marta Irla, Marina Gil López, Trygve Brautaset, and Luciana Fernandes Brito. Unravelling formaldehyde metabolism in bacteria: Road towards synthetic methylotrophy. *Microorganisms*, 10(2), 2022. ISSN 2076-2607. URL https://www.mdpi.com/2076-2607/10/2/220.

[17] Tonje MB Heggeset, Anne Krog, Simone Balzer, Alexander Wentzel, Trond E Ellingsen, and Trygve Brautaset. Genome sequence of thermotolerant *Bacillus methanolicus*: features and regulation related to methylotrophy and production of l-lysine and l-glutamate from methanol. *Applied and environmental microbiology*, 78(15):5170–5181, 2012. URL https://doi.org/10.1128/AEM.00703-12.

[18] Kerstin Schultenkämper, Luciana F Brito, Marina Gil López, Trygve Brautaset, and Volker F Wendisch. Establishment and application of CRISPR interference to affect sporulation, hydrogen peroxide detoxification, and mannitol catabolism in the methylotrophic thermophile *Bacillus methanolicus*. *Applied microbiology and biotechnology*, 103:5879–5889, 2019. URL https://doi.org/10.1007/s00253-019-09907-8.

[19] Marina Gil López, Marta Irla, Luciana F Brito, and Volker F Wendisch. Characterization of d-arabitol as newly discovered carbon source of *Bacillus methanolicus*. *Frontiers in Microbiology*, 10:1725, 2019. URL https://doi.org/10.3389/fmicb.2019.01725.

[20] Marta Irla, Tonje MB Heggeset, Ingemar Naerdal, Lidia Paul, Tone Haugen, Simone B Le, Trygve Brautaset, and Volker F Wendisch. Genome-based genetic tool development for *Bacillus methanolicus*: theta-and rolling circle-replicating plasmids for inducible gene expression and application to methanol-based cadaverine production. *Frontiers in microbiology*, 7:1481, 2016. URL http://dx.doi.org/10.3389/fmicb.2016.01481.

[21] Eivind B Drejer, Sigrid Hakvåg, Marta Irla, and Trygve Brautaset. Genetic tools and techniques for recombinant expression in thermophilic bacillaceae. *Microorganisms*, 6(2):42, 2018. URL https://doi.org/10.3390/microorganisms6020042.

[22] Marta Irla, Sigrid Hakvåg, and Trygve Brautaset. Developing a riboswitch-mediated regulatory system for metabolic flux control in thermophilic *Bacillus methanolicus*. *International Journal of Molecular Sciences*, 22(9):4686, 2021. URL https://doi.org/10.3390/ijms22094686.

[23] Baudoin Delépine, Marina Gil López, Marc Carnicer, Cláudia M Vicente, Volker F Wendisch, and Stéphanie Heux. Charting the metabolic landscape of the facultative methylotroph *Bacillus methanolicus*. *Msystems*, 5(5):e00745–20, 2020. URL https://doi.org/10.1128/mSystems.00745-20.

[24] Marta Irla and Volker F Wendisch. Efficient cell factories for the production of N-methylated amino acids and for methanol-based amino acid production. *Microbial Biotechnology*, 15(8):2145–2159, 2022. URL https://doi.org/10.1111/1751-7915.14067.

[25] Ingemar Nærdal, Johannes Pfeifenschneider, Trygve Brautaset, and Volker F Wendisch. Methanol-based cadaverine production by genetically engineered *Bacillus methanolicus* strains. *Microbial biotechnology*, 8(2):342–350, 2015. URL https://doi.org/10.1111/1751-7915.12257.

[26] Dian Zou, Ziyue Zhao, Lu Li, Yu Min, Daiyuan Zhang, Anying Ji, Cong Jiang, Xuetuan Wei, and Xian Wu. A comprehensive review of spermidine: Safety, health effects, absorption and metabolism, food materials evaluation, physical and chemical processing, and bioprocessing. *Comprehensive Reviews in Food Science and Food Safety*, 21(3):2820–2842, 2022. URL https://doi.org/10.1111/1541-4337.12963.

[27] Volker F Wendisch, Melanie Mindt, and Fernando Pérez-García. Biotechnological production of mono-and diamines using bacteria: recent progress, applications, and perspectives. *Applied microbiology and biotechnology*, 102:3583–3594, 2018. URL https://doi.org/10.1007/s00253-018-8890-z.

[28] Bioplastics market data. www.european-bioplastics.org/market, 2023.

[29] Li Wang, Guohui Li, and Yu Deng. Diamine biosynthesis: Research progress and application prospects. *Applied and Environmental Microbiology*, 86(23):e01972–20, 2020. URL https://doi.org/10.1128/AEM.01972-20.

[30] Fernando Pérez-García. *Microbial Production of Diamines*, pages 1–31. Springer Netherlands, Dordrecht, 2020. ISBN 978-94-007-6724-9. URL https://doi.org/10.1007/978-94-007-6724-9_14-1.

[31] Zhi-Gang Qian, Xiao-Xia Xia, and Sang Yup Lee. Metabolic engineering of *Escherichia coli* for the production of putrescine: a four carbon diamine. *Biotechnology and bioengineering*, 104(4):651–662, 2009. URL https://doi.org/10.1002/bit.22502.

[32] Yi Liu, Xing Guo, Xin Wang, Kequan Chen, and Pingkai Ouyang. A two-enzyme cascade system for the bio-production of spermidine from putrescine. *Molecular Catalysis*, 504:111439, 2021. URL https://doi.org/10.1016/j.mcat.2021.111439.

[33] Jens Schneider and Volker F Wendisch. Putrescine production by engineered *Corynebacterium glutamicum*. *Applied microbiology and biotechnology*, 88:859–868, 2010. URL https://doi.org/10.1007/s00253-010-2778-x.

[34] Kegg pathway database. https://www.kegg.jp/kegg/pathway.html, 2023.

[35] Shin Kurihara, Kenji Kato, Kei Asada, Hidehiko Kumagai, and Hideyuki Suzuki. A putrescine-inducible pathway comprising PuuE-YneI in which γ-aminobutyrate is degraded into succinate in *Escherichia coli* K-12. *Journal of bacteriology*, 192(18):4582–4591, 2010. URL https://doi.org/10.1128/JB.00308-10.

[36] Shin Kurihara, Yuichi Tsuboi, Shinpei Oda, Hyeon Guk Kim, Hidehiko Kumagai, and Hideyuki Suzuki. The putrescine importer PuuP of *Escherichia coli* k-12. *Journal of bacteriology*, 191(8):2776–2782, 2009. URL https://doi.org/10.1128/JB.01314-08.

[37] Jae Ho Shin and Sang Yup Lee. Metabolic engineering of microorganisms for the production of l-arginine and its derivatives. *Microbial cell factories*, 13:1–12, 2014. URL https://doi.org/10.1186/s12934-014-0166-4.

[38] Jens Schneider, Karin Niermann, and Volker F Wendisch. Production of the amino acids l-glutamate, l-lysine, l-ornithine and l-arginine from arabinose by recombinant *Corynebacterium glutamicum*. *Journal of biotechnology*, 154(2-3):191–198, 2011. URL https://doi.org/10.1016/j.jbiotec.2010.07.009.

[39] Jens Schneider, Dorit Eberhardt, and Volker F Wendisch. Improving putrescine production by *Corynebacterium glutamicum* by fine-tuning ornithine transcarbamoylase activity using a plasmid addiction system. *Applied microbiology and biotechnology*, 95:169–178, 2012. URL https://doi.org/10.1007/s00253-012-3956-9.

[40] Anh QD Nguyen, Jens Schneider, and Volker F Wendisch. Elimination of polyamineN-acetylation and regulatory engineering improved putrescine production by *Corynebacterium glutamicum*. *Journal of Biotechnology*, 201:75–85, 2015. URL https://doi.org/10.1016/j.jbiotec.2014.10.035.

[41] Kullathida Thongbhubate, Kanako Irie, Yumi Sakai, Akane Itoh, and Hideyuki Suzuki. Improvement of putrescine production through the arginine decarboxylase pathway in *Escherichia coli* K-12. *AMB Express*, 11:1–13, 2021. URL https://doi.org/10.1186/s13568-021-01330-5.

[42] Seok Hyun Park, Hyun Uk Kim, Tae Yong Kim, Jun Seok Park, Suok-Su Kim, and Sang Yup Lee. Metabolic engineering of *Corynebacterium glutamicum* for l-arginine production. *Nature communications*, 5(1):4618, 2014. URL https://doi.org/10.1038/ncomms5618.

[43] Sun-Ki Kim, Jung-Hyun Jo, Yong-Cheol Park, Yong-Su Jin, and Jin-Ho Seo. Metabolic engineering of *Saccharomyces cerevisiae* for production of spermidine under optimal culture conditions. *Enzyme and Microbial Technology*, 101:30–35, 2017. URL https://doi.org/10.1016/j.enzmictec.2017.03.008.

[44] Jiufu Qin, Anastasia Krivoruchko, Boyang Ji, Yu Chen, Mette Kristensen, Emre Özdemir, Jay D Keasling, Michael Krogh Jensen, and Jens Nielsen. Engineering yeast metabolism for the discovery and production of polyamines and polyamine analogues. *Nature Catalysis*, 4(6):498–509, 2021. URL https://doi.org/10.1038/s41929-021-00631-z.

[45] Dian Zou, Lu Li, Yu Min, Anying Ji, Yingli Liu, Xuetuan Wei, Jing Wang, and Zhiyou Wen. Biosynthesis of a novel bioactive metabolite of spermidine from *Bacillus amyloliquefaciens*: gene mining, sequence analysis, and combined expression. *Journal of Agricultural and Food Chemistry*, 69(1):267–274, 2020. URL https://doi.org/10.1021/acs.jafc.0c07143.

[46] Kyohei Higashi, Hiroyuki Ishigure, Risa Demizu, Takeshi Uemura, Kunihiko Nishino, Akihito Yamaguchi, Keiko Kashiwagi, and Kazuei Igarashi. Identification of a spermidine excretion protein complex (MdtJI) in *Escherichia coli*. *Journal of bacteriology*, 190(3):872–878, 2008. URL https://doi.org/10.1128/JB.01505-07.

[47] Adam J Potter and James C Paton. Spermidine biosynthesis and transport modulate pneumococcal autolysis. *Journal of bacteriology*, 196(20):3556–3561, 2014. URL https://journals.asm.org/doi/abs/10.1128/JB.01981-14.

[48] Dokyun Na, Seung Min Yoo, Hannah Chung, Hyegwon Park, Jin Hwan Park, and Sang Yup Lee. Metabolic engineering of *Escherichia coli* using synthetic small regulatory RNAs. *Nature biotechnology*, 31(2):170–174, 2013. URL https://doi.org/10.1038/nbt.2461.

[49] Hee Taek Kim, Kei-Anne Baritugo, Young Hoon Oh, Sung Min Hyun, Tae Uk Khang, Kyoung Hee Kang, Sol Hee Jung, Bong Keun Song, Kyungmoon Park, Il-Kwon Kim, et al. Metabolic engineering of *Corynebacterium glutamicum* for the high-level production of cadaverine that can be used for the synthesis of biopolyamide 510. *ACS Sustainable Chemistry & Engineering*, 6(4):5296–5305, 2018. URL https://doi.org/10.1021/acssuschemeng.8b00009.

[50] Leibniz institute. https://www.dsmz.de/collection/catalogue/details/culture/DSM-18039, 2023.

[51] Alessandro Bertero, Stephanie Brown, and Ludovic Vallier. Methods of cloning. In *Basic science methods for clinical researchers*, pages 19–39. Elsevier, 2017.

[52] D Peter Snustad and Michael J Simmons. *Principles of genetics*. John Wiley & Sons, 2015.

[53] Daniel G Gibson, Lei Young, Ray-Yuan Chuang, J Craig Venter, Clyde A Hutchison, and Hamilton O Smith. Enzymatic assembly of dna molecules up to several hundred kilobases. *Nature methods*, 6 (5):343–345, 2009. URL https://doi.org/10.1038/nmeth.1318.

[54] Carsten Haupka, Luciana F Brito, Tobias Busche, Daniel Wibberg, and Volker F Wendisch. Genomic and transcriptomic investigation of the physiological response of the methylotroph *Bacillus methanolicus* to 5-aminovalerate. *Frontiers in Microbiology*, 12:664598, 2021. URL https://doi.org/10.3389/fmicb.2021.664598.

[55] Makoto Masuda, Satoru Takamatsu, Noriyuki Nishimura, Saburo Komatsubara, and Tetsuya Tosa. Improvement of nitrogen supply for l-threonine production by a recombinant strain of *Serratia marcescens*. *Applied biochemistry and biotechnology*, 37:255–265, 1992. URL https://doi.org/10.1007/BF02788877.

[56] H Brückner, S Flassig, and J Kirschbaum. Determination of biogenic amines in infusions of tea (camellia sinensis) by HPLC after derivatization with 9-fluorenylmethoxycarbonyl chloride (fmoc-cl). *Amino Acids*, 42:877–885, 2012. URL https://doi.org/10.1007/s00726-011-1003-2.

[57] Sci ed software: Clone manager v9. https://www.scied.com/pr_cmpro.htm, 2023.

[58] Benchling. https://www.benchling.com/, 2023.

[59] Blast: *B. methanolicus* MGA3, complete genome. https://www.ncbi.nlm.nih.gov/nuccore/662717320, 2023.

[60] Leibniz institute dsmz: BRENDA enzyme database. https://www.brenda-enzymes.org/index.php, 2023.

[61] Biorad: Image lab software. https://www.bio-rad.com/en-no/product/image-lab-software?ID=KRE6P5E8Z, 2023.

[62] Xia Sun, Wei Song, and Liming Liu. Enzymatic production of agmatine by recombinant arginine decarboxylase. *Journal of Molecular Catalysis B: Enzymatic*, 121:1–8, 2015. URL https://doi.org/10.1016/j.molcatb.2015.06.008.

[63] Matthew Burrell, Colin C Hanfrey, Ewan J Murray, Nicola R Stanley-Wall, and Anthony J Michael. Evolution and multiplicity of arginine decarboxylases in polyamine biosynthesis and essential role in *Bacillus subtilis* biofilm formation. *Journal of Biological Chemistry*, 285(50):39224–39238, 2010. URL https://doi.org/10.1074/jbc.M110.163154.

[64] HJ Rosenfeld and J Roberts. Arginine decarboxylase from a *Pseudomonas* species. *Journal of bacteriology*, 125(2):601–607, 1976. URL https://doi.org/10.1128/jb.125.2.601-607.1976open_in_new.

[65] Mashkoor Alam, Abhishek Srivastava, Ankita Dutta, and Apurba Kumar Sau. Biochemical and biophysical studies of helicobacter pylori arginine decarboxylase, an enzyme important for acid adaptation in host. *IUBMB life*, 70(7):658–669, 2018. URL https://doi.org/10.1002/iub.1754.

[66] C Satishchandran and Stephen M Boyle. Purification and properties of agmatine ureohydrolyase, a putrescine biosynthetic enzyme in *Escherichia coli*. *Journal of bacteriology*, 165(3):843–848, 1986. doi: 10.1128/jb.165.3.843-848.1986.

[67] Mon-Juan Lee, Ya-Ting Yang, Vivian Lin, and Haimei Huang. Site-directed mutations of the gatekeeping loop region affect the activity of *Escherichia coli* spermidine synthase. *Molecular biotechnology*, 54:572–580, 2013. URL https://doi.org/10.1007/s12033-012-9599-3.

[68] William H Bowman, Celia White Tabor, and Herbert Tabor. Spermidine biosynthesis: purification and properties of propylamine transferase from *Escherichia coli*. *Journal of Biological Chemistry*, 248(7):2480–2486, 1973. URL https://doi.org/10.1016/S0021-9258(19)44133-1.

[69] Celia White Tabor. [103a] adenosylmethionine decarboxylase. In *Methods in enzymology*, volume 5, pages 756–760. Elsevier, 1962. URL https://doi.org/10.1016/S0076-6879(62)05309-4.

[70] Celia White Tabor and Herbert Tabor. S-adenosylmethionine synthetase and S-adenosylmethionine decarboxylase. *Advances in enzymology and related areas of molecular biology*, 56(25):1–282, 1984.

[71] George D Markham, Celia White Tabor, and Herbert Tabor. [37] s-adenosylmethionine decarboxylase (*Escherichia coli*). In *Methods in Enzymology*, volume 94, pages 228–230. Elsevier, 1983. URL https://doi.org/10.1016/S0076-6879(83)94039-9.

[72] Dexter B Northrop. On the meaning of Km and V/K in enzyme kinetics. *Journal of Chemical Education*, 75(9):1153, 1998. URL https://doi.org/10.1021/ed075p1153.

[73] Zhi-Gang Qian, Xiao-Xia Xia, and Sang Yup Lee. Metabolic engineering of *Escherichia coli* for the production of cadaverine: a five carbon diamine. *Biotechnology and bioengineering*, 108(1):93–103, 2011. URL https://doi.org/10.1002/bit.22918.

[74] Marta Tous Mohedano, Oliver Konzock, and Yun Chen. Strategies to increase tolerance and robustness of industrial microorganisms. *Synthetic and Systems Biotechnology*, 7(1):533–540, 2022. URL https://doi.org/10.1016/j.synbio.2021.12.009.

[75] Marta Irla, Ingemar Nærdal, Trygve Brautaset, and Volker F Wendisch. Methanol-based γ-aminobutyric acid (gaba) production by genetically engineered *Bacillus methanolicus* strains. *Industrial Crops and Products*, 106:12–20, 2017. URL https://doi.org/10.1016/j.indcrop.2016.11.050.

[76] Akihiko Sakamoto, Junpei Sahara, Gota Kawai, Kaneyoshi Yamamoto, Akira Ishihama, Takeshi Uemura, Kazuei Igarashi, Keiko Kashiwagi, and Yusuke Terui. Cytotoxic mechanism of excess polyamines functions through translational repression of specific proteins encoded by polyamine modulon. *International Journal of Molecular Sciences*, 21(7):2406, 2020. URL https://doi.org/10.3390/ijms21072406.

[77] Minho Noh, Seung Min Yoo, Won Jun Kim, and Sang Yup Lee. Gene expression knockdown by modulating synthetic small rna expression in *Escherichia coli*. *Cell systems*, 5(4):418–426, 2017. URL https://doi.org/10.1016/j.cels.2017.08.016.

[78] Carmen Keilhauer, L Eggeling, and H Sahm. Isoleucine synthesis in *Corynebacterium glutamicum*: molecular analysis of the ilvb-ilvn-ilvc operon. *Journal of bacteriology*, 175(17):5595–5603, 1993. URL https://doi.org/10.1128/jb.175.17.5595-5603.1993.

[79] Peng Yang, Yanan Chen, and An-dong Gong. Development of a defined medium for *Corynebacterium glutamicum* using urea as nitrogen source. *3 Biotech*, 11(9):405, 2021. URL https://doi.org/10.1007/s13205-021-02959-6.

[80] Sanjoy K Bhattacharya and Ashok K Dubey. Metabolic burden as reflected by maintenance coefficient of recombinant *Escherichia coli* overexpressing target gene. *Biotechnology letters*, 17:1155–1160, 1995. URL https://doi.org/10.1007/BF00128377.

[81] Roman Jansen, Niklas Tenhaef, Matthias Moch, Wolfgang Wiechert, Stephan Noack, and Marco Oldiges. Feeder: a feedback-regulated enzyme-based slow-release system for fed-batch cultivation in microtiter plates. *Bioprocess and biosystems engineering*, 42(11):1843–1852, 2019. URL https://doi.org/10.1007/s00449-019-02180-z.

[82] Trygve Brautaset, Øyvind M Jakobsen, Michael C Flickinger, Svein Valla, and Trond E Ellingsen. Plasmid-dependent methylotrophy in thermotolerant *Bacillus methanolicus*. *Journal of bacteriology*, 186(5):1229–1238, 2004. URL https://doi.org/10.1128/jb.186.5.1229-1238.2004.

[83] Kinga Umenhoffer, Tamás Fehér, Gabriella Balikó, Ferhan Ayaydin, János Pósfai, Frederick R Blattner, and György Pósfai. Reduced evolvability of *Escherichia coli* MDS42, an IS-less cellular chassis for molecular and synthetic biology applications. *Microbial Cell Factories*, 9(1):1–12, 2010. URL https://doi.org/10.1038/s41467-021-21210-7.

[84] Marta Irla, Armin Neshat, Trygve Brautaset, Christian Rückert, Jörn Kalinowski, and Volker F Wendisch. Transcriptome analysis of thermophilic methylotrophic *Bacillus methanolicus* MGA3 using RNA-sequencing provides detailed insights into its previously uncharted transcriptional landscape. *BMC genomics*, 16:1–22, 2015. URL https://doi.org/10.1186/s12864-015-1239-4.

[85] Elke EE Noens and Juke S Lolkema. Convergent evolution of the arginine deiminase pathway: the ArcD and ArcE arginine/ornithine exchangers. *Microbiologyopen*, 6(1):e00412, 2017. URL https://doi.org/10.1002/mbo3.412.

Appendices

A Media and solution recipes

Table A.1 and A.2 shows the recipe for all media and solutions used in this project, respectively. All media were autoclaved at 121 °C for 20 minutes unless otherwise stated in the table. For the preparation of agar plates, 15 gL^{-1} of agar was added to the media before autoclaving, and required antibiotics were added after autoclaving. Unless stated otherwise, the media pH was adjusted to 7.2 with HCl, KOH, or NaOH before adjusting the volume and autoclaving.

Table A.1: Recipe of media used to cultivate bacterial strains. The purpose of each meidum is stated in the table.

Solution	Compound	Amount (g)	Volume (mL)
LB medium	Growth medium for bacterial strains		
	Tryptone	10	
	NaCl	10	
	Yeast extract	5	
	MilliQ H_2O, to		1000
SOB medium	Rich medium for *B. methanolicus*		
	Hannah's broth (SOB)	28	
	MilliQ H_2O, to	1000	
MVcM(Y) medium	Minimal medium for *B. methanolicus* cultivation *		
	MVcM High Salt Buffer 10x		100
	(Yeast extract)	0.25	
	MilliQ H_2O, to	1000	
Additions:	Added to 100 mL of MVcM(Y) buffer before use		
	$MgSO_4$ stock solution		0.1
	Trace metals stock solution (Table A.2)		0.1
	Complete vitamin stock solution (Table A.2)		0.1
	Methanol		0.811
CGXII medium	Minimal medium developed for *C. glutamicum*[78]		
	CGXII buffer		80
	MilliQ H_2O, to		100
Additions:	Additions presented under MVcM media, added to 100 mL of medium before use		
Psi media	Applied in preparation of chemically competent *E. coli* DH5α cells		
	Tryptone	20	
	Yeast extract	5	
	$MgCl_2$	5	
	MilliQ H_2O, to		1000

*Yeast extract only applies to MVcMY, while MVcM is prepared with no addition of yeast extract.

Table A.2: Recipe of buffers and solutions used in this work. The purpose of each solution is stated in the table.

Solution	Compound	Amount (g)	Volume (mL)
Tris-acetate-EDTA (TAE) buffer	Running buffer in agarose gel electrophoresis.		
	Tris	4.85	
	Glacial acetic acid	1.14	
	0.5M EDTA		20
	MilliQ H_2O, to		1000
Transformation buffer 1 (TFB1)	For the preparation of chemically competent *E. coli* DH5α cells. The pH was adjusted to 5.8 with acetic acid (10%). Sterile filtrated into an autoclaved bottle		
	Potassium acetate	0.588	
	$RbCl_2$	2.42	
	$CaCl_2$ -$2H_2O$	0.294	
	$MnCl_2$	2.0	
	Glycerol		30
	MilliQ H_2O, to		200
Transformation buffer 2 (TFB2)	For the preparation of chemically competent *E. coli* DH5α cells. pH adjusted to 6.5 with NaOH. Sterile filtrated into an autoclaved bottle.		
	MOPS	0.21	
	$CaCl_2$ -$2H_2O$	1.1	
	Glycerol		15
	MilliQ H_2O, to		100
Electroporation buffer (EPB)	For the preparation of electrocompetent *B. methanolicus* MGA3 cells. Sterile filtrated into an autoclaved bottle.		
	MOPS	0.21	
	$CaCl_2$ -$2H_2O$	1.1	
	Glycerol		15
	MilliQ H_2O, to		100
MVcM High Salt Buffer 10x	Contains the salts for the MVcMY and MVcM medium.		
	K_2HPO_4	40.93	
	NaH_2PO_4*H_2O	14.9	
	$(NH_4)_2SO_4$	21.14	
	MilliQ H_2O, to		1000
CGXII 80% concentrated	Buffer for CGXII medium preparation		
	K_2HPO_4	0.10	
	KH_2PO_4	0.10	
	Urea	0.10	
	$(NH_4)_2SO_4$	1.00	
	MilliQ H_2O, to		80
$MgSO_4$ stock solution	Applied in cultivation of *B. methanolicus*. Sterile filtered into an autoclaved bottle. Stored in -4 °C.		
	$MgSO_4$*$7H_2O$	246.47	
	MilliQ H_2O, to		1000
Trace metals stock solution	Applied in cultivation of *B. methanolicus*. Sterile filtered into an autoclaved bottle. Stored in -4 °C.		
	$FeSO_4$*$7H_2O$	5.56	
	$CuSO_4$*$2H_2O$	0.02728	
	$CaCl_2$*$2H_2O$	7.35	
	$CoCl_2$*$6H_2O$	0.04050	
	$MnCl_2$*$4H_2O$	9.90	
	$ZnSO_4$*$7H_2O$	0.28754	
	Na_2MoO_4*$2H_2O$	0.04840	
	H_3BO_3	0.0392	
	HCl		80
	MilliQ H_2O, to		1000
Complete vitamin stock solution	Applied in cultivation of *B. methanolicus*. Sterile filtered and aliquoted 1 mL in autoclaved Eppendorf tubes. Stored in -20 °C.		
	Biotin	0.1	
	Thiamine hydrochloride	0.1	
	Riboflavin	0.1	
	d-Calcium pantothenate	0.1	
	Pyridoxine hdyrochloride	0.1	
	Nicotinamide	0.1	
	p-Aminobenzoic acid	0.02	
	Folic acid	0.01	
	Vitamin B_{12}	0.01	
	Lipoic acid	0.01	
	MilliQ H_2O, to		1000

All solutions used for the derivatization of HPLC samples are stated in Table A.3. No internal standards were used, and external standards used are 1 mM arginine, 1 mM putrescine dichloride, and 1 mM spermidine. External standards were diluted with MilliQ water, and filtrated before use.

Table A.3: Solutions used for derivatization of samples prior to quantification by HPLC.

Solution	Compound	Amount (g)	Volume (mL)
Sodium borate buffer (pH 9 and pH 7)	Chemical used for the derivatization of HPLC samples by the FMOC method to neutralize the samples. pH was adjusted to 9 or 7 with 30 % NaOH before completing the volume to 100 mL.		
	Boric acid	3.09	
	MilliQ H_2O, to		100
Elution buffer (50 mM sodium acetate pH 4.2)	Chemical used as mobile phase for HPLC. pH was adjusted to 4.2 with 30 % NaOH. Buffer was filtered before use.		
	Acetic acid - glacial		7.5
	MilliQ H_2O, to		2500
Dilution buffer	Used for dilution of the derivatized HPLC samples by FMOC method.		
	Elution buffer		30
	Acetonitrile		70
EVA reagent (40 mM)	Reagent for the derivatization of HPLC samples.		
	Glycine	0.150	
	Borate buffer pH 7 to		25
FMOC	Reagent for the derivatization of HPLC samples.		
	FMOC-Chloride	12.95	
	Acetone		10

B Oligonucleotides

Primers used in this study for PCR amplification of DNA fragments, colony PCR, and sequencing of generated constructs are listed below (Table B.1). The purpose of each primer is specified in the table along with the sequence (5' à 3'). For Gibson assembly, relevant primers were designed with overlapping regions with a respective plasmid backbone or neighboring gene.

Table B.1: Primers used in the present study. Overlapping regions are denoted by bases in **bold**.

Name	Purpose	Sequence 5' à 3'
speebmfw	Gibson assembly forward primer for amplification of *speE* using *B. methanolicus* MGA3 gDNA	**GTAAACAATTACATAAATAGGAGGTAGTAgtac** ATGGGACTTTGGTTTACT-GAAAAACAAACAG
speebm2rv	Gibson assembly reverse primer for amplification of *speE* using *B. methanolicus* MGA3 gDNA	**GGATCCCCGGGAATTCAAGCTTTAAACATG** TTATTTTGTTAGGTCGCT-GACGAACTTCG
speeecfw	Gibson assembly forward primer for amplification of *speE* using *E. coli* K-12 MG1655 gDNA	**GTAAACAATTACATAAATAGGAGGTAGTAgtac** ATGAGCACCTTAGGTCAT-CAATACGATAAC
speeec2rv	Gibson assembly reverse primer for amplification of *speE* using *E. coli* K-12 MG1655 gDNA	**GGATCCCCGGGAATTCAAGCTTTAAACATG** TTACTCGCCCTTTTTCGCCGCCTG
PTH 112	Standard forward primer for pTH1mp multiple cloning site sequencing	GCGTCAAAATCACTTTTCCTTTGG
PTH 113	Standard reverse primer for pTH1mp multiple cloning site sequencing	GGCTGCGCAACTGTTGGGAAGGGC

C Growth curves

Figure C.1 show the growth curve of *B. methanolicus* WT strain MGA3 cultivated in the presence of arginine (A), putrescine (B), spermidine (C), or putrescine andspermidine together (D) with increasing concentration from 0 to 30 mM.

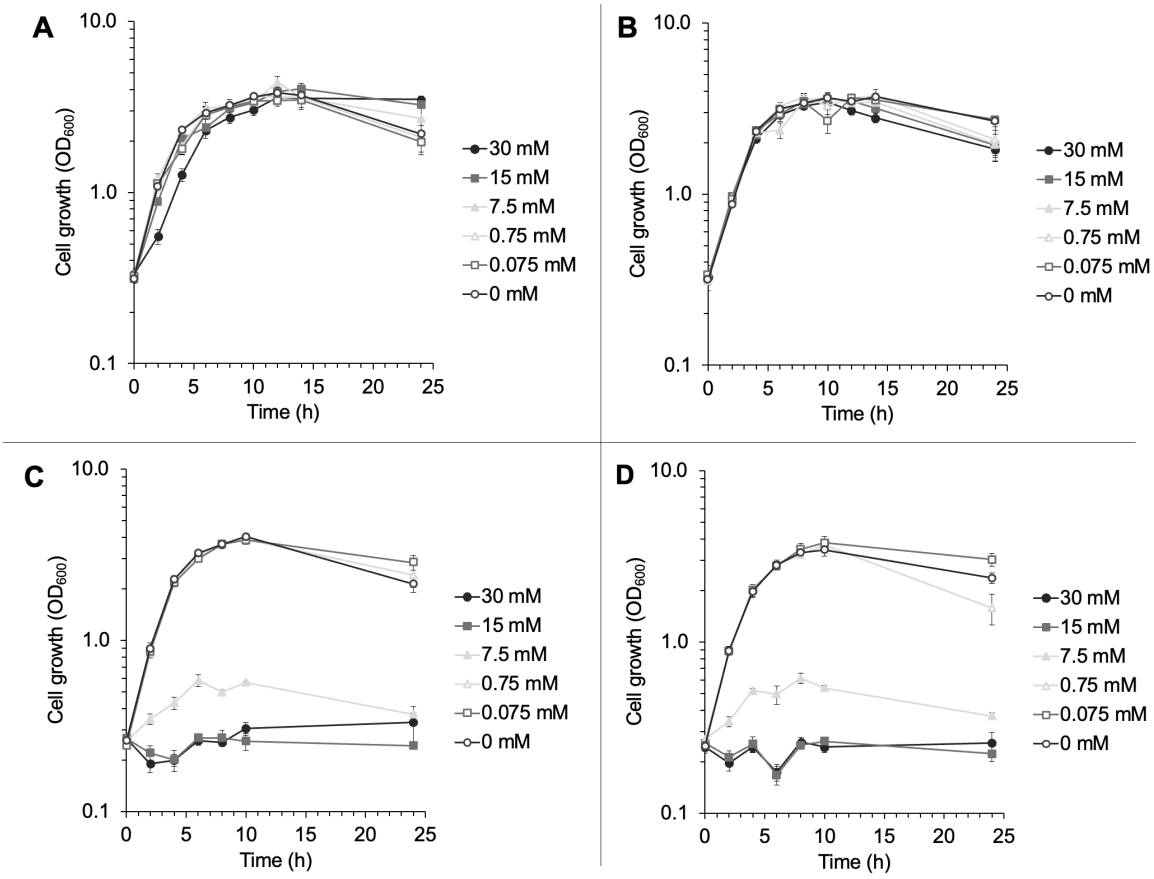

Figure C.1: Growth of *B. methanolicus* WT strain MGA3 in the presence of arginine (A), putrescine (B), spermidine (C) and putrescine and spermidine together (D).
B. methanolicus MGA3 WT was cultivated in SOB medium supplemented with 0, 0.075, 0.75, 7.5, 15, and 30 mM arginine (A), putrescine (B), spermidine (C), and putrescine and spermidine together (D). Values are presented as the mean OD_{600} of triplicates. Standard deviations are presented as error bars.

Figure C.2 show the growth curve of PBV, PUT^{Ec}, and PUT^{Bm} induced to a final concentration of 0 (A), 0.01 (B), 0.1 (C), or 1% (D) xylose. All strains were induced after 2 hours of growth.

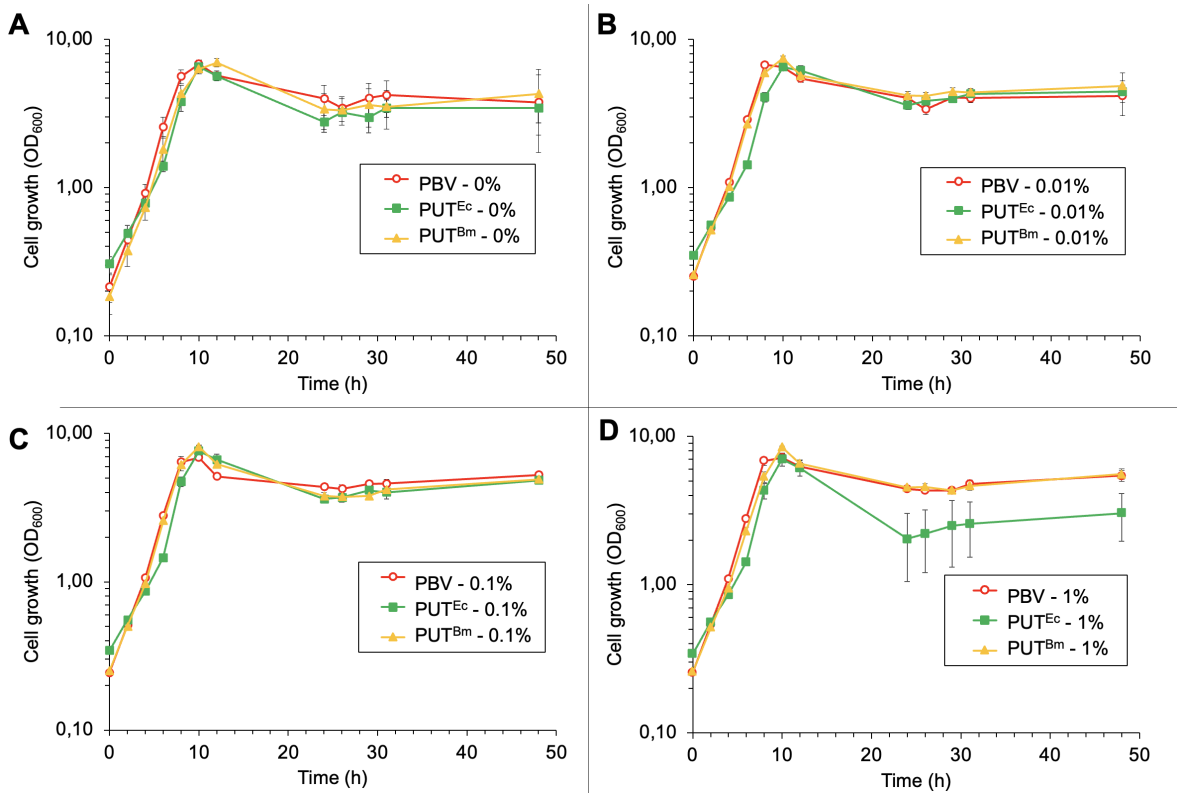

Figure C.2: Growth of *B. methanolicus* MGA3 strains PBV, PUT^{Ec}, and PUT^{Bm} under varying gene expression induction levels.
PBV, PUT^{Ec}, and PUT^{Bm} was cultivated in MVcM medium and plasmid-borne gene expression were induced with a final concentration of 0 (A), 0.01 (B), 0.1 (C), and 1% (D) xylose. Induction occured after 2 hours of growth. Values are presented as mean OD_{600} of triplicates with standard deviations displayed as error bars.

Figure C.3 shows the growth curve of PBV, and PUT^{Ec} cultivated in MVcM and MVcM supplemented with 1mM of glutamate, arginine, or ornithine. All strains were induced with xylose 0.1% after 2 hours of growth.

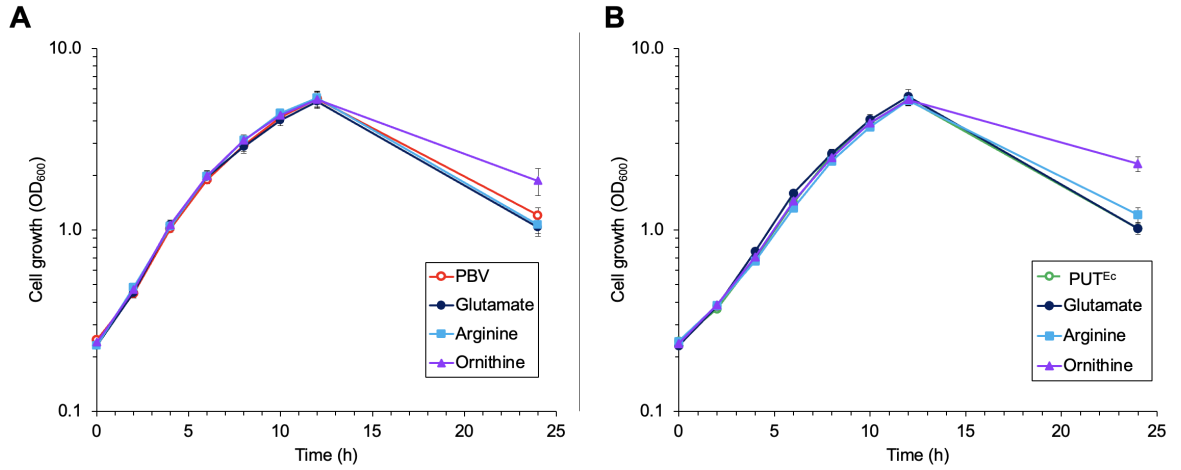

Figure C.3: Growth of *B. methanolicus* MGA3 strains PBV, and PUT^{Ec} supplemented with precursors of putrescine and spermidine.
PBV (A) and PUT^{Ec} (B) was cultivated in MVcM medium supplemented with either 1 mM glutamate, arginine, ornithine, or no supplementation. Induction with a final concentration of 0.1% xylose occurred after 2 hours of growth. Values are presented as mean OD_{600} of triplicates with standard deviations displayed as error bars.

Figure C.4 presents the growth curve of PBV, and PUT^{Ec} cultivated in MVcM, MVcM2, or CGXII. All strains were induced with xylose 0.1% after 3 hours of growth.

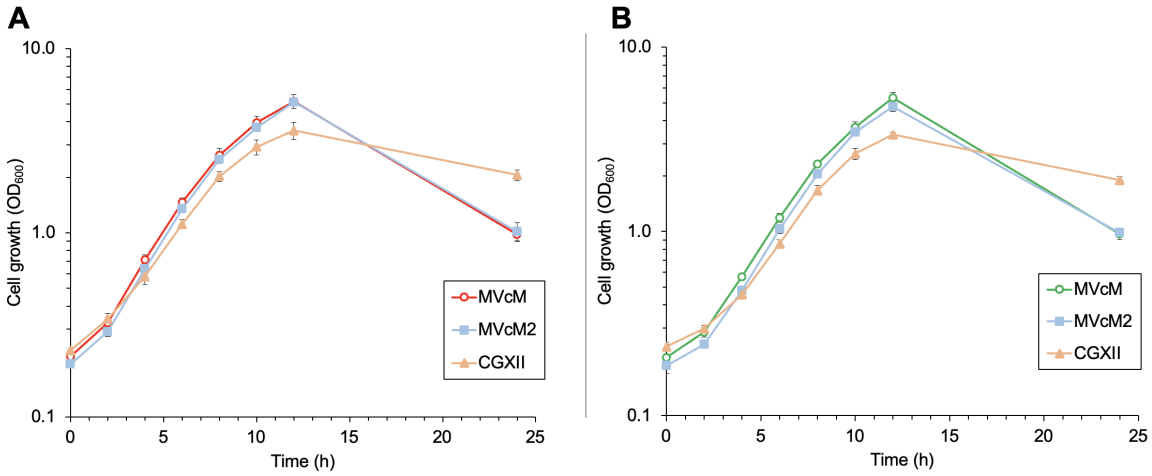

Figure C.4: Growth curves of *B. methanolicus* MGA3 strains PBV and PUT^{Ec} cultivated in MVcM, MVcM2, or CGXII. PBV (A) and PUT^{Ec} (B) was cultivated in MVcM, MVcM2, or CGXII. Induction with a final concentration of 0.1% xylose occurred after 3 hours of growth. Values are presented as mean OD_{600} of triplicates with standard deviations displayed as error bars.

Figure C.5 presents the growth curve of PTH, SPE^{Bm}, SPE$_{ii}^{Ec}$, and SPE$_{ii}^{Bm}$ cultivated in MVcM media.

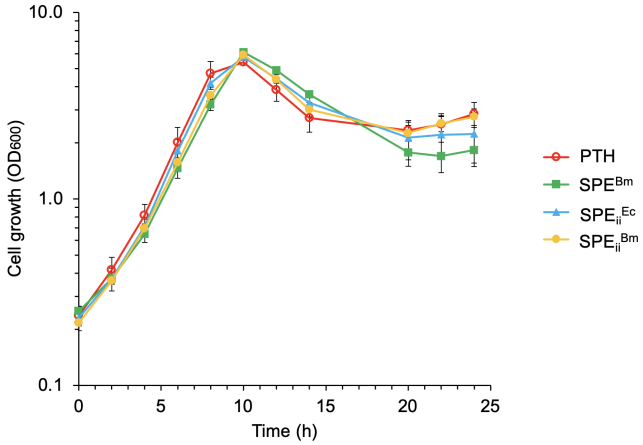

Figure C.5: Growth of *B. methanolicus* strains PTH, SPE^{Bm}, SPE$_{ii}^{Ec}$, and SPE$_{ii}^{Bm}$.
The strains PTH, SPE^{Bm}, SPE$_{ii}^{Ec}$, and SPE$_{ii}^{Bm}$ was cultivated in MVcM medium. Values are presented as mean OD_{600} of triplicates with standard deviations displayed as error bars.

Figure C.6 presents the growth curve of PUT^{Ec}SPE^{Bm}, PUT^{Ec}SPE$_{ii}^{Ec}$, and PUT^{Ec}SPE$_{ii}^{Bm}$ cultivated in MVcM media.

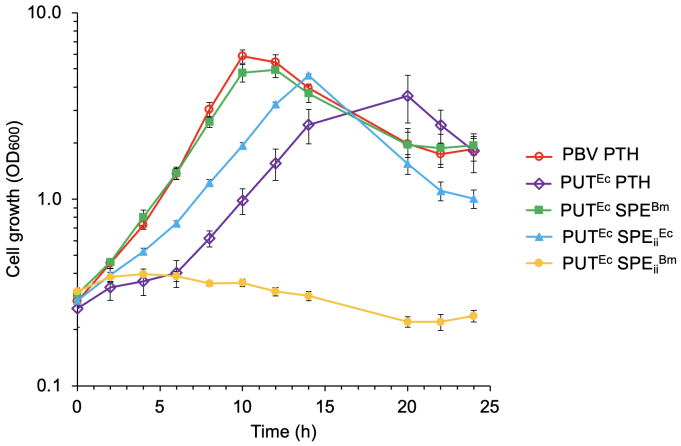

Figure C.6: Growth of *B. methanolicus* strains, PBV PTH, PUT^{Ec}PTH, PUT^{Ec}SPE^{Bm}, PUT^{Ec}SPE$_{ii}{}^{Ec}$, and PUT^{Ec}SPE$_{ii}{}^{Bm}$. The PBV PTH, PUT^{Ec}PTH, PUT^{Ec}SPE^{Bm}, PUT^{Ec}SPE$_{ii}{}^{Ec}$, and PUT^{Ec}SPE$_{ii}{}^{Bm}$ strains were cultivated in MVcM medium induced with xylose after 4 hours. Values are presented as the mean OD_{600} of triplicates. Standard deviations are presented as error bars.

D Example calculation of growth rates, final biomass and IC_{50}

A calculation example of the growth rate and final biomass of a bacterial strain after 24 hours of cultivation is presented here. The growth curve shown in Figure D.1-A was recorded as previously presented in Section 2.3. The growth rate is calculated as the slope of an exponential fitted trend line of the exponential growth phase during cultivation, as shown in Figure D.1-B. From the exponential fitted trend line ($y = 0.1914e^{0.3939x}$), the slope is found to be 0.3939 which results in a growth rate of 0.39 h^{-1}.

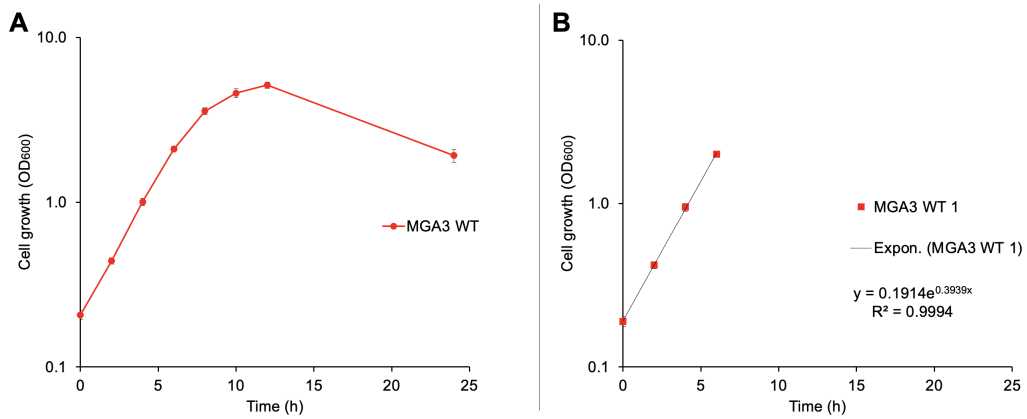

Figure D.1: Example calculation of growth rate
Growth curve (A) of *B. methanolicus* WT strain MGA3 in SOB (rich) medium. Values are presented as mean OD_{600} of triplicates with standard deviations displayed as error bars. Exponential fitter trend line (B) of the exponential phase of one of the triplicates presented in A for calculation of growth rate using the equation $y = 0.1914e^{0.3939x}$.

A calculation example of IC_{50} value, here for the *B. methanolicus* WT strain MGA3 cultivated in SOB (rich) medium containing increasing concentrations of spermidine. The growth rates were calculated as presented above, followed by plotting the growth rates against spermidine concentrations (Figure D.2). A linear fitted trend line was created between the two data points with the steepest decline (between 0.75 and 7.5 mM spermidine), where the equation of the linear trend line was y = -0.0616x + 0.5909. To determine the half-inhibitory concentration, the value of y was set to 0.5909 multiplied by 0.5, and the corresponding value of x was calculated as the IC_{50} value = 4.8 mM.

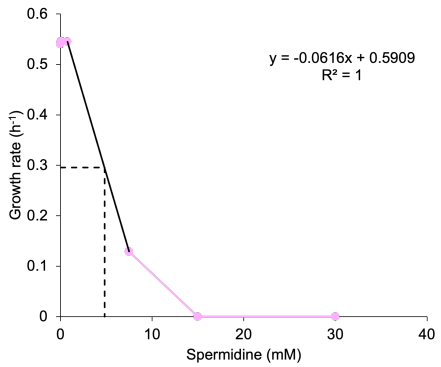

Figure D.2: Example calculation of IC_{50}
Growth rates of *B. methanolicus* WT strain MGA3 in cultivation with increasing concentrations of spermidine plotted against the respective concentrations. The equation of the linear fitted trend line (y = -0.0616x + 0.5909) between the data point with the steepest decline was used for the calculation of the IC_{50} value.

E Example calculation of quantitative analysis by HPLC

A calculation example of the quantification of arginine, putrescine, and spermidine, in samples, is presented here. During HPLC analysis, a derivatized sample passes through the HPLC column, and the different compounds within the sample elute at varying retention times. These compounds are detected by an FLR detector, resulting in peaks with different heights, areas, and retention times. To establish calibration, mixtures of arginine, putrescine dichloride, and spermidine were prepared at concentrations of 0.1 mM, 0.05 mM, 0.025 mM, and 0.0125 mM through appropriate dilution with MilliQ H_2O. The height of each peak was computed by integration, which is proportional to the respective concentrations. A calibration curve was then created by plotting the integrated peak heights against the concentrations of arginine, putrescine dichloride, and spermidine, as shown in Figure E.1. Linear trend lines were fitted for each compound, and the slope (a) of the trend line was used for subsequent calculations of unknown samples using Equation E.1.

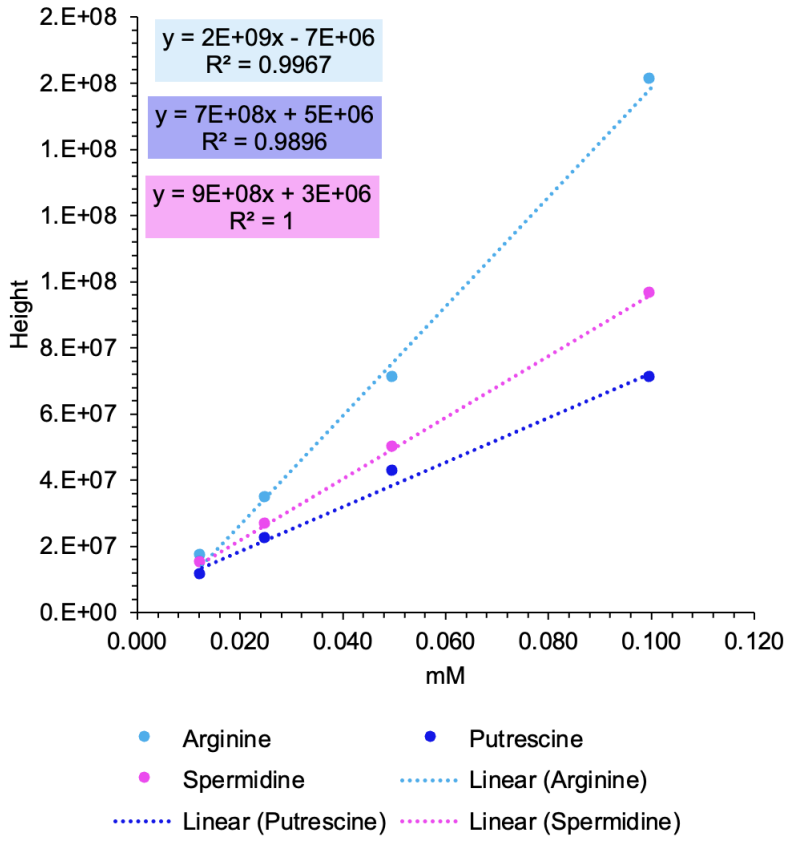

Figure E.1: Linear calibration curve for calculation of l-arginine, putrescine, and spermidine concentration in samples analyzed by HPLC.
For each compound, the integrated peak heights of each concentration were plotted against the respective concentration.

$$\text{Concentration sample } (\mu M) = \frac{\frac{\text{Height of peak}}{a}}{1000} \tag{E.1}$$

F Plasmid maps

Plasmid maps of constructs donated by Luciana F. Brito for the establishment of methanol-based production of putrescine (Figure F.1-A, and F.1-B) and spermidine (Figure F.1-C, and F.1-D) is presented here. The construct created in this study for methanol-based production of spermidine is presented in Figure F.1-E, while Figure F.1-F shows the construct attempted to be created in this study.

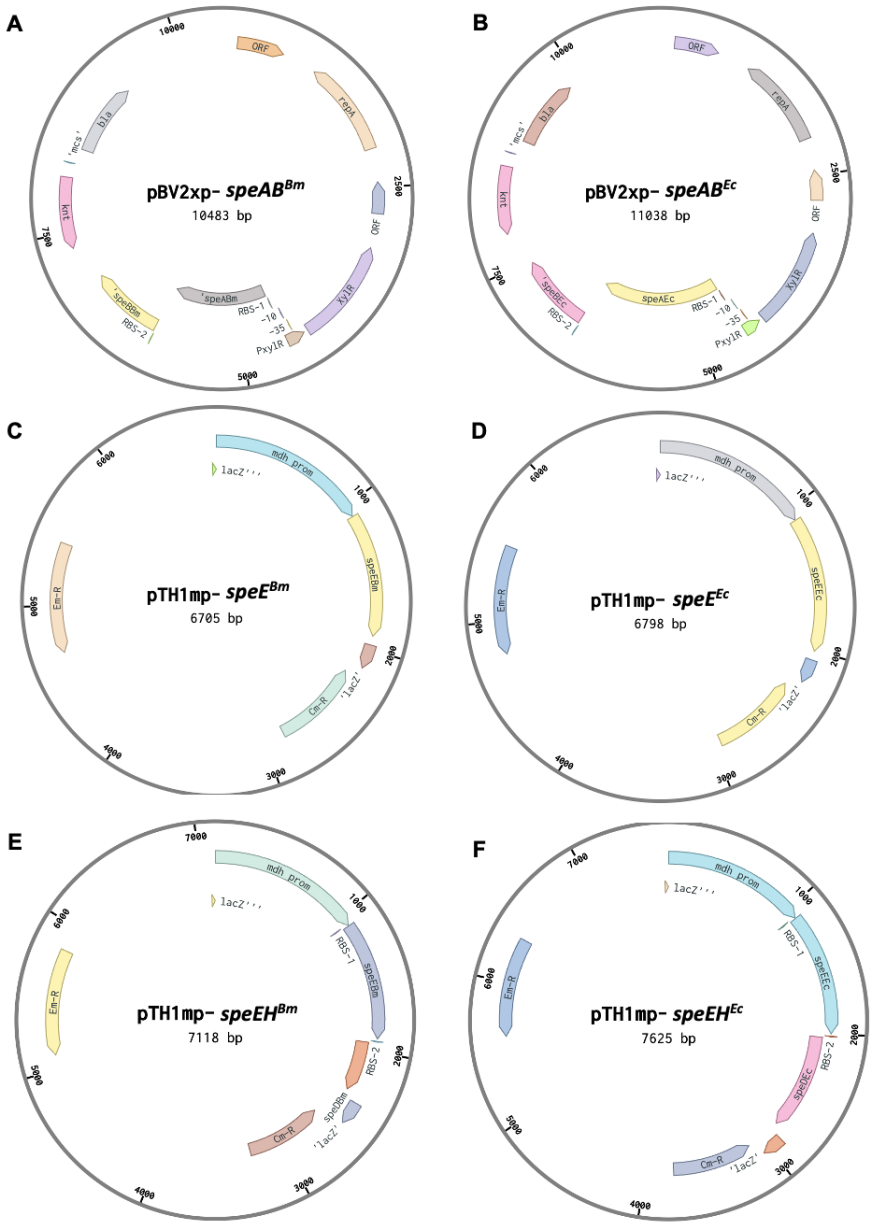

Figure F.1: Plasmid maps of constructed and donated pBV2xp-*speAB*^{Bm} (A) and pBV2xp-*speAB*^{Ec} (B), pTH1mp-*speEH*^{Bm} (C), pTH1mp-*speEH*^{Ec} (D), pTH1mp-*speE*^{Bm} (E), and pTH1mp-*speE*^{Ec} (F)

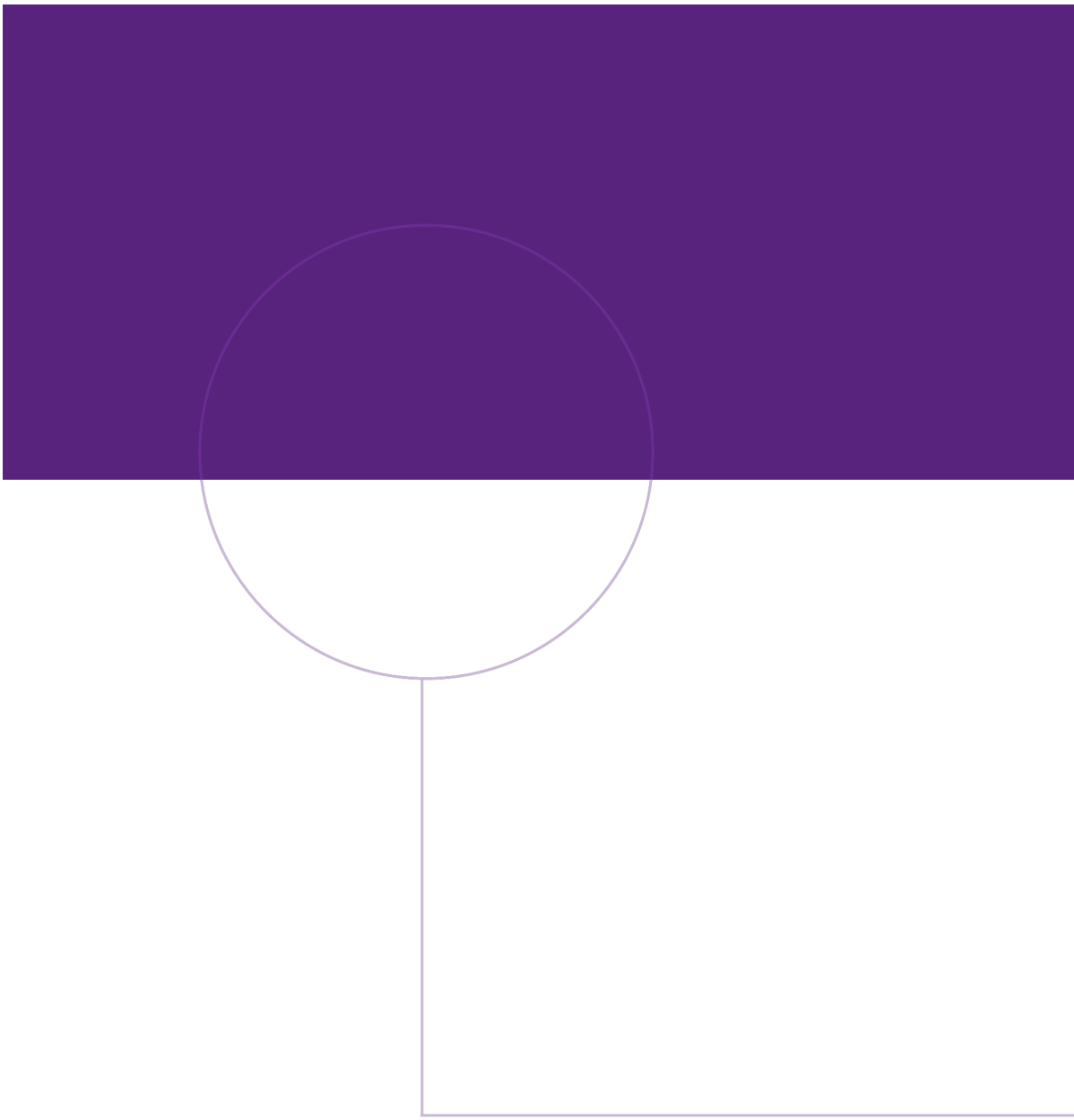

NTNU

Norwegian University of
Science and Technology